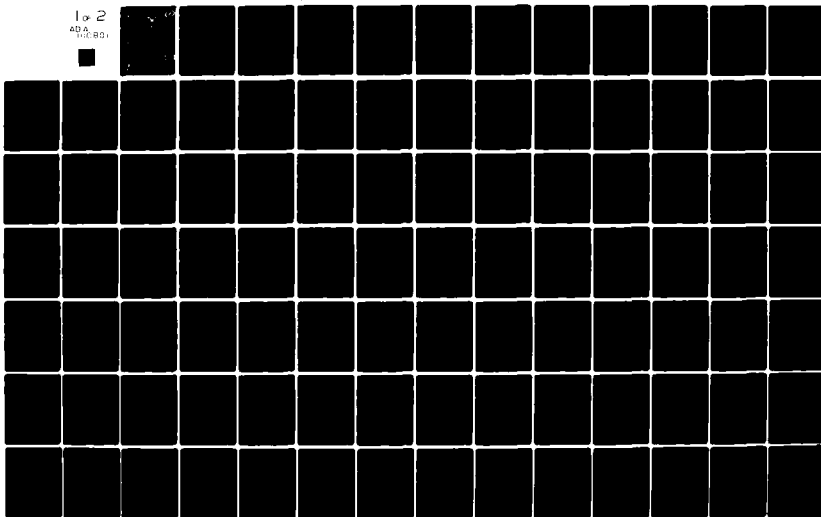


AD-A100 801 AIR FORCE INST OF TECH WRIGHT-PATTERSON AFB OH SCHOO--ETC F/G 12/1  
ANALYTICAL AND NUMERICAL PROBLEMS ASSOCIATED WITH EXTENDING TH--ETC(U)  
JUN 81 J C SOUNDRS  
UNCLASSIFIED AFIT/DS/PH/81-2 NL

1 of 2  
40A  
100-801

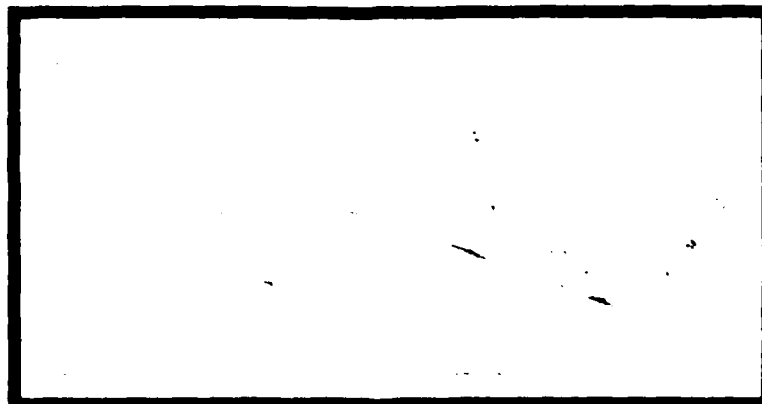


AD A100301



DDP. CV  
①

LEVEL 1



DTIC FILE COPY

DTIC  
ELECTE  
S JUL 1 1981

D

UNITED STATES AIR FORCE  
AIR UNIVERSITY  
AIR FORCE INSTITUTE OF TECHNOLOGY  
Wright-Patterson Air Force Base, Ohio

DISTRIBUTION STATEMENT A

Approved for public release;  
Distribution Unlimited

81 6 30 035

AFIT/DS/PH/81-2

Accession For	
NTIS GRA&I	<input checked="checked" type="checkbox"/>
DTIC TAB	<input type="checkbox"/>
Unannounced	<input type="checkbox"/>
Justification	
By	
Distribution/	
Availability Codes	
Dist	Avail and/or Special
A	

ANALYTICAL AND NUMERICAL PROBLEMS  
ASSOCIATED WITH EXTENDING THE USE  
OF THE SECOND ORDER EVEN-PARITY  
TRANSPORT EQUATION.

DISSERTATION

AFIT/DS/PH/81-2

John C. Souders, Jr.  
Captain USAF

DTIC  
ELECTRONIC  
JUL 1 1981

D

Approved for public release; distribution unlimited

AFIT/DS/PH/81-2

ANALYTICAL AND NUMERICAL PROBLEMS ASSOCIATED WITH  
EXTENDING THE USE OF  
THE SECOND ORDER EVEN-PARITY TRANSPORT EQUATION

DISSERTATION

Presented to the Faculty of the School of Engineering  
of the Air Force Institute of Technology  
Air University  
in Partial Fulfillment of the  
Requirements for the Degree of  
Doctor of Philosophy

by

John C. Souders, Jr., B.S., M.E.  
Captain USAF

June 1981

Approved for public release; distribution unlimited.

AFIT/DS/PH/81-2

ANALYTICAL AND NUMERICAL PROBLEMS ASSOCIATED WITH  
EXTENDING THE USE OF  
THE SECOND ORDER EVEN-PARITY TRANSPORT EQUATION

by

John C. Souders, Jr., B.S., M.E.  
Captain USAF

Approved:

<u>David D. Harden</u> Chairman, DAVID D. HARDIN	<u>2 June 1981</u>
<u>John Jones Jr.</u> JOHN JONES, JR.	<u>2 June 1981</u>
<u>D. Kelleher</u> DERMOD KELLEHER	<u>22/5/81</u>
<u>George M. Nickel</u> GEORGE M. NICKEL	<u>2 June 1981</u>
<u>Charles J. Bridgman</u> CHARLES J. BRIDGMAN	<u>2 June 81</u>

ACCEPTED:

<u>J. Przemieniecki</u> Dean, School of Engineering	<u>2 June 81</u>
--	------------------

## Preface

The first step in problem solving is determining the reasons and causes that underlie the problem. Such has been the purpose of this dissertation. Previous work involving the second order even-parity form of the Boltzmann transport equation successfully demonstrated its ability to generate ray effect free solutions. These solutions were obtained in transport media requiring relatively simple geometry and isotropic scatter. The obvious extension of this work was to attempt a more complex transport problem. An air-over-ground problem was chosen since it adds the necessary complication to meaningfully test the feasibility of such an extension. Additionally, the solution of this problem is important in predicting the survivability and vulnerability of military systems in a nuclear environment. Thus, a successful extension would yield a worthwhile product. Unfortunately such an extension was not possible using the standard solution techniques currently available. The positive aspect of this research is that the problems associated with applying this equation to more complex transport problems are identified and the causes are known. The results of this research will provide direction for future efforts aimed at developing new solution techniques that will successfully solve the even-parity form of the Boltzmann equation formulated for these more complex problems.

As in all research efforts, several people played an important role. I would like to particularly thank Captain David Hardin for the technical guidance he provided. His contribution to this research effort was significant. I would also like to express my gratitude to Dr. Bridgman, Dr. Jones, and Dr. Kelleher, the other members of my committee, for their suggestions and constant encouragement. Two members of the Air Force Weapons Laboratories (AFWL) deserve special recognition, Mr. John Burgio and Mr. Harry

Murphy. These two individuals sponsored this research through the Technology Division of the AFWL. Additionally they provided computer support and several DOT 3.5 runs for use in analyzing specific problems encountered during this research. My family deserves my sincerest gratitude and love. Their patience and sacrifices during this research have been immense. Finally, I wish to thank the good Lord for providing me the strength to overcome the frustration that was abundant during this effort.

John C. Souders, Jr.

## Contents

	<u>Page</u>
Preface . . . . .	iii
List of Figures . . . . .	vii
Abstract . . . . .	viii
I. Introduction . . . . .	1
Even-Parity Equation and Space Angle Synthesis . . . . .	8
Purpose of the Research . . . . .	12
II. Weak Form Equation and Galerkin Method . . . . .	14
Introduction . . . . .	14
Weak Form and Functional Representations . . . . .	14
Galerkin Method . . . . .	15
Numerical Integration . . . . .	18
Analytical Integration . . . . .	30
III. Collocation Method . . . . .	39
Criteria . . . . .	39
Collocation Method and Trial Solution . . . . .	40
Problems . . . . .	46
Problem Analysis . . . . .	54
IV. Multigroup Considerations . . . . .	69
Background . . . . .	69
Multigroup Analysis . . . . .	70
V. Summary, Conclusions, and Recommendations . . . . .	75
Summary and Conclusions . . . . .	75
Recommendations . . . . .	80
Bibliography . . . . .	83
Appendix A: Derivation of Even-Parity Form of the Boltzmann Neutron Transport Equation . . . . .	86
Appendix B: Derivation of the $K_u$ Operator . . . . .	90
Appendix C: Derivation of the Weak Form of Second Order Even- Parity Fluence Equation . . . . .	93
Appendix D: Bilinear Lagrange Polynomials . . . . .	98
Appendix E: Canonical Techniques . . . . .	101

Appendix F: Total Terms in $\hat{A} \cdot \nabla \varepsilon(\vec{r}, \hat{A}) K_{\mu} \hat{A} \cdot \nabla \psi(\vec{r}, \hat{A})$ . . . . .	105
Appendix G: Derivation of Angular Synthesis Function . . . . .	108
Appendix H: Flow Charts . . . . .	113
Appendix I: Derivation of Normalized B Splines of Order 4 . . . . .	121
Vita . . . . .	124

## List of Figures

<u>Figure</u>		<u>Page</u>
1	Coordinate Systems Used in Neutral Particle Transport Problems for 2-D Cylindrical Geometry . . . . .	4
2	First Scatter Source Coordinate System Definition . . . . .	7
3	Tent Function Defined Over Four Rectangular Elements . . . . .	20
4	Results Using Galerkin Weak Form Equation . . . . .	28
5	Ellipsoidal Synthesis Function . . . . .	35
6	Representative Angular Fluence Shapes (Polar Plots) . . . . .	37
7	Collocation Spatial Mesh . . . . .	47
8	Global Collocation Matrix . . . . .	48
9	Program Logic . . . . .	50
10	Interpolation Problem 1 . . . . .	59
11	Interpolation Problem 2 (1 of 2) . . . . .	61
12	Interpolation Problem 2 (2 of 2) . . . . .	62
13	Even and Odd-Parity Fluence . . . . .	65
14	Boltzmann Fluence . . . . .	66
15	Polar Plot of Boltzmann Fluence . . . . .	67
16	Rectangular Element . . . . .	99
17	Standard Rectangular Element . . . . .	101
18	Canonical Element . . . . .	102
19	Derivation of Collocation Angular Synthesis Function . . . . .	109
20	Definition of Collocation Angular Synthesis Function . . . . .	111
21	Galerkin Program Flow Chart . . . . .	116
22	Collocation Program Flow Diagram . . . . .	120
23	B Spline Node Sequence . . . . .	121

Abstract

Published work indicated that a finite element solution of the even-parity form of the Boltzmann equation (EPFBE) provided a means for curing the ray effect in transport problems. This conclusion was made after examining the solutions of some simply defined problems involving plane geometry and isotropic scatter. The purpose of this research was to determine the feasibility of applying this equation to more complex problems. The air-over-ground problem was chosen. This problem is important in nuclear weapon effects calculations and requires two-dimensional cylindrical geometry, anisotropic scatter, and a multigroup solution. Additionally, the discrete ordinates method applied to this problem generates solutions with severe ray effects. Several numerical approaches based on the finite element method were attempted. The Galerkin method was applied to the weak form of the EPFBE. A bilinear Lagrange polynomial trial solution and specially derived synthesis function trial solution were used. The Galerkin method proved infeasible because the integrals resulting from this method could not be efficiently evaluated either numerically or analytically. To solve this integration problem, the collocation method was attempted. A trial solution consisting of cubic splines and a simply defined angular synthesis function was used. The collocation method allowed the analytic evaluation of the resulting integrals but forced a fixed anisotropy on the solution. The multigroup method applied to the EPFBE resulted in a nested integral problem involving the source terms of this equation. The complexity of this nesting problem increased proportionately with the number of energy group used. This research demonstrated that the finite element method cannot be cost effectively used in solving the EPFBE for transport problems requiring

complex geometries, anisotropic scatter, and a multigroup solution. Criteria were developed from this research that provides guidelines for pursuing future work related to the EPFBE. Recommendations based on these criteria are made.

## I. Introduction

The steady-state transport of neutrons and gamma rays from a point source of simulated nuclear weapon radiation in the atmosphere is a problem of fundamental importance in nuclear effects calculations. The equation whose solution prescribes the steady-state, neutral-particle distribution in the phase space of position, particle direction, and particle energy is the Boltzmann transport equation. This equation is a linear form of the Boltzmann equation used in several fields of physics and is a statement of particle conservation as applied to an infinitesimal element of volume, direction and energy, and may be written as

$$\hat{\lambda} \cdot \nabla \Phi(\vec{r}, \hat{\lambda}, E) + \sigma_T(\vec{r}, E) \Phi(\vec{r}, \hat{\lambda}, E) = S(\vec{r}, \hat{\lambda}, E) + \int_0^\infty dE' \int_{4\pi} d\hat{\lambda}' \sigma_S(\vec{r}, \hat{\lambda}' \rightarrow \hat{\lambda}, E' \rightarrow E) \Phi(\vec{r}, \hat{\lambda}', E') \quad (1.1)$$

where

$\vec{r}$  = the spatial position vector, in units of distance,

$E$  = the particle energy,

$\hat{\lambda}$  = a unit vector in the direction of particle motion,

$\nabla$  = the gradient operator

$S(\vec{r}, \hat{\lambda}, E)$  = the particle source density, in particles/unit volume/unit energy,

$\Phi(\vec{r}, \hat{\lambda}, E)$  = the angular particle fluence, in particles/unit area/steradian/unit energy,

$\sigma_T(\vec{r}, E)$  = the macroscopic total interaction cross section at position  $\vec{r}$  and for energy  $E$ , per unit distance, per unit energy,

$\sigma_S(\vec{r}, \hat{\lambda}' \rightarrow \hat{\lambda}, E' \rightarrow E)$  = the macroscopic differential scattering cross section at position  $\vec{r}$  for a particle of direction  $\hat{\lambda}'$  with energy

$E'$  scattering to a direction  $\hat{\lambda}$  and energy  $E$ . The units are per unit distance per steradian per unit energy.

Analytical solutions to this equation occur in only special cases where simplifying assumptions can be applied (Reference 1). Unfortunately, these assumptions do not generate a realistic scenario for performing nuclear effects calculations, thus requiring the use of numerical methods in these types of transport problems.

The scenario most used in performing nuclear effects calculations is a nuclear air burst detonation. Analytically this scenario is modeled by a two-dimensional cylindrical geometry (azimuthal symmetry assumed) composed of air with an exponentially varying density over a flat ground. This type of configuration is referred to as air-over-ground geometry. In this type of configuration, there is an interface at the air-ground boundary across which a discontinuous change in density occurs. The importance of including the ground was demonstrated by Straker (Ref. 2) who showed a significant effect on the atmospheric neutron distribution due to the presence of this relatively high density medium.

The conservative form of the Boltzmann transport equation for the selected cylindrical geometry can be written as

$$\begin{aligned} & \frac{\sqrt{1-\mu^2} \cos(\chi)}{\rho} \frac{\partial(\rho \Phi(\rho, z, \hat{\lambda}, E))}{\partial \rho} - \frac{1}{\rho} \frac{\partial(\sin(\chi) \sqrt{1-\mu^2} \Phi(\rho, z, \hat{\lambda}, E))}{\partial \chi} \\ & + \mu \frac{\partial \Phi(\rho, z, \hat{\lambda}, E)}{\partial z} + \sigma_T(\rho, z, E) \Phi(\rho, z, \hat{\lambda}, E) = \\ & S(\rho, z, \hat{\lambda}, E) + \int_0^\infty dE' \int_{4\pi} d\hat{\lambda}' \sigma_s(\rho, z, \hat{\lambda} \rightarrow \hat{\lambda}, E' \rightarrow E) \Phi(\rho, z, \hat{\lambda}', E') \end{aligned} \quad (1.2)$$

where

$\rho$  = the distance in the radial spatial direction

$z$  = the distance in the axial spatial direction

$\mu$  = direction cosine with respect to the z-axis

$\chi$  = azimuthal angle describing particle direction

Figure 1 describes the coordinate relation between  $\rho, z, \mu, \chi$ .

In Eq. (1.2) the energy dependence of the angular particle fluence is represented as a continuous function. In practice the energy variable is divided into a number of finite, discrete energy groups. This discretization of the energy variable is known as the multigroup method (Ref. 1) and is used to derive the set of multigroup transport equations by integrating Eq. (1.2) over each discrete energy group. Applying the multigroup method to Eq. (1.2) yields

$$\begin{aligned} & \frac{\sqrt{1-\mu^2} \cos(\chi)}{\rho} \frac{\partial(\rho \Phi_g^g(\rho, z, \hat{n}))}{\partial \rho} - \frac{1}{\rho} \frac{\partial(\sin(\chi) \sqrt{1-\mu^2} \Phi_g^g(\rho, z, \hat{n}))}{\partial \chi} \\ & + \mu \frac{\partial \Phi_g^g(\rho, z, \hat{n})}{\partial z} + \sigma_T^g(\rho, z) \Phi_g^g(\rho, z, \hat{n}) = \\ & S^g(\rho, z, \hat{n}) + \sum_{g'=1}^G \int_{4\pi} d\hat{n}' \sigma_s^{g' \rightarrow g}(\rho, z, \hat{n}' \rightarrow \hat{n}) \Phi_g^g(\rho, z, \hat{n}') \end{aligned} \quad (1.3)$$

where

$g$  = the energy group designator,  $g=1$  being highest energy group

$G$  = total number of energy groups

$\Phi_g^g(\rho, z, \hat{n})$  = the angular particle fluence for energy group  $g$ , and

$\sigma_s^{g' \rightarrow g}(\rho, z, \hat{n}' \rightarrow \hat{n})$  = the macroscopic differential scattering cross section at position  $(\rho, z)$  for a particle of direction  $(\mu', \chi')$  in energy group  $g'$  scattering to a direction  $(\mu, \chi)$  and to energy group  $g$ .

To complete the specification of this analytical problem, boundary conditions must be assigned to Eq. (1.3). One boundary condition often used is referred to as a vacuum boundary condition and is represented as

$\Omega$  = PARTICLE DIRECTION

$\mu = \cos \phi$

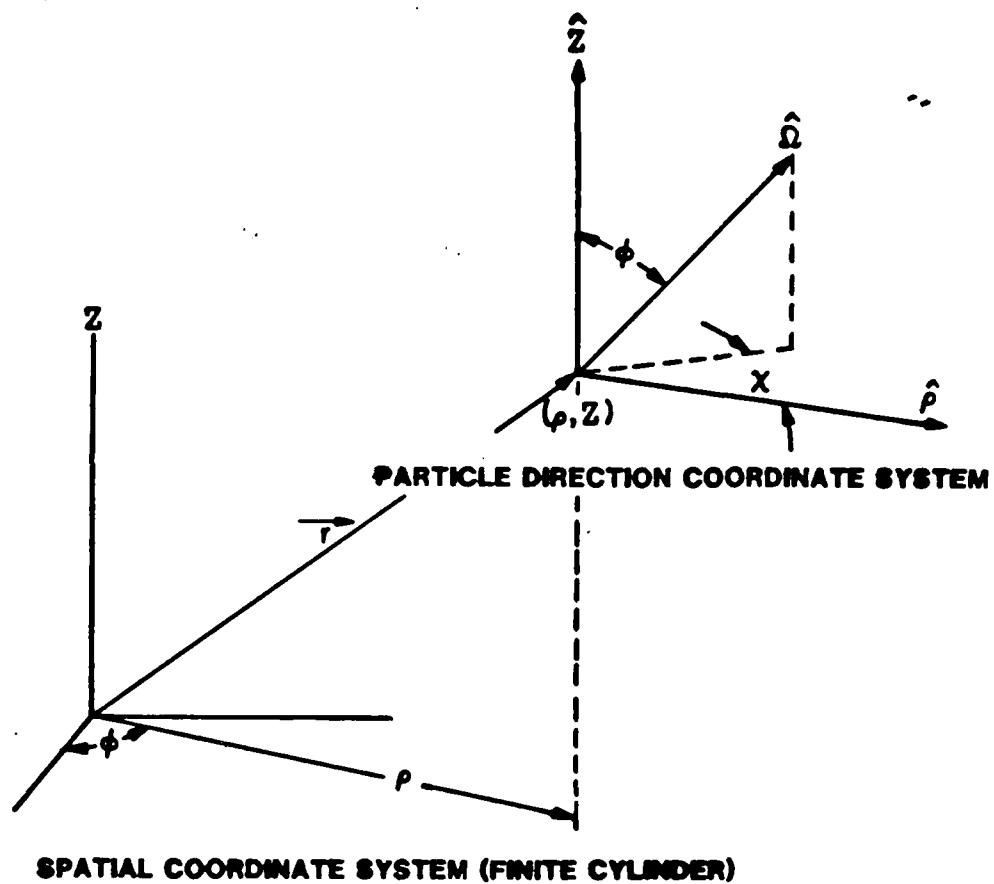


Fig 1. Coordinate Systems Used In Neutral Particle Transport Problems For 2-D Cylindrical Geometry

$$\Phi^g(\vec{r}_s, \hat{n}) = 0, \quad \hat{n} \cdot \hat{n} < 0 \quad (1.4)$$

where

$\vec{r}_s$  = the position vector representing a spatial location on an exterior surface

$\hat{n}$  = a unit vector normal to the exterior surface located at  $\vec{r}_s$

The second boundary condition is applied along the axis of the cylinder at  $\rho=0$  and is referred to as the symmetry or reflective boundary condition. This boundary condition can be written as

$$\Phi^g(0, z, \hat{n}) = \Phi^g(0, z, \hat{n}') \quad (1.5)$$

where  $\hat{n}'$  is defined by  $\hat{n} \cdot \hat{n}' = -\hat{n} \cdot \hat{n}$ , and  $(\hat{n} \times \hat{n}') \cdot \hat{n} = 0$ .

A nuclear burst is represented as an isotropic point source in the atmosphere. In the cylindrical air-over-ground geometry the isotropic point source is located along the axis of the cylinder ( $\rho=0$ ) at the desired burst altitude ( $z_B$ ). Mathematically this point source can be represented as

$$\frac{S_o^g \delta(z-z_B) \delta(\rho)}{4\pi} \quad (1.6)$$

where

$S_o^g$  = isotropic source in group g

$\delta(z-z_B) \delta(\rho)$  = Dirac delta function

During the course of this dissertation it became necessary to define another source term known as the first-scatter source. This source can be expressed as

$$\frac{S_o^g \sigma_s^{g \rightarrow g}(\rho, z, \hat{n}_o \rightarrow \hat{n}_s) e^{-\lambda}}{4\pi |\vec{r} - \vec{r}_s|^2} \quad (1.7)$$

where

$\vec{r}_s$  = position vector of the nuclear burst

$\vec{r}$  = position vector in spatial domain

$\hat{\lambda}_0$  = direction vector aligned with the  $\vec{r} - \vec{r}_s$  vector at the spatial position  $\vec{r}$ .

$$\lambda = \int_0^{|\vec{r} - \vec{r}_s|} \sigma_T^g(\vec{r}_s + s\hat{\lambda}_0) ds \quad \text{along the ray defined by } \hat{\lambda}_0 = \frac{\vec{r} - \vec{r}_s}{|\vec{r} - \vec{r}_s|}$$

See Fig. 2 for a clarification of the above definitions. The reason for using the first-scatter source will be explained in latter chapters.

Combining the previously derived results leads to the following form of the Boltzmann transport equation:

$$\begin{aligned} & \frac{\sqrt{1-\mu^2} \cos(\chi)}{e} \frac{\partial(e \Phi^g(e, z, \hat{\lambda}))}{\partial e} - \frac{1}{e} \frac{\partial(\sin(\chi) \sqrt{1-\mu^2} \Phi^g(e, z, \hat{\lambda}))}{\partial \chi} \\ & + \mu \frac{\partial \Phi^g(e, z, \hat{\lambda})}{\partial z} + \sigma_T^g(e, z) \Phi^g(e, z, \hat{\lambda}) = \\ & \frac{S_0^g \sigma_s^g(\vec{r}_s, z, \hat{\lambda}_0 \rightarrow \hat{\lambda}) e^{-\lambda}}{4\pi |\vec{r} - \vec{r}_s|^2} + \sum_{g'=1}^g \int_0^{2\pi} d\chi' \int_1^1 d\mu' \sigma_s^{g'g}(\vec{r}_s, z, \hat{\lambda}' \rightarrow \hat{\lambda}) \Phi^g(e, z, \hat{\lambda}') \end{aligned} \quad (1.8)$$

The sum over energy groups has been terminated at g because scatter occurs only from higher to equal or lower energies.

The most common techniques used to solve the Boltzmann equation for the air-over-ground problem are Monte Carlo, discrete ordinates, and Mass Integral Scaling (MIS). Each method is deficient in some respect. Monte Carlo demands a substantial amount of computational time due to its statistical nature (Ref. 3). Discrete ordinates (Refs. 4 and 5) is susceptible to a computational anomaly called the ray effect. All attempts to eliminate or mitigate this computation anomaly in the discrete ordinates method have resulted in a substantial increase in computational time (Refs. 6-12). MIS (Refs. 13-15) cannot provide accurate results

$\hat{\Omega}_D$  = STREAMING DIRECTION AT  $(\rho, Z)$   
 $\hat{\Omega}$  = PARTICLE DIRECTION  
 $\mu = \cos \phi$

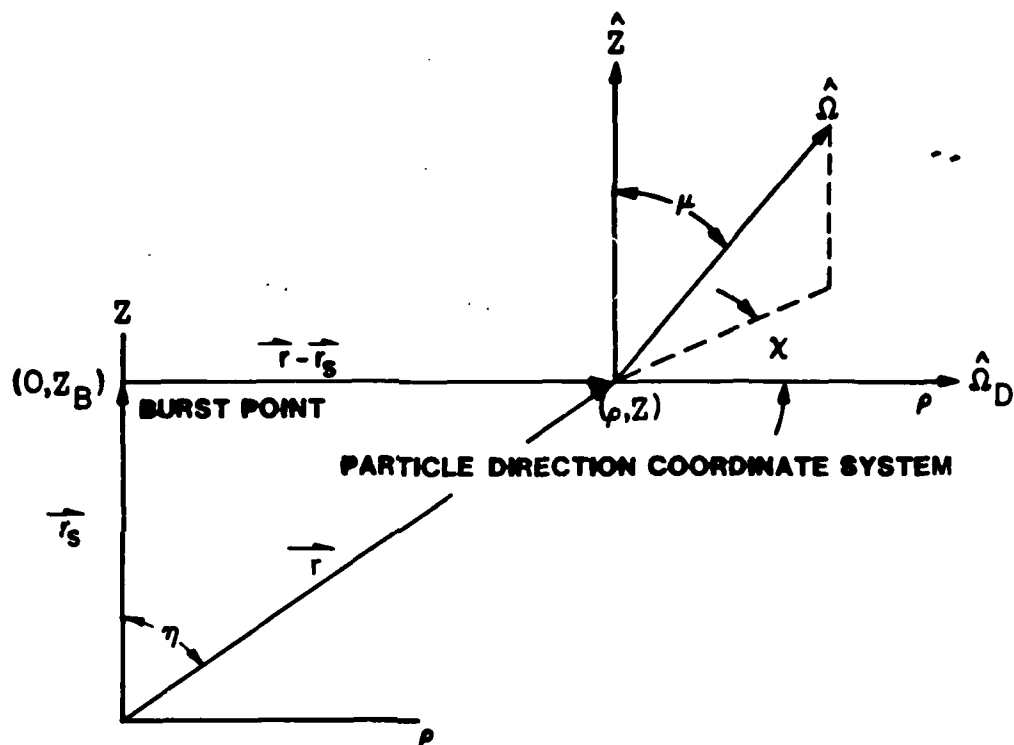


Fig 2. First Scatter Source Coordinate System Definition

near the air-ground interface at slant ranges less than 1000 feet. The deficiencies exhibited by these commonly used solution techniques motivated several new approaches for solving transport problems.

### Even-Parity Equation and Space Angle Synthesis

In 1961 Vladimirov (Ref. 16) derived a self-adjoint form of the Boltzmann transport equation known as the second-order even-parity fluence form (EPFBE). The monoenergetic form of this equation can be represented as

$$-\hat{\lambda} \cdot \nabla K_{\mu} \hat{\lambda} \cdot \nabla \Psi(\vec{r}, \hat{\lambda}) + G_g \Psi(\vec{r}, \hat{\lambda}) = -\hat{\lambda} \cdot \nabla K_{\mu} S_{\mu}(\vec{r}, \hat{\lambda}) + S_g(\vec{r}, \hat{\lambda}) \quad (1.9)$$

where all previous definitions apply and the following are presented

$$\Psi = \frac{1}{2} (\Phi(\vec{r}, \hat{\lambda}) + \Phi(\vec{r}, -\hat{\lambda})) \quad (\text{even-parity fluence}) \quad (1.10)$$

$$S_{\mu} = \frac{1}{2} (S(\vec{r}, \hat{\lambda}) - S(\vec{r}, -\hat{\lambda})) \quad (\text{odd-parity source}) \quad (1.11)$$

$$S_g = \frac{1}{2} (S(\vec{r}, \hat{\lambda}) + S(\vec{r}, -\hat{\lambda})) \quad (\text{even-parity source}) \quad (1.12)$$

The two operators  $K_{\mu}$  and  $G_g$  are positive definite and self-adjoint (Ref. 17) and can be represented as

$$K_{\mu} f(\hat{\lambda}) = \frac{1}{\sigma_T(\vec{r})} \left( f(\hat{\lambda}) + \int_{4\pi} \sigma_{K\mu}(\vec{r}, \hat{\lambda}; \hat{\lambda}') f(\hat{\lambda}') d\hat{\lambda}' \right) \quad (1.13)$$

$$G_g f(\hat{\lambda}) = \sigma_T(\vec{r}) f(\hat{\lambda}) - \int_{4\pi} \sigma_{Sg}(\vec{r}, \hat{\lambda}; \hat{\lambda}') f(\hat{\lambda}') d\hat{\lambda}' \quad (1.14)$$

where

$$\sigma_{K\mu}(\vec{r}, \hat{\lambda}; \hat{\lambda}') = \sum_{l=\text{odd}}^{\infty} \frac{\sigma_l^{\mu}(\vec{r})}{\sigma_T(\vec{r}) - \sigma_l^{\mu}(\vec{r})} P_l(\hat{\lambda} \cdot \hat{\lambda}') \quad (1.15)$$

$\sigma_l^{\mu}(\vec{r})$  = odd Legendre coefficients

$P_l(\hat{\lambda} \cdot \hat{\lambda}')$  =  $l$ th order Legendre polynomial

$$\sigma_{sg}(\vec{r}, \hat{\lambda}, \hat{\lambda}) = \frac{1}{2} (\sigma_s(\vec{r}, \hat{\lambda}, \hat{\lambda}) + \sigma_s(\vec{r}, \hat{\lambda}, -\hat{\lambda})) \quad (1.16)$$

(even-parity differential scattering cross section)

The vacuum boundary condition becomes

$$\Psi(\vec{r}, \hat{\lambda}) + K_\mu (\vec{S}_\mu(\vec{r}, \hat{\lambda}) - \hat{\lambda} \cdot \nabla \Psi(\vec{r}, \hat{\lambda})) = 0$$

for  $\vec{r}$  on the vacuum surface and  $\hat{\lambda} \cdot \vec{n} < 0$

For the reflective boundary condition

$$\Psi(\vec{r}, \hat{\lambda}) = \Psi(\vec{r}, \hat{\lambda}')$$

where  $\vec{r}$  is on the reflective boundary and  $\hat{\lambda}'$  is defined by  $\hat{\lambda} \cdot \hat{\lambda}' = \pm \hat{\lambda} \cdot \hat{\lambda}$  and  $(\hat{\lambda} \times \hat{\lambda}') \cdot \hat{n} = 0$ . The derivation of Eq. (1.9), Eq. (1.13) and the boundary condition is presented in Appendices A and B respectively.

In conjunction with this self-adjoint form, a functional was derived whose Euler equation is the even-parity fluence equation (Ref. 17). Kaplan and Davis (Ref. 18) used this functional to solve a simple monoenergetic Milne problem with isotropic scatter. They derived a coupled set of differential equations that represented the Euler equations of the functional for the various regions of the spatial domain. This set of equations was solved by finite difference methods. The angular dependence of the neutron distribution in their problem was represented by trial functions obtained from an intuitive knowledge of the true solution. The use of such predetermined functions is known as flux synthesis (Refs. 19-22) and provides a method of introducing a priori knowledge of the particle distribution into the trial solution. This a priori knowledge may come from experience, subsidiary calculations, or intuition.

Further success of the flux synthesis technique was achieved by Roberds and Bridgman (Ref. 23) who applied the flux synthesis method to an air-over-ground problem using a weighted residual formulation of the Boltzmann transport equation. Their results were within ten percent of those generated by discrete ordinates and reduced the computational time by a factor of seven. Also significant is the fact that their results had no ray effects, since the chosen synthesis functions changed the angular mesh at each spatial point and thus did not allow any specific rays to penetrate the entire spatial domain.

Miller, Lewis, and Rossow (Refs. 24 and 25) applied the even-parity fluence functional with a finite element trial solution in space and angle to solve both a one and two-dimensional monoenergetic neutron transport problem in plane geometry. In the 2-D problem isotropic sources and scattering were used. From these solutions, the authors concluded that the finite element method could produce results with a computational time savings that were comparably accurate to discrete ordinates results. Also, as in the case of synthesis functions, finite elements used with the EPFBE are not subject to ray effects. A finite element method has been incorporated into a production computer code called TRIPLET (Ref. 26). This code uses the finite element method to represent only the spatial variation of the neutron distribution in the first-order Boltzmann equation. The angular variation is represented by discrete ordinates and thus this code is subject to ray effects.

In 1974 Kaper, Leaf, and Lindeman published a study (Ref. 27) which evaluates several finite element methods for solving the multigroup

neutron transport equation using the variational form of the even-parity equation. Their final conclusions were unfavorable and lead to the recommendation that "the use of high order approximation procedures, based on finite element methods and applied to the self-adjoint form of the transport equation does not provide a viable alternative to the use of the discrete ordinates methods, applied in combination with either finite differences or finite element methods to the standard form of the transport equation."

These authors made this conclusion based on their experience in solving reactor type problems. In this problem ray effects do not occur and thus would not have influenced the quoted conclusion. In the air-over-ground problem the ray effect is predominant and the elimination of this effect from a transport solution is important. Though the EPFBE is applicable for use in both types of transport problems, its value in mitigating or eliminating the ray effect is most pronounced in an air-over-ground problem. Kaper, Leaf, and Lindeman's conclusion does not apply to transport problems that exhibit the ray effect.

In 1975 Briggs, Miller, and Lewis (Ref. 28) did an extensive theoretical study to determine the reasons behind the ray effect eliminating property of the EPFBE. Their approach was to solve the self-adjoint form of the Boltzmann equation cast in a variational formulation using three different angular representations. One angular formulation was the standard discrete ordinates treatment of the angular domain. The other two formulations incorporated either piecewise constant or piecewise bilinear finite elements as angular trial functions. Solutions obtained from these various formulations demonstrated that both finite

element angular representations eliminated ray effects, while the discrete ordinates treatment of the angular variable did not. To explain their computational results Briggs, et al, demonstrated that the operator of the self-adjoint form of the Boltzmann equation changed from a hyperbolic to an elliptic form when the finite element angular representation replaced the discrete ordinates treatment. This change was synonymous with the disappearance of the characteristic lines along the discrete ordinates directions of neutron travel and was equivalent to introducing into the streaming operators fictitious derivatives normal to these lines (Ref. 29). These derivatives result from the averaging of the transport operator over the solid angle support of the finite element basis functions. This averaging allows a coupling of angular directions not present in the discrete ordinates method and eliminates the ray effect from transport solutions.

#### Purpose of the Research

The second order even-parity form of the Boltzmann transport equation offered a sound theoretical basis for eliminating the ray effect. However, a method based on this equation is much more difficult to program than the discrete ordinates method and requires the added expense of evaluating many integrals. Previous applications of this equation had been limited to one dimensional problems with linear anisotropic scatter and two-dimensional plane geometry with only isotropic scatter. Extending the use of this equation to two-dimensional cylindrical geometry with anisotropic scatter represented a significant departure from past work. The purpose of this research was to determine the feasibility of eliminating the ray effect when solving the air-over-ground problem by using the EPFBE.

In Chapter II the Galerkin method is applied to the weak form of the EPFBE. Both a finite element and synthesis trial solution were used. The finite element trial solution was a tensor product consisting of bilinear Lagrange polynomials. The synthesis trial solution used bilinear Lagrange polynomials to represent the spatial variation of the neutron fluence and a ellipsoidal synthesis function expansion to approximate the angular dependence. The results of this chapter demonstrate that neither the Galerkin or Ritz method would provide a feasible means of solving the air-over-ground problem since the resulting integrals cannot be efficiently evaluated either numerically or analytically.

In Chapter III the collocation method is applied to the EPFBE. A trial solution consisting of cubic splines and specially derived angular synthesis functions were used. This method allowed the analytic integration of the resulting integrals, but introduced a numerical deficiency associated with the odd-parity fluence transformation. This deficiency is related to the requirement that the derivatives with respect to all phase space variables of the selected trial solution contain the necessary information to accurately represent the anisotropic portion of the Boltzmann fluence.

In Chapter IV the problems that result from applying a multigroup method to the EPFBE are outlined. These problems center on the odd-parity source term and the dependence of this term on the odd-parity fluence. The nested integrals that result are complex and their evaluation would lead to problems similar to those encountered in Chapter II.

Chapter V presents recommendations and conclusions.

## II. Weak Form Equation and Galerkin Method

### Introduction

In this chapter the weak form of the EPFBE is formulated for the air-over-ground problem using the Galerkin method. Evaluation of the integrals that result from this method is attempted using both analytical and numerical integration techniques. Trial solutions consisting of linear Lagrange polynomials in space and a specially derived synthesis function in angle are used to approximate the even-parity fluence. Different combinations of the above integration techniques and trial solutions are attempted. The results demonstrate that the Galerkin and Ritz methods introduce too much complexity to efficiently assemble a global matrix representation of the EPFBE for an air-over-ground problem. This statement applies in general to the Lagrange polynomial trial solution and specifically to the synthesis trial solution.

### Weak Form and Functional Representations

The Galerkin and Ritz methods are commonly used in the finite element method. The Galerkin method is applied to the weak form of an equation. The weak form of the EPFBE can be represented as (see Appendix C)

$$\int_V \{ \langle -\hat{n} \cdot \nabla E(\vec{r}, \hat{n}), K_\mu(\hat{n} \cdot \nabla \Psi(\vec{r}, \hat{n})) \rangle + \langle E(\vec{r}, \hat{n}), G_y \Psi(\vec{r}, \hat{n}) \rangle \} d\vec{r} = \quad (2.1)$$

$$\int_V \{ \langle E(\vec{r}, \hat{n}), K_\mu S_\mu(\vec{r}, \hat{n}) \rangle + \langle E(\vec{r}, \hat{n}), S_g(\vec{r}, \hat{n}) \rangle \} d\vec{r} - \int_{S_v} \langle E(\vec{r}, \hat{n}), \Psi(\vec{r}, \hat{n}) | \hat{n} \cdot \hat{n} | \rangle d\vec{r}$$

where  $E(\vec{r}, \hat{n})$  is referred to as a weight function.  $V$  represents the spatial domain,  $S_v$  is the part of the surface bounding the spatial domain on which the vacuum boundary condition is applied, and

$$\langle a(\vec{r}, \hat{n}), b(\vec{r}, \hat{n}) \rangle = \int_{4\pi} a(\vec{r}, \hat{n}) b(\vec{r}, \hat{n}) d\hat{n} \quad (2.2)$$

The Ritz method is applied to a functional that represents an equation.

For the EPFBE a functional representation exists and can be written as

$$F[\Psi(\vec{r}, \hat{n})] = \langle \frac{1}{\sigma_T(\vec{r})} \{ \hat{n} \cdot \nabla \Psi(\vec{r}, \hat{n}) \}^2 + \sigma_T(\vec{r}) \Psi^2(\vec{r}, \hat{n}) - \Psi(\vec{r}, \hat{n}) \int_{4\pi} \sigma_{Tg}(\vec{r}, \hat{n}; \hat{n}') \Psi(\vec{r}, \hat{n}') d\hat{n}' \rangle_{\vec{r}} \quad (2.3)$$

$$+ \{ \hat{n} \cdot \nabla \Psi(\vec{r}, \hat{n}) \} \int_{4\pi} \sigma_{\mu}(\vec{r}, \hat{n}; \hat{n}') \hat{n} \cdot \nabla \Psi(\vec{r}, \hat{n}') d\hat{n}' - 2 \Psi(\vec{r}, \hat{n}) S_g(\vec{r}, \hat{n})$$

$$- \frac{2}{\sigma_T(\vec{r})} S_{\mu}(\vec{r}, \hat{n}) \{ \hat{n} \cdot \nabla \Psi(\vec{r}, \hat{n}) \} - 2 \{ \hat{n} \cdot \nabla \Psi(\vec{r}, \hat{n}) \} \int_{4\pi} \sigma_{\mu}(\vec{r}, \hat{n}; \hat{n}') S_{\mu}(\vec{r}, \hat{n}') d\hat{n}' \rangle_{\vec{r}}$$

$$+ 2 \langle \langle \Psi^2(\vec{r}, \hat{n}) \rangle \rangle_{\vec{r}}$$

where

$$\langle a(\vec{r}, \hat{n}) \rangle_{\vec{r}} = \int_{\vec{r}} d\vec{r} \int_{4\pi} a(\vec{r}, \hat{n}) d\hat{n} \quad (2.4)$$

$$\langle \langle a(\vec{r}, \hat{n}) \rangle \rangle_{\vec{r}} = \int_{S_V} d\vec{s} \int_{\hat{n} \cdot \hat{n}' > 0} (\hat{n} \cdot \hat{n}') a(\vec{r}, \hat{n}) d\hat{n} \quad (2.5)$$

The solutions to Eqs. (2.1) and (2.3) naturally satisfy the vacuum boundary condition. The reflective boundary condition is essential for both equations and must be imposed.

If the same trial solution is used in solving the EPFBE, the Ritz and Galerkin methods generate an identical set of simultaneous algebraic equations. This occurs because the  $K_U$  and  $G_g$  operators in this equation are both positive definite and self-adjoint. The Galerkin method was selected for use in this chapter, because it represented a convenient starting point for determining the feasibility of applying the finite element method to the EPFBE.

#### Galerkin Method

The Galerkin method falls under the broader category of weighted residual methods. These methods assume that the exact solution of a differential equation is not known and must be approximated, thus introducing into the equation an error called the residual. The weighted residual method requires this residual to vanish in some average sense

over the domain of definition of the dependent variable. As an example consider a function  $\phi(\vec{x})$  defined over some domain D dependent on the variables represented by the vector  $\vec{x}$ . Let the behavior of  $\phi(\vec{x})$  in D be given by

$$L \phi(\vec{x}) = f(\vec{x}) \quad (2.6)$$

where  $f(\vec{x})$  is a known function of the same independent variables. Eq. (2.6) can be rearranged to give

$$L \phi(\vec{x}) - f(\vec{x}) = 0 \quad (2.7)$$

Since  $\phi(\vec{x})$  is not known, an approximate solution must be used. Let the approximate solution be represented by  $\tilde{\phi}(\vec{x})$ . Substituting  $\tilde{\phi}(\vec{x})$  into Eq. (2.7) yields

$$L \tilde{\phi}(\vec{x}) - f(\vec{x}) \neq 0 \quad (2.8)$$

or stated in another manner

$$L \tilde{\phi}(\vec{x}) - f(\vec{x}) = R(\vec{x}) \quad (2.9)$$

$R(\vec{x})$  is called the residual and results from the use of the approximate solution  $\tilde{\phi}(\vec{x})$ . Multiplying Eq. (2.9) by the weight function  $\epsilon(\vec{x})$  and integrating over the domain D results in

$$\int_D \{ L \tilde{\phi}(\vec{x}) - f(\vec{x}) \} \epsilon(\vec{x}) d\vec{x} = \int_D R(\vec{x}) \epsilon(\vec{x}) d\vec{x} \quad (2.10)$$

$\tilde{\phi}(\vec{x})$  is often represented by a linear combination of a linearly independent set of known functions:

$$\tilde{\phi}(\vec{x}) = \sum_{i=1}^M a_i Q_i(\vec{x}) \quad (2.11)$$

In Eq. (2.11) the  $a$ 's are the constant coefficients and the  $Q$ 's represent the known functions. Eq. (2.11) is called a trial solution. Inserting Eq (2.11) into Eq. (2.10) gives

$$\int_0 \left\{ L \sum_{i=1}^M a_i Q_i(\vec{x}) - f(\vec{x}) \right\} \epsilon(\vec{x}) d\vec{x} = \int_0 R(\vec{x}) \epsilon(\vec{x}) d\vec{x} \quad (2.12)$$

Requiring that the weighted residual vanish (Ref. 30) yields

$$\int_0 R(\vec{x}) \epsilon(\vec{x}) d\vec{x} = 0. \quad (2.13)$$

Eq. (2.13) implies that the weighted residual method determines a set of coefficients that requires the residual function to be orthogonal to the weight function and thus forces the residual to vanish in an integral or average sense. The final form of the weighted residual method is

$$\int_0 \left\{ L \sum_{i=1}^M a_i Q_i(\vec{x}) - f(\vec{x}) \right\} \epsilon(\vec{x}) d\vec{x} = 0$$

If the weight function is allowed to be any linear combination of the same known function as the trial solution, i.e.

$$\epsilon(\vec{x}) = \sum_{j=1}^M b_j Q_j(\vec{x}) \quad (2.14)$$

then the Galerkin method is defined and requires

$$\int_0 \left\{ L \sum_{i=1}^M a_i Q_i(\vec{x}) - f(\vec{x}) \right\} Q_j(\vec{x}) d\vec{x} = 0, j = 1, 2, \dots, M \quad (2.15)$$

Transport problems are normally of such complexity that an analytical solution is not possible. These problems necessitate the use of a trial solution that describes both the spatial and angular variation of the neutron fluence. Such a trial solution for the even-parity fluence can be presented as

$$\psi(\vec{r}, \hat{\lambda}) = \sum_{i=1}^N \sum_{j=1}^M a_{ij} S_i(\vec{r}) A_j(\hat{\lambda}) \quad (2.16)$$

where  $S_i(\vec{r})$  represents a known function to approximate the spatial variation and  $A_j(\hat{\lambda})$  plays a similar role for the angular dependence. If the Galerkin method is used with the trial solution in Eq. (2.16), then the proper form of the weight function is

$$\varepsilon(\vec{r}, \hat{\lambda}) = \sum_{k=1}^N \sum_{L=1}^M b_{kL} S_k(\vec{r}) A_L(\hat{\lambda}) \quad (2.17)$$

Substituting Eqs. (2.16) and (2.17) into the weak form of the EPFBE, Eq. (2.1), yields

$$\begin{aligned} & \sum_{i=1}^N \sum_{j=1}^M a_{ij} \left\{ \int_V \left( \langle -\hat{\lambda} \cdot \nabla S_k(\vec{r}) A_L(\hat{\lambda}), K_{\mu} \hat{\lambda} \cdot \nabla S_i(\vec{r}) A_j(\hat{\lambda}) \rangle + \right. \right. \\ & \quad \left. \left. \langle S_k(\vec{r}) A_L(\hat{\lambda}), G_g S_i(\vec{r}) A_j(\hat{\lambda}) \rangle \right) d\vec{r} + \int_{S_V} \langle S_k(\vec{r}) A_L(\hat{\lambda}), S_i(\vec{r}) A_j(\hat{\lambda}) | \hat{\lambda} \cdot \hat{n} \rangle d\vec{s} \right\} \\ & = \int_V \left\{ S_k(\vec{r}) A_L(\hat{\lambda}), K_{\mu} S_{\mu}(\vec{r}, \hat{\lambda}) \rangle + \langle S_k(\vec{r}) A_L(\hat{\lambda}), S_g(\vec{r}, \hat{\lambda}) \rangle \right\} d\vec{r} \\ & \quad \text{for } k = 1, 2, \dots, N \\ & \quad \text{for } L = 1, 2, \dots, M \end{aligned} \quad (2.18)$$

Eq. (2.18) is referred to as the Galerkin weak form equation throughout the remainder of this dissertation.

#### Numerical Integration

The trial solution initially used with Eq. (2.18) consisted of piecewise bilinear Lagrange polynomials to approximate both the spatial and angular variation of the fluence. These polynomials have only  $C_0$  continuity (continuity of the function only). This degree of continuity is all that is required since the highest derivative in the Galerkin

weak form equation equals one (Ref 31). In any given element, the form of these polynomials is given by

$$L_i(x,y) = a_i x y + b_i x + c_i y + d_i \quad (2.19)$$

where the  $i$  subscript refers to a particular node in the discretized domain consisting of rectangular elements. Since four nodal degrees of freedom exist in each rectangular element, the coefficients in Eq. (2.19) can be determined. These coefficients satisfy the requirements that at one node  $L_i(x,y)$  equals one and at the other three the polynomial is zero. These constraints lead to the classic tent function illustrated in Fig. 3. The same procedure is followed in determining the other tent functions for the remaining nodes in the rectangular element and also the remaining elements in the mesh. This procedure is given in more detail in Appendix D.

The Lagrange polynomials representing the spatial and angular variation of the fluence are combined using a tensor product. In this tensor product, the spatial and angular dependence of the fluence is assumed separable in a manner similar to the  $P_n$  method (Ref. 1). Using the Galerkin method with this bilinear Lagrange polynomial tensor product trial solution, one defines the following representations for the even-parity fluence and weight function respectively:

$$\Psi(\vec{r}, \hat{n}) = \sum_{i=1}^M \sum_{j=1}^N a_{ij} L_i(\vec{r}) L_j(\hat{n}) \quad (2.20)$$

$$\mathcal{E}(\vec{r}, \hat{n}) = \sum_{k=1}^M \sum_{l=1}^N b_{kl} L_k(\vec{r}) L_l(\hat{n}) \quad (2.21)$$

where  $M$  represents the total number of spatial nodes and  $N$  the number of angular nodes.

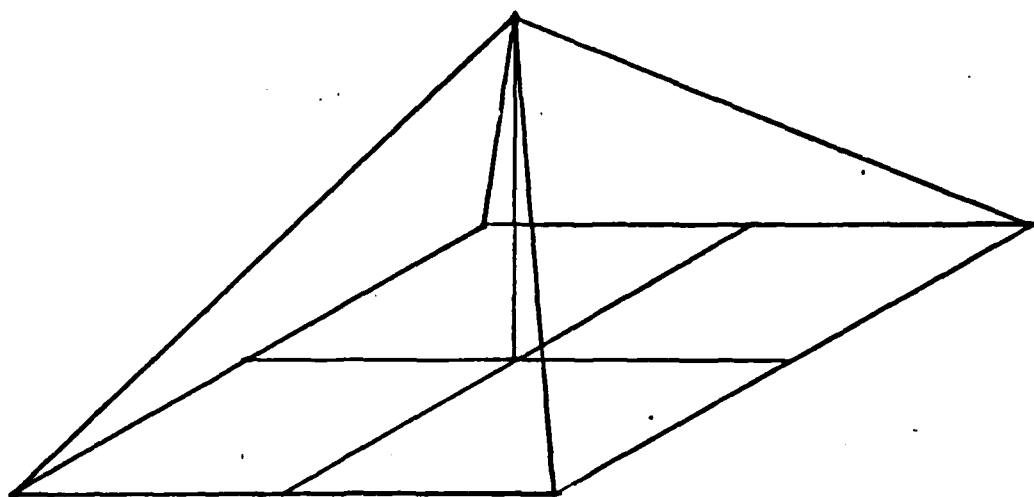


Fig 3. Tent Function Defined Over Four Rectangular Elements

The trial solution presented in Eq. (2.20) was used (Ref. 26) to find the solution of a monoenergetic transport problem involving two-dimensional plane geometry and isotropic scatter. The success of this application depended in part on the simplicity that the isotropic scatter assumption introduced. Scattering from one angular direction to another is represented in the first order Boltzmann equation by the differential scattering cross section  $\sigma_s(\vec{r}, \hat{\lambda}' \rightarrow \hat{\lambda})$  for scattering from  $\hat{\lambda}'$  to  $\hat{\lambda}$ . The differential scattering cross section is normally approximated by an expansion in terms of Legendre polynomials, i.e.

$$\sigma_s(\vec{r}, \hat{\lambda}' \rightarrow \hat{\lambda}) = \sum_{\ell=0}^P \sigma_{s\ell} P_{\ell}(\hat{\lambda}' \rightarrow \hat{\lambda}) \quad (2.22)$$

where  $P_{\ell}$  is the  $\ell^{\text{th}}$  order Legendre polynomial,  $\sigma_{s\ell}$  is a spatially dependent coefficient, and  $P$  represents the order of the approximation. In the case of isotropic media the  $\hat{\lambda}' \rightarrow \hat{\lambda}$  variable is replaced with  $\mu_{\phi}$  which represents the cosine of the angle between  $\hat{\lambda}'$  and  $\hat{\lambda}$  and is expressed as

$$\mu_{\phi} = \mu \mu' + \sqrt{1 - \mu^2} \sqrt{1 - \mu'^2} \cos(\chi - \chi') \quad (2.23)$$

For the EPFBE the definition presented in Eq. (1.15) and (1.16) leads to

$$\sigma_{sg}(\vec{r}, \mu_{\phi}) = \sum_{\ell=\text{even}}^P \sigma_{s\ell}(\vec{r}) P_{\ell}(\mu_{\phi}) \quad (2.24)$$

$$\sigma_{km}(\vec{r}, \mu_{\phi}) = \sum_{\ell=\text{odd}}^P \frac{\sigma_{s\ell}(\vec{r})}{\sigma_t(\vec{r}) - \sigma_{s\ell}(\vec{r})} P_{\ell}(\mu_{\phi}) \quad (2.25)$$

The assumption of isotropic scattering reduces the complexity of Eq. (2.24) and (2.25) to

$$\sigma_{sg}(\vec{r}, \mu_{\phi}) = \sigma_{s\phi}(\vec{r}) \quad (2.26)$$

$$\sigma_{\mu\mu}(\vec{r}, \mu_\phi) = 0 \quad (2.27)$$

In an air-over-ground problem, the differential scattering cross section is expressed as a third order Legendre expansion (P=3). The introduction of anisotropic scattering significantly complicates Eq. (2.18) and the process of reducing this equation to a matrix form. The complication that occurs in the  $G_g$  and  $K_u$  operators can be seen by comparing the isotropic scattering case with an anisotropic representation. Combining the definition of these operators presented in Eqs. (1.13) and (1.14) with the isotropic scatter results of Eqs. (2.26) and (2.27), leads to the following representation of these operators in Eq. (2.1):

$$G_g \Psi(\vec{r}, \hat{\lambda}) = \sigma_T(\vec{r}) \Psi(\vec{r}, \hat{\lambda}) - \sigma_{s4}(\vec{r}) \int_{4\pi} \Psi(\vec{r}, \hat{\lambda}') d\hat{\lambda}' \quad (2.28)$$

$$K_\mu \hat{\lambda} \cdot \nabla \Psi(\vec{r}, \hat{\lambda}) = \frac{1}{\sigma_T(\vec{r})} \{ \hat{\lambda} \cdot \nabla \Psi(\vec{r}, \hat{\lambda}) \} \quad (2.29)$$

Eqs. (2.28) and (2.29) demonstrate two simplifications that result from the isotropic scatter assumption. The first is the absence of the integral term in the  $K_u$  operators, since  $\sigma_{\mu\mu}(\vec{r}, \mu_\phi) = 0$ . The second is the simple form of the integral in the  $G_g$  term that results from the  $P_0$  Legendre polynomial equaling one. Using the trial solution of Eq. (2.20), this global integral becomes an evaluation of the bilinear Lagrange polynomials over the angular domain. Since these polynomials are identically defined over each angular element, the integral can be evaluated using the results of a single canonical element evaluation. The value of this integral for any angular element can be found by simply multiplying the area of the angular element by the canonical result. (See Appendix E for more detail.) If a more precise value is necessary, only the single

canonical evaluation must be repeated. This simple procedure is possible due to the definition of this integral.

The integrals resulting from both the  $G_g$  and  $K_u$  operators couple all scattering directions in the angular domain and thus must be evaluated over all angular finite elements. This global definition is contrary to the other integrals resulting from the definition of the weak form equation. These integrals are defined locally over a single spatial and angular finite element and during the assembly of the global matrix are evaluated over a single element at a time. The difference between a local and global definition can be clarified by examining the term in Eq (2.1) that contains the  $G_g$  operator.

$$\int_{\vec{r}} \int_{4\pi} E(\vec{r}, \hat{n}) \left\{ \sigma_T(\vec{r}) \Psi(\vec{r}, \hat{n}) - \int_{4\pi} \sigma_{sg}(\vec{r}, \mu_0) \Psi(\vec{r}, \hat{n}') d\hat{n}' \right\} d\vec{r} \quad (2.30)$$

To determine the value of one element in the global matrix, the two outer integrals of Eq. (2.30) are evaluated over a few spatial and angular finite elements. For the same single value the inner integral must be evaluated over the entire angular domain. Since the neutron fluence is highly anisotropic near the source in an air-over-ground problem the angular domain requires a refined discretization to accurately approximate this type of distribution. Thus evaluating the global integrals resulting from the  $K_u$  and  $G_g$  operator could be quite costly, if the definition of the integrand prohibited the effective use of canonical integration. Such is the case, when an anisotropic scattering process is used.

The  $G_g$  and  $K_u$  operators take within Eq. (2.1) the following forms in the anisotropic case:

$$G_g \Psi(\vec{r}, \hat{n}) = \sigma_T(\vec{r}) \Psi(\vec{r}, \hat{n}) - \int_{4\pi} \sigma_{sg}(\vec{r}, \hat{n}, \hat{n}') \Psi(\vec{r}, \hat{n}') d\hat{n}' \quad (2.31)$$

$$K_{\mu} \hat{n} \cdot \nabla \Psi(\vec{r}, \hat{n}) = \frac{1}{\sigma_T(\vec{r})} \left( \hat{n} \cdot \nabla \Psi(\vec{r}, \hat{n}) + \int_{4\pi} \sigma_{SM}(\vec{r}, \hat{n}, \hat{n}') \hat{n}' \cdot \nabla \Psi(\vec{r}, \hat{n}') d\hat{n}' \right) \quad (2.32)$$

The degree by which these forms deviate from the isotropic case depends on the order of the even and odd-parity differential scattering cross sections. To illustrate the complications introduced by anisotropic scattering in these terms, assume a first order scattering representation involving the  $P_0$  and  $P_1$  terms of the Legendre expansion. This order of scattering approximation does not alter the definition of the  $G_g$  term presented in Eq. (2.28), but does add the integral term to the  $K_u$  operator, i.e.

$$K_{\mu} \hat{n} \cdot \nabla \Psi(\vec{r}, \hat{n}) = \frac{1}{\sigma_T(\vec{r})} \left( \hat{n} \cdot \nabla \Psi(\vec{r}, \hat{n}) + \sigma_{s1}(\vec{r}) \int_{4\pi} P_1(\mu_{\phi}) \hat{n}' \cdot \nabla \Psi(\vec{r}, \hat{n}') d\hat{n}' \right) \quad (2.33)$$

Substituting the definition of  $\mu_{\phi}$  into Eq. (2.33) results in the following formulation for the global integral term.

$$I(\vec{r}, \hat{n}) = \sigma_{s1}(\vec{r}) \left( \int_{\mu} \int_{x'} \mu' \hat{n}' \cdot \nabla \Psi(\vec{r}, \hat{n}') dx' d\mu' + \sqrt{1-\mu^2} \int_{\mu} \int_{x'} \sqrt{1-\mu'^2} \cos(x-x') \hat{n}' \cdot \nabla \Psi(\vec{r}, \hat{n}') dx' d\mu' \right) \quad (2.34)$$

The two integrals in Eq. (2.34) are considerably more complex than those resulting from the  $G_g$  operator due to the presence of the gradient term. The increased complexity of these integrands affect the order of quadrature needed to accurately evaluate them and thus the computational time required. Another significant deviation from the isotropic case is the presence of  $\sqrt{1-\mu^2}$  and  $\cos(x-x')$  within these integrands. These functions cause the integrand to be defined differently in each angular finite element, thus altering the basic premise that allowed the efficient evaluation of the integral in the isotropic case. The presence of these functions in the integrand now force the global integral to be evaluated over each angular finite element, rather than a single canonical element.

Since this global evaluation must be repeated for each angular quadrature point, the expense of forming a global matrix representing the Galerkin weak form equation is greatly increased.

The problems demonstrated with a  $P_1$  anisotropic scattering representation for the  $K_u$  operator become more severe with a  $P_3$  representation and spread to the global integral term of the  $G_g$  operator. This  $G_g$  operator is affected by the  $P_2$  term of the Legendre expansion that introduces  $\sqrt{1-\mu'^2}$  and  $\cos(x-x')$  to the integrand of this integral. The Legendre expansion of the angular scattering significantly increases the complexity of an anisotropic scattering problem compared to an isotropic scattering problem. This complexity is primarily concentrated in the global integrals resulting from the  $G_g$  and  $K_u$  operators.

A modified computer code (Ref. 32) was used to determine the exact effect anisotropic scattering had on computer execution time and accuracy. This code assembled the global matrix resulting from the Galerkin weak form equation Eq. (2.18) using a bilinear Lagrange tensor product trial solution. The evaluation of all integrals resulting from this equation was performed during assembly using numerical integration. This integration was carried out over a canonical representation of the spatial and angular elements. A flow diagram of this code appears in Appendix H.

The problem selected to examine the effect of anisotropic scattering was a simple air burst problem. The spatial domain consisted only of air and was discretized into a single rectangular finite element extending from 0 to 100 meters in both the  $\phi$  and  $z$  directions. The angular domain was zoned into a single rectangular finite element with the  $u$  variable extending from 0 to 1 and  $x$  from 0 to  $\pi$ . The symmetry of the even-parity

fluence allowed this reduced angular domain. All cross sections were taken from the first energy group of the DLC-31 set generated by the Radiation Shielding Information Center, Oak Ridge, Tennessee (Ref. 34). The vacuum boundary condition was satisfied naturally on three boundaries and the reflective boundary condition was enforced on the cylinder axis. The global matrix resulting from the definition of this problem was  $16 \times 16$ .

Four problems were run on the CDC-6600 computer using this code. These problems differed only in the order of the scattering approximation and quadrature set used. The effect of increasing the order of the scattering representation was measured by two parameters. One parameter was the computational time required to compute and assemble a global matrix. The second parameter was concerned with the sign of the eigenvalues related to this matrix. The sign of all eigenvalues of a global matrix from the Galerkin weak form equation should be positive. This results from the positive definiteness of the  $K_u$  and  $G_g$  operators used in this equation. A negative eigenvalue would indicate that the elements contained within a global matrix were inaccurately computed. Since all computations in the Galerkin weak form equation center around the evaluation of integrals, this would indicate that the order of the quadrature set used was inadequate and would need to be increased. Increasing the order of the quadrature would increase the computational time required to assemble a global matrix. Thus, it can be seen that the two evaluation parameters are related and together indicate the relative efficiency of assembling an accurate global matrix representation of the Galerkin weak form equation.

The results of the four sample problems are presented in Fig. 4 and substantiate the analysis previously presented. Problem one is analogous to the analysis that used an isotropic scattering representation. Here a simple two point Gaussian quadrature set was adequate to generate an accurate global matrix. Problem two and three demonstrated the increasing complexity that occurred as the order of the scatter approximation increased. For both problems a two point Gaussian quadrature set was used. The increased complexity was reflected in the number of negative eigenvalues associated with the respective global matrices. Problem four was an attempt to increase the order of the quadrature set for a P=1 scattering approximation. This problem demonstrated that changing the order of the quadrature set substantially increased the computational time required to generate a global matrix. This occurred because of the six nested integrals that are contained in the Galerkin weak form equation. If Eq. (2.33) is substituted into the first term of Eq. (2.1) the following would result

$$\int_{\rho} \int_{\mu} \int_{\mathbf{z}} \int_{\mathbf{x}} \hat{\mathbf{n}} \cdot \nabla \epsilon(\hat{\mathbf{r}}, \hat{\mathbf{n}}) \left\{ \frac{1}{\sigma_r(\hat{\mathbf{r}})} (\hat{\mathbf{n}} \cdot \nabla \psi(\hat{\mathbf{r}}, \hat{\mathbf{n}}) + I(\hat{\mathbf{r}}, \hat{\mathbf{n}})) \right\} d\mathbf{x} d\mathbf{z} d\mu d\rho \quad (2.35)$$

Eq. (2.35) clearly illustrates these nested integrals. Evaluating these integrals requires  $Q^6$  evaluations per matrix element, where  $Q$  represents the number of quadrature points for each variable. For a two point quadrature set 64 evaluations are needed per matrix element and four quadrature points would require 4096 evaluations per element. Considering the 256 elements in the matrix the substantial increase in computational time is not surprising.

The numerical integration procedure used in the computer code that generated the results presented in Fig. 4 was not efficient. An analysis

Problem Number	Order of Scatter Approximation ( $P_s$ )	Number of Quadrature Pts/ Independent Variable	Number of Positive Eigenvalues	Number of Negative Eigenvalues	Computational Time (Sec)
1	0	2	16	0	38
2	1	2	10	6	41
3	3	2	9	7	45
4	1	4	---	---	>180

Fig 4. Results Using Galerkin Weak Form Equation

of the second term in Eq. (2.35) demonstrated it could be separated into 9 spatial and 27 angular integrals. The evaluation of these integrals using a four point quadrature set would require 576 evaluations per matrix element. Though the 576 evaluations represented a significant reduction from the 4096 previously required, it still was not enough reduction to support the use of numerical integration.

Certain requirements of the air-over-ground problem oppose the cost efficient implementation of a finite element solution technique using numerical integration. This transport problem requires the use of a third order Legendre expansion to approximate the scattering process. This expansion used in the weak form of the EPFBE would significantly increase the complexity of the resulting integrals. As demonstrated in Fig. 4, complex integrals require the use of higher order quadrature sets to assure the positive definiteness of a global matrix. The air-over-ground problem also requires a very finely zoned angular and spatial domain. Such zoning intensifies the problems associated with evaluating the globally defined angular integrals and increases the number of local element integrations that must be done. Since the angular integrals resulting from the weak form of the EPFBE can not be efficiently evaluated by canonical techniques, a computational cost inefficiency results. The combined effect of high order quadrature sets and refined meshing significantly offset even substantial gains made in improving the efficiency of a numerical integration process. For this reason further work based on a finite element method using numerical integration was stopped and the use of analytical integration techniques were attempted.

The success of previous work using the EPFBE functional was based on the isotropic scattering assumption. This assumption automatically

resolved all the problems that rendered either this formulation or the weak form equation too complex for efficient numerical solution.

The numerical integration problems encountered using the Galerkin weak form equation are not unique. Strang and Fix (Ref. 33) devote an entire section in a chapter entitled "Variational Crimes" to this problem. In this section they theoretically discuss problems similar to those presented in this chapter and conclude that "it is very important to control properly the fraction of computer time spent on numerical integration." As evidenced by the sample problems, the computer time necessary to evaluate the integrals resulting from the Galerkin weak form equation has not been properly controlled.

#### Analytical Integration

A natural solution to the numerical integration problem was to attempt the analytical evaluation of the integrals associated with the Galerkin weak form equation. This method of integration would alleviate both the accuracy problem and computational time problems met in the previous section. Analytical integration would be precise and require only a single function evaluation per finite element, instead of the many evaluations required by numerical integration. The structure of the integrals resulting from this equation were known to be complicated; however, it was hoped that the MACSYMA (Ref. 34) symbolic algebraic manipulating system would provide the necessary simplification. Two different trial solutions were used in attempting this analytical integration.

The first trial solution was the tensor product consisting of bilinear Lagrange polynomials used in the previous section. The first term on the right-hand side of Eq. (2.18) was input to the MACSYMA program by defining the individual terms that composed it. As an example,

the  $\mu_4$  variable represented by Eq. (2.23) was defined in MACSYMA. Next the  $P_1$  and  $P_3$  Legendre polynomials were defined in terms of  $\mu_4$ . Using the preceding two definitions the odd-parity differential scattering cross section was constructed. The Lagrange polynomials representing both the spatial and angular variation of the neutron fluence were next defined. In the first term of the Galerkin weak form equation both the weight function and trial solution is operated upon by  $\hat{n} \cdot \nabla$ . In cylindrical geometry this operator is defined as

$$\hat{n} \cdot \nabla f(\hat{r}, \hat{n}) = \frac{\sqrt{1-\mu^2} \cos(x)}{\rho} \frac{\partial(\rho f(\hat{r}, \hat{n}))}{\partial \rho} - \frac{\sqrt{1-\mu^2}}{\rho} \left( \frac{\partial(f(\hat{r}, \hat{n}) \sin(x))}{\partial x} \right) + \mu \frac{\partial f(\hat{r}, \hat{n})}{\partial z} \quad (2.36)$$

MACSYMA was programmed to perform the operation defined in Eq. (2.36) on both the previously defined weight function and trial solution. With all the individual components defined, MACSYMA assembled the first term of the Galerkin weak form equation.

Several different techniques were attempted to perform analytical integration over the required six nested integrals. One attempt involved integrating the whole assembled term. This attempt was only successful in performing the two intermost integrations over the  $u'$  and  $x'$  variables. Further integration was impossible, since the number of terms generated by the successful integrations exceeded the memory capacity of MACSYMA. This large number of terms developed because of the indefinite integration limits and the complex nature of the trigonometric functions that result from the assembled term. The integration limits were arbitrarily set so the dimensions of the finite elements in the angular and spatial domain could be varied without repeating the work on MACSYMA. The use of these arbitrary limits always generated two terms for each integration, since an upper and lower limit evaluation was necessary. The complex trigonometric terms resulted from the product of those involved in Eq. (2.36)

and the definition of  $\mu_4$ . Integrals involving these terms required reduction techniques for evaluation. These reduction techniques always generated several additional terms. The exact number of the terms was dependent on the power of the exponent associated with the trigonometric function.

To resolve the memory capacity problem, several different MACSYMA functions that optimized the use of memory were tried. The use of these functions did not solve the memory problem thus motivating the use of a new approach.

The previous approach attempted to evaluate the entire first term of the Galerkin weak form equation, while this new approach sought to simplify the expression into a number of smaller less complex terms. To accomplish this goal a special MACSYMA function was written that automatically searched the string of simplified terms to identify those that have the same form of variable dependence. Once identified the coefficients of these terms were added together, thus reducing the total number of terms requiring evaluation. Several attempts were made to implement this approach and use this specially derived MACSYMA function. In all cases memory capacity again was exceeded during the simplification process. A careful examination of the first term of the Galerkin weak form equation demonstrates this expression can be simplified into over 29,000 distinct terms (see Appendix F). MACSYMA does not have the capacity to generate this number of terms and no successful means was found to generate only a small portion of these terms at one time.

These two approaches failed for reasons similar to those found in attempting numerical integration. Once again the complexity of the integrands contributed to the failure of using the Galerkin weak form equation.

The integral evaluation of these functions necessitated the use of reduction formulas that required the use of significant amounts of memory in MACSYMA. The nested integral problem also surfaced. In the analytical integration attempt this problem manifested itself by taxing the limited memory resources available to MACSYMA. Therefore, any means that would reduce the requirement for this memory would improve the chances of successfully using this program.

The space angle synthesis (SAS) method discussed in Chapter I offered the possibility of reducing these memory requirements. The Lagrange polynomial trial solution used in an air-over-ground problem requires sixteen distinct terms. Substituting a global synthesis function representation for the angularly dependent Lagrange polynomials would condense the form of the trial solution. This reduction would result from replacing the four terms of the bilinear Lagrange representation with a single term. The choice of synthesis functions was influenced by the work of Roberds and Bridgman (Ref. 23). These authors used an off-centered ellipsoidal function to represent the angular variation of the neutron fluence in an air-over-ground problem. The most significant feature of this ellipsoidal function was its ability to be analytically integrated in a weighted residual formulation of the first order Boltzmann equation. Additionally, the effectiveness of this function was demonstrated by accurately representing the angular variation of the neutron fluence and generating ray effect free scalar fluence solutions.

The off-centered ellipsoidal function used by Roberds and Bridgman needed modification for use in the Galerkin weak form equation. The even-parity fluence as defined in Eq. (1.10) is an even function in the angular variable. This property forces the ellipsoid to be centered.

The expression for a centered ellipsoid, symmetric about the position vector from the point source to position  $(\rho, z)$  is (see Fig. 5).

$$E(\lambda) = b \sqrt{\frac{1}{1 - (b^2 - 1) f(\mu, \chi)}} \quad (2.37)$$

where

$E(\lambda)$  is the distance from  $(\rho, z)$  to the ellipsoidal surface.

$b$  denotes the length of the minor axis,  $f(\mu, \chi)$  = the cosine of the angle between  $R$  and the axis of revolution

$$f(\mu, \chi) = \cos(\eta) \mu + \sin(\eta) \sqrt{1 - \mu^2} \cos(\chi)$$

The  $\eta$  parameter is now a function of the  $(\rho, z)$  coordinates, since it is dependent on the spatial location. This dependence is defined in the following manner:

$$\sin(\eta) = \frac{(\rho - \rho_0)}{\sqrt{(\rho - \rho_0)^2 + (z - z_0)^2}}$$

$$\cos(\eta) = \frac{(z - z_0)}{\sqrt{(\rho - \rho_0)^2 + (z - z_0)^2}}$$

where the coordinates  $(\rho_0, z_0)$  represent the spatial location of the point source of weapon radiation. In the air-over-ground problem, since the point source is on the axis of the cylinder.

The angularly dependent part of the trial solution Eq. (2.20) was modified to include these ellipsoidal synthesis functions. The trial solution chosen replaced the angularly defined bilinear Lagrange polynomials with a three term ellipsoidal expansion

$$\Psi(r, \lambda) = \sum_{i=1}^M \sum_{j=1}^3 a_{ij} S_i(r) E_j(\lambda) \quad (2.38)$$

where  $S_i(r)$  is still the spatially defined bilinear Lagrange polynomials.

The three ellipsoidal functions were chosen to represent the expected

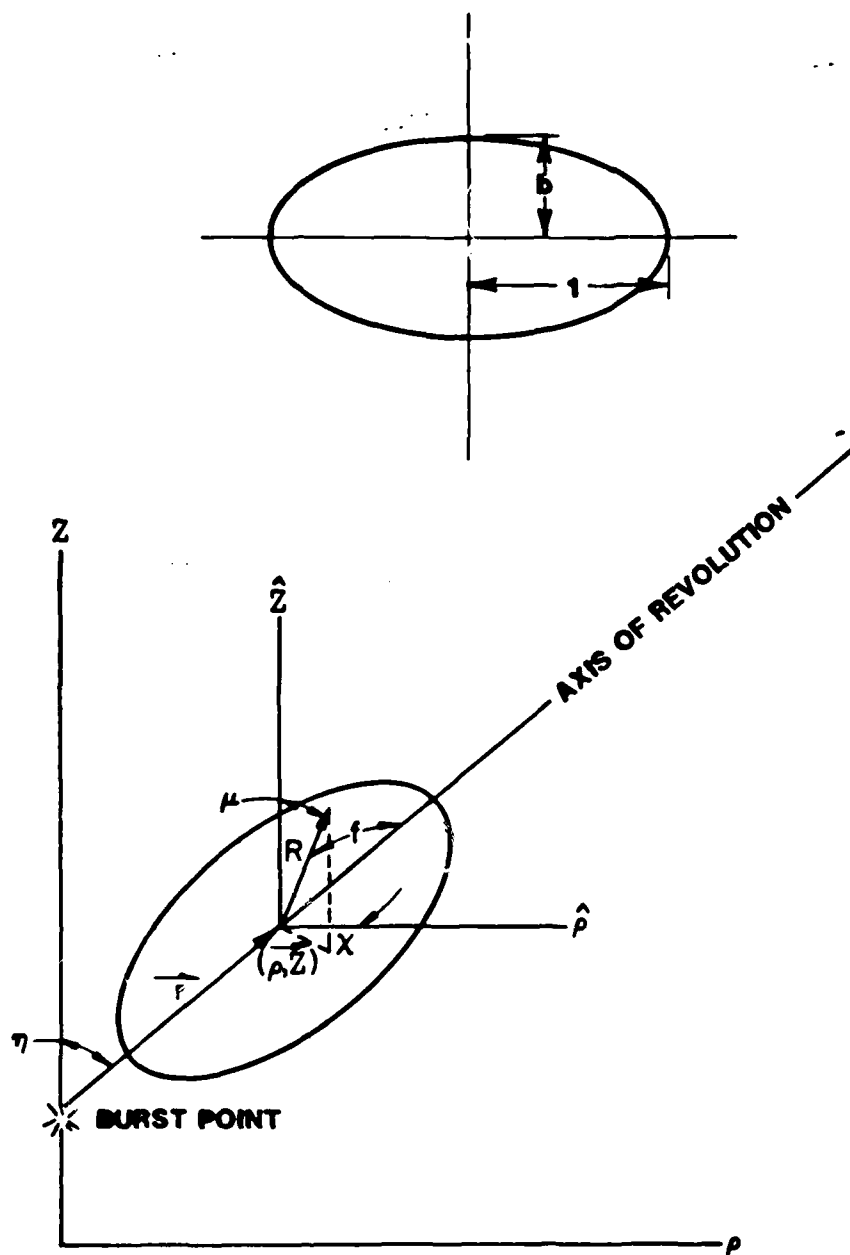


Fig 5. Ellipsoidal Synthesis Function

spectrum of angular variation that would exist for an air-over-ground problem (see Fig. 6).  $E_1(\hat{r})$  was chosen to represent the extremely anisotropic nature of the angular fluence near the point source.  $E_3(\hat{r})$  represented the isotropic nature of the angular fluence at large distances from the source.  $E_2(\hat{r})$  was chosen to act as a transitional shape between the two others. The  $b$  parameter in Eq. (2.37) determined these shapes. The mixing of these shapes is accomplished by the coefficients. The value of these coefficients is determined by solving the global matrix representing the weak form of the even-parity equation.

Analytical integration of these ellipsoidal synthesis functions in the weak form of the even-parity equation was not possible. This can be illustrated by examining the simplest term in Eq. (2.1).

$$\int_F \langle \epsilon(\hat{r}, \hat{r}), G_g \Psi(\hat{r}, \hat{r}) \rangle d\hat{r} \quad (2.39)$$

Substituting Eq. (2.38) and the proper definition of  $\epsilon(\hat{r}, \hat{r})$  for the Galerkin method results in:

$$\sum_{i=1}^M \sum_{j=1}^3 a_{ij} \int_F \langle S_k(\hat{r}) E_L(\hat{r}), G_g (S_i(\hat{r}) E_j(\hat{r})) \rangle d\hat{r} \quad (2.40)$$

for  $k = 1, \dots, M$   
 $L = 1, 2, 3$

If isotropic scatter is assumed the following angular integral would result from Eq. (2.40)

$$\int_{4\pi} E_L(\hat{r}) E_j(\hat{r}) d\hat{r} \quad (2.41)$$

By substituting Eq. (2.37) into the above, the following results:

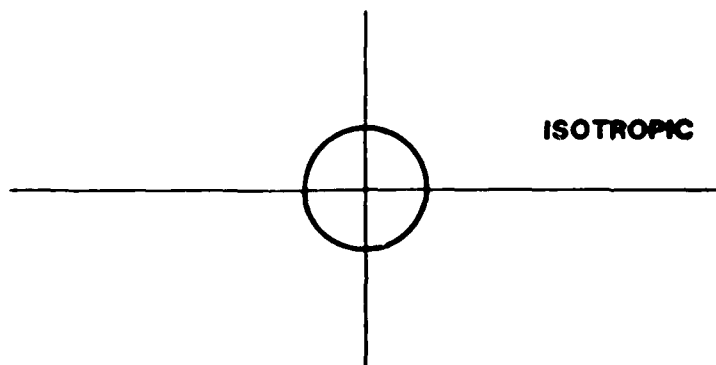
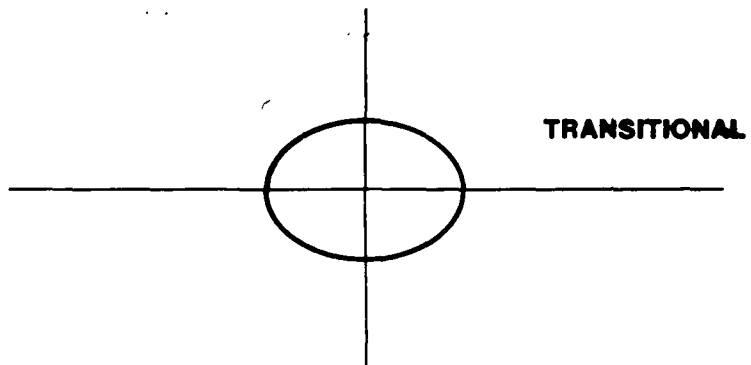
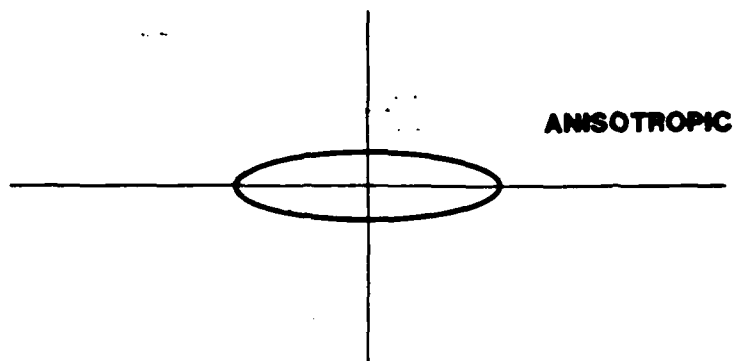


Fig 6. Representative Angular Fluence Shapes (Polar Plots)

$$b_i b_j \int_{\Omega} \sqrt{\frac{1}{1-(b_i^2-1)f(\mu, x)}} \sqrt{\frac{1}{1-(b_j^2-1)f(\mu, x)}} d\hat{n} \quad (2.42)$$

Eq. (2.42) could not be analytically integrated by the MACSYMA program.

The weighted residual technique applied to the first order Boltzmann equation by Roberds and Bridgman never produced a multiplication of two ellipsoidal functions. This multiplication occurred because the Galerkin method was used.

Numerical integration of the ellipsoidal trial function was also attempted. The computer program previously described was modified to replace the bilinear Lagrange polynomials defined over the angular domain with the ellipsoidal functions. All derivatives of this function needed for an evaluation of the Galerkin weak form equation were analytically calculated and formulated in FORTRAN by MACSYMA. Sample problems using this modified code demonstrated the need for high order quadrature sets to accurately evaluate the resulting integrals and thus properly define the global matrix. As before, the use of these higher order quadrature sets made the computational time necessary to evaluate one spatial finite element prohibitive for an air-over-ground problem.

Further efforts to use the Galerkin weak form equation to obtain solutions to an air-over-ground problem were not attempted. The complexity of this equation formulated for this problem had been demonstrated. Neither numerical nor analytical integration could efficiently form an accurately defined global matrix representation.

The next logical step in attempting to generate a solution to the EPFBE was to use a less complex numerical method. The numerical method selected was collocation as described in the next chapter.

### III. Collocation Method

#### Criteria

The results obtained from the previous chapter identified two criteria that must be met to successfully generate a global matrix representation of the EPFBE for an air-over-ground problem. The first criterion is to use a numerical method that allows the efficient computation of this matrix. The Galerkin method failed this criterion by requiring the use of a weight function that significantly added to the complexity. Additionally this method generated the nested integrals that contributed to the problems in attempting both analytical and numerical integration. The second criterion is to use a trial solution that is simply defined and analytically integrable. The bilinear Lagrange polynomials were simple in form; however, they expanded the number of distinct terms in the Galerkin weak form equation beyond the memory requirements available in MACSYMA. The ellipsoidal angular synthesis function had only one term but proved not analytically integrable. Also the complexity of this synthesis function prohibited the efficient use of numerical integration, since high order quadrature sets were needed for accurate evaluation.

The main purposes of this chapter are to present a numerical method that satisfies the first criterion, to develop a trial solution that meets the requirements of the second criterion, and to identify the problems that result from applying this combination to an air-over-ground problem.

The numerical technique chosen is the collocation method. This method was selected after reviewing the work of Houstis, Lynch, Rice, and Papatheodorou (Ref. 35). These authors generated solutions to seventeen different elliptic partial differential equations using the numerical

methods of finite differences, collocation, least squares, and Galerkin. The purpose of this paper was to compare the efficiency and accuracy of these numerical methods. This research indicated that the collocation method offered an efficient and accurate alternative to the other three techniques. Additionally, this work demonstrated the ability of the collocation method to produce a more simplified formulation than the Galerkin method. The successes reported in this paper motivated the idea of developing a numerical method based on collocation for solving the EPFBE. To insure that this attempt did not violate the second criterion, a special trial solution, derived using the concept of space-angle-synthesis, was used.

This combination of trial solution and numerical method allowed the successful approximation of the EPFBE. The simplicity of the trial solution allowed all integrals in this formulation to be analytically evaluated on MACSYMA. Attempts at solving the air-over-ground problem demonstrated a numerical problem associated with the definition of the odd-parity fluence. The severity of this problem eliminated the use of the collocation method for solving the EPFBE when a standard finite element or combination finite element synthesis trial solution was used.

#### Collocation Method and Trial Solution

Collocation is classified as a weighted residual method. In the previous chapter a derivation was presented to illustrate the weighted residual method. From this derivation the following equation resulted.

$$\int_D \left\{ L \sum_{i=1}^M a_i Q_i(\vec{x}) - f(\vec{x}) \right\} \epsilon(\vec{x}) d\vec{x} = 0 \quad (3.1)$$

The difference between the collocation method and Galerkin method is in the definition of the weight function,  $\epsilon(\vec{x})$ . As previously demonstrated this weight function is defined in the following manner for the Galerkin method.

$$\varepsilon(\vec{x}) = \sum_{i=1}^M b_i Q_i \quad (3.2)$$

For the collocation method the weight function is defined as

$$\varepsilon(\vec{x}) = \delta(\vec{x} - \vec{x}_0) \quad (3.3)$$

where  $\delta(\vec{x} - \vec{x}_0)$  is the Dirac delta function. Substituting Eq. (3.3) into Eq. (3.1) gives

$$\int_D \left\{ L \sum_{i=1}^M a_i Q_i(\vec{x}) - f(\vec{x}) \right\} \delta(\vec{x} - \vec{x}_0) d\vec{x} = 0 \quad (3.4)$$

Since the Dirac delta function is defined as

$$\delta(\vec{x} - \vec{x}_0) = \begin{cases} 0, & \vec{x} \neq \vec{x}_0 \\ \infty, & \vec{x} = \vec{x}_0 \end{cases} \quad (3.5)$$

$$\int_{-\infty}^{\infty} \delta(\vec{x} - \vec{x}_0) d\vec{x} = 1$$

Eq. (3.4) becomes

$$L \sum_{i=1}^M a_i Q_i(\vec{x}_0) = f(\vec{x}_0) \quad (3.6)$$

To solve for the  $a_i$  coefficients, Eq. (3.6) must be specified at  $M$  points in the domain  $D$ . Thus, Eq. (3.6) can be written as

$$\sum_{i=1}^M a_i L Q_i(\vec{x}_i) = f(\vec{x}_i) \quad (3.7)$$

Eq. (3.7) is a general expression representing the collocation method.

For the EPFBE, using the trial solution presented in Eq. (2.16), this expression becomes

$$\sum_{i=1}^M \sum_{j=1}^N a_{ij} \left( -\hat{n} \cdot \nabla K_{\mu} \hat{n} \cdot \nabla S_i(\vec{r}_i) A_j(\vec{r}_j) + G_y S_i(\vec{r}_i) A_j(\vec{r}_j) \right) = \quad (3.8)$$

$$-\hat{n} \cdot \nabla K_{\mu} S_{\mu}(\vec{r}_i, \vec{r}_j) - S_g(\vec{r}_i, \vec{r}_j)$$

The coefficients  $\alpha_j$  are determined by solving a system of simultaneous equations resulting from the evaluation of Eq. (3.8) at NXM phase space points.

Comparing Eq. (3.8) to Eq. (2.18) demonstrates the simplification resulting from the collocation method. Most significant is the absence of the weight function and outer integrals that caused complications in the Galerkin weak form equation. Eliminating these two complicating factors allows the first criterion specified earlier to be met.

The collocation method does introduce some new complexities. The most obvious is that the vacuum boundary condition is no longer treated naturally. This condition must now be enforced by using

$$\Psi(\vec{r}, \hat{n}) = K_\mu \{ S_\mu(\vec{r}, \hat{n}) - \hat{n} \cdot \nabla \Psi(\vec{r}, \hat{n}) \} = 0, \quad \hat{n} \cdot \hat{n} < 0 \quad (3.9)$$

as presented in Chapter I. Unlike the Galerkin method, the collocation method does not generate a symmetric global matrix. This lack of symmetry and positive definiteness increases the cost of solving the resulting matrix and eliminates the use of some very efficient and fast linear equation solving algorithms. Another complication results from the required continuity of the trial solution. In the Galerkin weak form equation, the functions chosen for use in the trial solution were required to be continuous. The variational nature of this equation eliminated continuity constraints on the derivatives of these functions and thus allowed the use of piecewise continuous Lagrange polynomials. The collocation method requires the trial solution to have continuous second derivatives at the mesh nodes. The simplification gained by using the collocation method forces higher continuity requirements on the trial solution.

A trial solution requiring continuity in the second derivative may be constructed from cubic splines. A derivation of the cubic spline function in one dimension is presented in Appendix I and is denoted as

. A tensor product consisting of cubic splines representing both the spatial and angular variation of the neutron fluence would result in a global matrix of large bandwidth. In an air-over-ground problem both the spatial and angular domain demand relatively fine zoning. This zoning requirement increases the bandwidth problem in the global matrix and increases the computational cost. To reduce the bandwidth a synthesis function was used instead of cubic splines to represent the angular variation of the neutron fluence.

An angular synthesis function was devised to represent the angular variation of the even-parity fluence and meet the second criterion described previously. This function can be represented as

$$A(\mu, x) = a_1 + a_2 (\mu \mu_0 + \sqrt{1 - \mu^2} \sqrt{1 - \mu_0^2} \cos(x - x_0))^2 \quad (3.10)$$

where  $\mu_0$  and  $x_0$  are the coordinates of the streaming direction with respect to the point source in the particle direction coordinate system. This synthesis function was devised by considering the expected angular variation of the neutron fluence. Appendix G describes this synthesis function.

Eq. (3.10) has properties similar to the ellipsoidal synthesis function used in Chapter II. Eq. (3.10) is pitched in line with the streaming direction at a particular spatial location. This equation can also be varied to represent the three expected angular fluence shapes presented in Fig. 6. A highly anisotropic flux distribution occurs when the coefficient  $a_2$  is much larger than the  $a_1$  coefficient. An isotropic flux distribution occurs when  $a_2 = 0$ .

The primary difference between the synthesis function defined in Eq. (3.9) and the ellipsoidal synthesis function presented in Chapter II is the meaning of the coefficients. The coefficients in the ellipsoidal synthesis function expansion allowed the blending of three ellipsoidal shapes to determine the angular approximation. In Eq. (3.10) the coefficients directly shape the synthesis function for approximating the angular variation of the even-parity fluence.

The use of a synthesis function to represent the angular dependence of the even-parity fluence reduces the bandwidth of the resulting global matrix. This reduction occurs since the synthesis function is globally defined over the entire angular domain, thus eliminating the need for zoning. One globally defined function replaces all the tensor product combinations that would result from an angular trial solution defined over a discretized domain. Since each tensor product combination occupies one element in the global matrix, the globally defined synthesis function can significantly reduce the bandwidth of this matrix. An additional advantage to using the synthesis function defined in Eq. (3.10) is that it satisfies the reflective boundary condition. The final form of the trial solution used with the collocation method is

$$\Psi(\vec{r}, \lambda) = \sum_{i=1}^M \sum_{j=1}^N \theta_i(\rho) \theta_j(z) \left\{ a_{1ij} + a_{2ij} (\mu \mu_0 + \sqrt{1-\mu^2} \sqrt{1-\mu_0^2} \cos(\chi - \chi_0))^2 \right\} \quad (3.11)$$

where  $\theta_i(\rho)$  and  $\theta_j(z)$  are cubic splines in the spatial domain.

The combination of the collocation method and the trial solution presented in Eq. (3.11) satisfied the two criteria determined from Chapter II. A computer program was written that used this combination to generate a global matrix representation of the EPFBE. This program used no numerical integration, since the simplicity of the trial solution and the collocation method allowed all integral and derivative operations to be

performed on MACSYMA. The results of these operations were translated into FORTRAN statements by MACSYMA, thus eliminating the possibility of erroneously transcribing these expressions.

A distributed first-scatter source term was used in this computer code. The angular distribution of the neutron fluence near the point source is extremely anisotropic. This anisotropy is so severe that the angular synthesis function represented by Eq. (3.10) would have difficulty in accurately approximating such an anisotropic shape. The use of the first-scatter source allows the scattered and unscattered neutrons at a point to be treated separately. Eq. (1.6) gives at  $\vec{r}$  the angular distribution of first-scattered neutrons which were emitted from a point source located at  $\vec{r}_s$ . The uncollided neutrons arriving at  $\vec{r}$  are given by

$$\frac{S(\vec{r}_s) e^{-\lambda (1 - \sigma_T(\vec{r}))}}{4\pi} \quad (3.12)$$

while those that interact either through absorption or scatter are represented by

$$\frac{S(\vec{r}_s) e^{-\lambda} \sigma_T(\vec{r})}{4\pi} \quad (3.13)$$

The scattered fluence is less anisotropic than the total fluence and may be represented by a function with a simple angular dependence. In the final solution the uncollided fluence is added to the calculated value of the neutron fluence in the streaming direction.

As previously mentioned, the collocation method requires an evaluation of Eq. (3.8) at a number of phase space points equal to the number of coefficients in the trial solution. The trial solution presented in Eq. (3.11) requires Eq. (3.8) to be evaluated in two distinct angular

directions at each spatial location. In the collocation based computer code, these angular directions were always selected as the streaming direction and a direction perpendicular to the streaming direction. The choice of these two directions allowed the coefficients to be defined in the most meaningful manner based on their role in properly shaping the angular synthesis function. The spatial collocation points were chosen as the nodes of the mesh. The only exception occurred along the mesh line  $\rho=0$ . On this mesh line the reflected boundary condition must be enforced. Since the chosen trial solution automatically satisfied this constraint, spatial collocation points were chosen at a value of  $\rho$  slightly greater than zero. Along the vacuum boundaries the code provided the option of either evaluating Eq. (3.9) at two angular directions or enforcing the EPFBE in one angular direction and the vacuum boundary condition in the other direction. A flow diagram of the collocation computer code appears in Appendix H.

The structure of the global matrix resulting from the use of the selected trial solution and the collocation method was primarily determined by the cubic splines. The structure of this matrix for the spatial mesh in Fig. 7 is illustrated in Fig. 8.

#### Problems

An air-over-ground problem was attempted using the collocation method. The spatial mesh used for this problem was identical to the one illustrated in Fig. 7. Collocation points were selected as previously described and the vacuum boundary condition was enforced along the appropriate boundary surfaces. To generate a solution to this problem the collocation global matrix assembly program was expanded. This expansion was necessary to determine the coefficients of the trial solution,

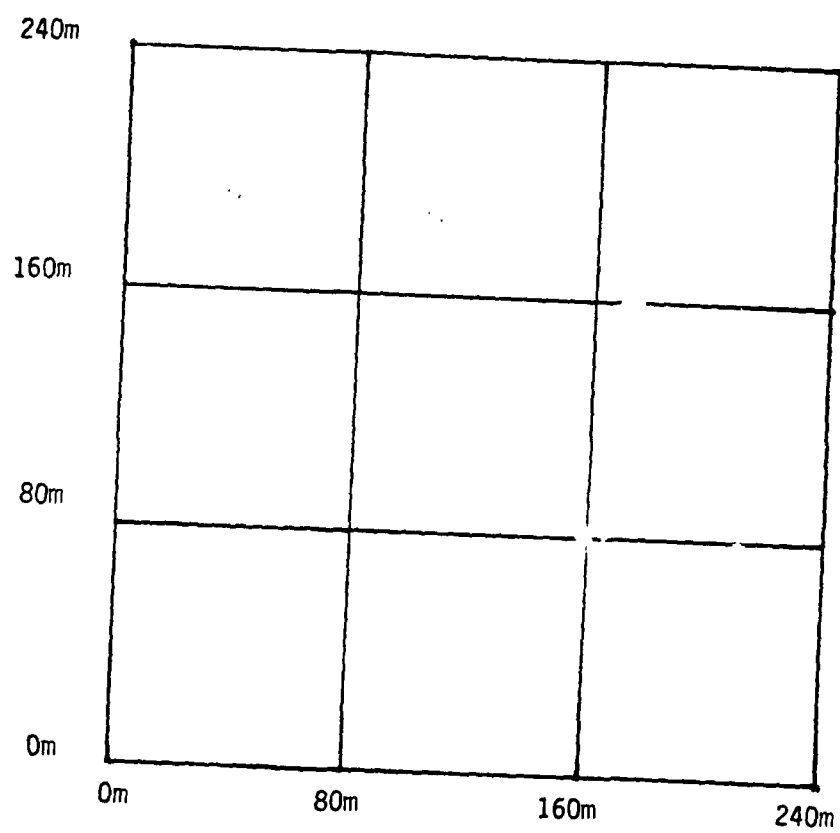


Fig 7. Collocation Spatial Mesh

# SPLINE COMBINATIONS

		$(s_1s_1)$	$(s_1s_2)$	$(s_1s_3)$	$(s_1s_4)$	$(s_2s_1)$	$(s_2s_2)$	$(s_2s_3)$	$(s_2s_4)$	$(s_3s_1)$	$(s_3s_2)$	$(s_3s_3)$	$(s_3s_4)$	$(s_4s_1)$	$(s_4s_2)$	$(s_4s_3)$	$(s_4s_4)$
$\rho_1$	$z_1$	$a_1$	xx	xx		xx	xx										
	$z_2$	$a_2$	xx	xx		xx	xx										
	$z_3$	$a_1$	xx	xx	xx	xx	xx	xx									
	$z_4$	$a_2$	xx	xx	xx	xx	xx	xx	xx								
$\rho_2$	$z_1$	$a_1$	xx	xx		xx	xx			xx	xx						
	$z_2$	$a_2$	xx	xx		xx	xx			xx	xx	xx					
	$z_3$	$a_1$	xx	xx	xx	xx	xx	xx		xx	xx	xx	xx				
	$z_4$	$a_2$	xx	xx	xx	xx	xx	xx	xx	xx	xx	xx	xx	xx			
$\rho_3$	$z_1$	$a_1$				xx	xx			xx	xx			xx	xx		
	$z_2$	$a_2$				xx	xx	xx		xx	xx	xx		xx	xx	xx	
	$z_3$	$a_1$				xx	xx	xx	xx	xx	xx	xx	xx	xx	xx	xx	xx
	$z_4$	$a_2$				xx	xx	xx	xx	xx	xx	xx	xx	xx	xx	xx	xx
$\rho_4$	$z_1$	$a_1$								xx	xx			xx	xx		
	$z_2$	$a_2$								xx	xx	xx		xx	xx	xx	
	$z_3$	$a_1$								xx	xx	xx	xx	xx	xx	xx	xx
	$z_4$	$a_2$								xx	xx	xx	xx	xx	xx	xx	xx

$(a_1, a_2)$  = angular collocations points

$(z_1, z_2, z_3, z_4)$  = (0, 80m, 160m, 240m)

= z coordinate collocation points

$(\rho_1, \rho_2, \rho_3, \rho_4)$  = (0, 80m, 160m, 240m)

=  $\rho$  coordinate collocation points

x = a nonzero matrix element

Fig 8. Global Collocation Matrix

analyze the resulting global matrix, and reconstruct in terms of the trial solution the even-parity, Boltzmann, and scalar fluences. Solution coefficients were determined using Gaussian elimination with full pivoting. The input to this linear equation solving routine was the collocation global matrix and source column vector computed from the global matrix assembly program. The global matrix was analyzed by determining its condition number which was calculated as the ratio of the largest to the smallest eigenvalue. (The eigenvalues were determined by the International Mathematical and Statistical Libraries routine entitled LSVDF.) Reconstruction of the desired fluences was accomplished from the solution coefficients and basis functions of the trial solution for the spatial location chosen. The reconstruction program used many of the same subroutines that were developed for the global matrix assembly program. The logic of this system of programs is illustrated in Fig. 9. Each subroutine contained within the global matrix assembly program and fluence reconstruction program was independently checked to assure that its logic, programming, and interface with the driver routines was correct.

The solution generated by the collocation method to this air-over-ground problem was disappointing. Most significant was that the scalar fluence was negative at several node locations in the spatial mesh. Also both the Boltzmann and even-parity fluence exhibited negative values for several angular locations at each spatial node point. Negative angular fluences values were not limited to spatial node points, but also appeared at off node spatial locations throughout the spatial domain. Those scalar fluence values that were positive did not make physical sense. The value of the scalar fluence was often larger on the boundaries than near the interior of the spatial mesh. Also the condition number of the resulting global matrix was  $10^5$ .

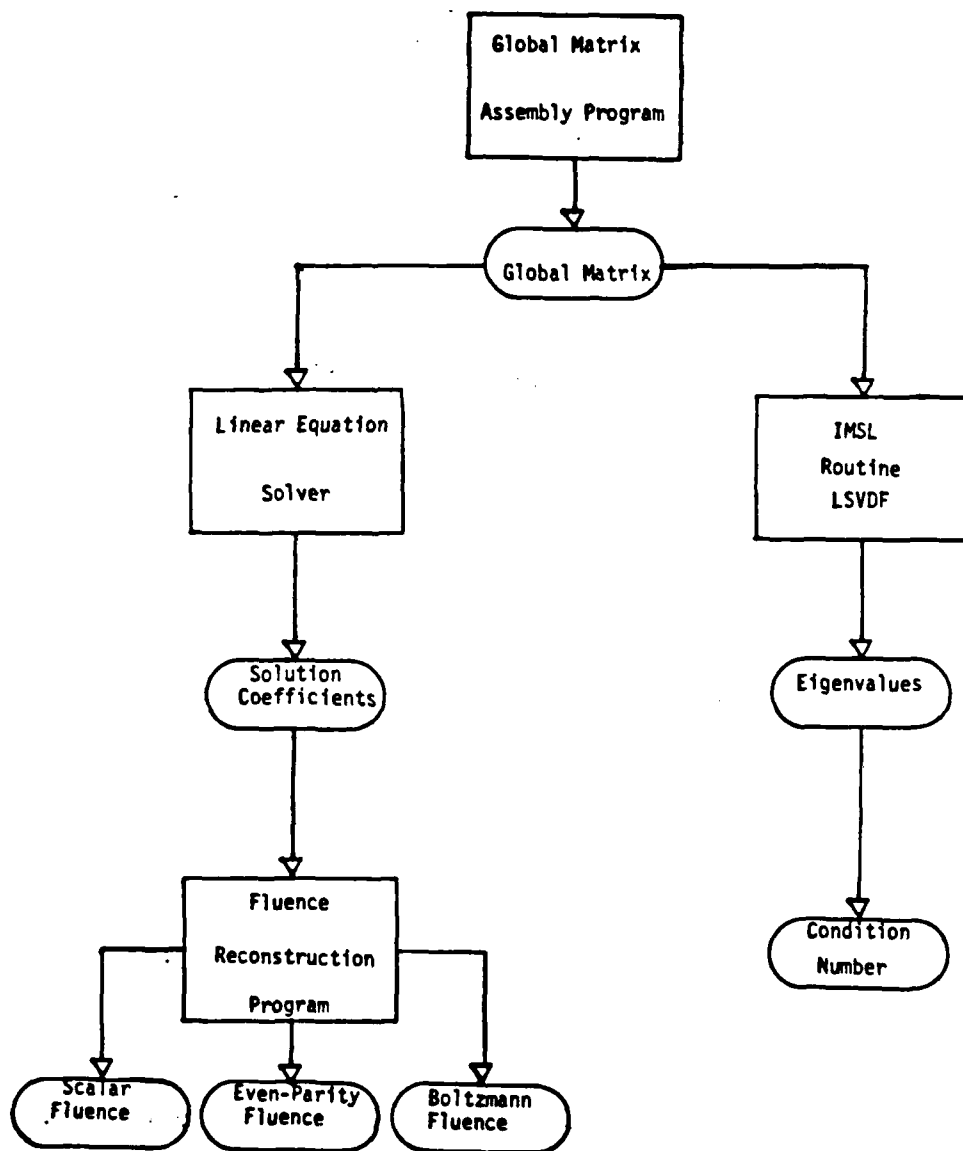


Fig 9. Program Logic

Several means were attempted to improve these poor results. The meshing of the spatial domain was refined. This refinement increased the number of nodes from sixteen to thirty-six, thus increasing the size of the global matrix to a  $72 \times 72$  system. This refinement produced no change in the previously observed behavior of the fluences and increased the condition number to  $10^8$ .

The method of selecting collocation points was altered. Spatial collocation points were selected at locations other than at the spatial nodes and angular collocation points were selected away from the streaming direction. Again the behavior of the fluence remained the same and the condition number did not change appreciably from the original value of  $10^5$ . In addition a new difficulty was encountered. This difficulty involved selecting spatial collocation points that were not located on either the vertical or horizontal mesh lines. Distributing these points evenly around the spatial mesh proved impossible and forced a random type of selection. The optimum way of picking these points from the unlimited number of combinations available was not clear. This random selection process was abandoned, since the resulting solution exhibited the same problems originally encountered.

Another attempt at resolving these solution problems used the option mentioned earlier of collocating either the EPFBE or vacuum boundary condition on the appropriate boundary surface. Two different approaches were tried. The first approach allowed the vacuum boundary condition to be used for both angular collocation points at a boundary spatial node. The second approach divided the two angular collocation evaluations between the EPFBE and vacuum boundary condition. In both cases the behavior of the scalar fluence and value of the condition number remained

effectively the same as the original result. At this point it was becoming increasingly clear that a fundamental problem existed with the collocation method. To uncover this problem a simple diagnostic problem was used.

This diagnostic problem assumed a uniform isotropic neutron source, isotropic scatter, and isotropic boundary conditions. Its solution, as verified by a DOT 3.5 calculation, is a flat spatial distribution isotropically distributed in angle. The simplicity of this problem allowed several different formulations of the EPFBE to be evaluated. These various formulations differed in complexity and all had the capacity of generating an accurate solution to this problem.

The simplest formulation was derived by using the isotropy of the known solution. This isotropy allowed all terms in the EPFBE related to the odd-parity fluence to be eliminated. The resulting formulation was

$$G_g \Psi(r, \hat{r}) = S_g(r, \hat{r}) \quad (3.14)$$

The collocation global matrix assembly program was modified to solve Eq. (3.14). This modification included replacing the first-scatter source term and vacuum boundary condition with those associated with the diagnostic problem. The source term and boundary condition for the diagnostic problem were respectively defined as

$$S_g(r, \hat{r}) = \frac{1}{4\pi (\sigma_T(r) + \sigma_{sp}(r))} \quad (3.15)$$

$$\Psi(r, \hat{r}) = \frac{1}{4\pi} \quad \text{for } \hat{r} \text{ on the boundary,} \quad (3.16)$$

The collocation method generated the correct solution to the diagnostic problem using this formulation of the EPFBE. This result was encouraging,

since it confirmed the logic and programming accuracy of the subroutines in the global matrix assembly program and reconstruction program.

A more complicated formulation was attempted next. This formulation was

$$-\hat{r} \cdot \nabla K_{\mu} \hat{r} \cdot \nabla \Psi(r, \hat{r}) + G_g \Psi(r, \hat{r}) = S_g(r, \hat{r}) \quad (3.17)$$

where  $S_g(r, \hat{r})$  and the boundary conditions were the same as the previous problem. For this formulation the collocation method did not generate a flat scalar fluence distribution. The boundary scalar fluences were correct, but the interior mesh values varied by as much as 20 percent. For this formulation all the scalar fluences were positive. The same formulation was solved again using a more refined spatial mesh. The solution was the same, indicating the original mesh was adequate.

The formulation presented in Eq. (3.14) was next used with the following form of the diagnostic problem boundary condition

$$\Psi(r, \hat{r}) + \chi(r, \hat{r}) = \frac{1}{4\pi} \quad (3.18)$$

Eq. (3.18) represents a statement of the diagnostic problem boundary condition in terms of the Boltzmann fluence. The collocation method must be able to handle this type of boundary condition formulation, since in all transport problems the physical constraints on the boundaries are specified in terms of this fluence. In the collocation computer program  $\chi(r, \hat{r})$  was replaced by the odd-parity fluence transformation Eq. (A.20). The solution generated by the collocation method for this problem was again incorrect. The interior scalar fluences were correct; however, the boundary scalar fluences varied by 120 percent.

The final formulation used Eq. (3.17) with the boundary condition presented in Eq. (3.18). The collocation method generated a solution for

this formulation that was utter nonsense. This solution had several negative fluence values both in the interior of the mesh and on the boundary. The scalar fluences that were positive were not equal and could not have generated a flat spatial distribution.

### Problem Analysis

The poor results generated by the collocation method can best be explained by using a 1-D plane geometry formulation of the diagnostic problem. In this simplified formulation a suitable synthesis trial solution for the standard Boltzmann equation is

$$\Phi(x, \mu) = \sum_{i=1}^N \beta_i(x) (a_{1i} + a_{2i} \mu) \quad (3.19)$$

where  $\beta_i(x)$  is a cubic spline basis function. Using the definition of the even-parity fluence with Eq. (3.19) generates the following trial solution

$$\Psi(x, \mu) = \sum_{i=1}^N a_{1i} \beta_i(x) \quad (3.20)$$

Applying the odd-parity fluence transformation presented in Eq. (A.20) to the trial solution of Eq. (3.20) results in

$$\chi(x, \mu) = - \sum_{i=1}^N a_{1i} \frac{\mu}{\sigma_T(x)} \frac{d}{dx} (\beta_i(x)) \quad (3.21)$$

for a  $P_0$  scatter process. The boundary condition of the diagnostic problem in terms of  $\Psi(x, \mu)$  and  $\chi(x, \mu)$  can be written as

$$\Phi(x, \mu) = \Psi(x, \mu) + \chi(x, \mu) = \frac{1}{4\pi} \quad (3.22)$$

Using Eqs. (3.20) and (3.21), Eq. (3.22) can be rewritten as

$$\Phi(x, \mu) = \sum_{i=1}^N a_{1i} \left( \beta_i(x) - \frac{\mu}{\sigma_T(x)} \frac{d}{dx} (\beta_i(x)) \right) \quad (3.23)$$

By the definition of the collocation method Eq. (3.23) can be satisfied for one selected angular collocation point at a particular spatial node. Eq. (3.23) can not be properly constrained to generate the isotropic boundary condition. In any other angular direction other than the selected collocation direction the value of the boundary condition is not  $\frac{1}{4\pi}$ . The odd-parity fluence transformation has forced the Boltzmann fluence to have an anisotropic component. This can be easily seen by the presence of the  $\mu$  variable in Eq. (3.23). Ideally for the diagnostic boundary condition the following relation should hold:

$$\chi(x, \mu) = \sum_{i=1}^N a_{i,i} \frac{\mu}{\sigma_T(x)} \frac{d}{dx} (\beta_i(x)) = 0 \quad (3.24)$$

however; this would require either

- (1) all the  $a_{i,i}$ 's to be zero in which case  $\psi(x, \mu) = 0$  at all phase space points.
- (2)  $\frac{d}{dx} (\beta_i(x)) \Big|_{x_b} = 0$ , which is only true for the spline centered at a node and since splines overlap in mesh intervals this is not in general true ( $x_b$  = boundary node location).
- (3)  $a_{i,i} \frac{\mu}{\sigma_T(x)} \frac{d}{dx} (\beta_i(x)) \Big|_{x_b} + a_{i,i+1} \frac{\mu}{\sigma_T(x)} \frac{d}{dx} (\beta_{i+1}(x)) \Big|_{x_b} + a_{i,i+2} \frac{\mu}{\sigma_T(x)} \frac{d}{dx} (\beta_{i+2}(x)) \Big|_{x_b} = 0$

which is not enforced in the collocation set of equations.

The conclusion is that the selected synthesis trial solution is not transformable through the odd-parity fluence transformation into a trial solution that accurately represents the anisotropy of the fluence.

The odd-parity fluence transformation is also present in the even-parity equation. As demonstrated in Appendix A the odd-parity fluence is contained in the first term of this equation. If the even-parity equation is being derived for the diagnostic problem, this first term would appear as

$$\mu \frac{d}{dx} (\chi(x, \mu)) \quad (3.25)$$

To eliminate the  $X$  variable from the even-parity equation the odd-parity fluence transformation is used. This is accomplished by substituting the value of  $\chi(x, \mu)$  from Eq. (3.24) into Eq. (3.25), thus generating

$$\mu \frac{d}{dx} \left( -\frac{\mu}{\sigma_T(x)} \frac{d}{dx} (\psi(x, \mu)) \right) \quad (3.26)$$

Simplifying Eq. (3.26) gives

$$-\frac{\mu^2}{\sigma_T(x)} \frac{d^2 \psi(x, \mu)}{dx^2} \quad (3.27)$$

The full even-parity equation for the 1-D plane geometry diagnostic problem is

$$-\frac{\mu^2}{\sigma_T(x)} \frac{d^2 \psi(x, \mu)}{dx^2} + \sigma_T(x) \psi(x, \mu) - \sigma_{S_0}(x) \int_{-4\pi} \psi(x, \mu') d\mu' = \frac{1}{4\pi} \quad (3.28)$$

Substituting the trial solution of Eq. (3.20) into Eq. (3.28) yields

$$\sum_{i=1}^N a_{i,c} \left( -\frac{\mu^2}{\sigma_T(x)} \frac{d^2 \beta_i(x)}{dx^2} + (\sigma_T(x) - \sigma_{S_0}(x)) \beta_i(x) \right) = \frac{1}{4\pi} \quad (3.29)$$

Obviously to generate a flat isotropic Boltzmann fluence, the first term of Eq. (3.28) must be zero, since its origin is the difference between the leakage in the  $\mu$  and  $-\mu$  angular directions. If  $-\frac{\mu^2}{\sigma_T(x)} \frac{d^2 \beta_i(x)}{dx^2}$  could be made equal to zero then Eq. (3.29) would be

$$\sum_{i=1}^N a_{i,c} (\sigma_T(x) - \sigma_{S_0}(x)) \beta_i(x) = \frac{1}{4\pi} \quad (3.30)$$

$$\sum_{i=1}^N a_{i,c} \beta_i(x) = \frac{1}{4\pi (\sigma_T(x) - \sigma_{S_0}(x))} \quad (3.31)$$

which generates the correct solution to the diagnostic problem. In the collocation method there is no means to set this term equal to zero.

Just as in the boundary condition, the odd-parity fluence transformation has forced an incorrect anisotropy into the solution.

To determine the form of the anisotropy resulting from the odd-parity fluence transformation, an analysis was performed. This analysis was based on an interpolation procedure similar to the one used to apply the Boltzmann fluence boundary condition to the even-parity equation. In this procedure three different trial solutions were used to represent the even-parity fluence. These trial solutions were selected because they illustrated specific problems related to the odd-parity fluence transformation. For each trial solution a simple spatial mesh was constructed and where necessary an angular mesh. All results were generated using the same sequence of programs that were used in solving the four versions of the diagnostic problem. Modifications to these programs were made to account for the different interpolating functions. All angular plots presented are typical of those seen at all the nodes in the spatial mesh.

The first problem used the trial solution presented in Eq. (3.19) and solved the interpolation problem of Eq. (3.22) with the  $1/4 \pi$  replaced by 100. Fig. 10 illustrates the results of this problem for various values of the total macroscopic cross section ( $\sigma_T(u)$ ). This interpolation problem demonstrates graphically the explanation that was presented using Eqs. (3.19) thru (3.31). The spatial mesh for this problem had nodes at 0, 10, 15, and 20 cm. The angular collocation point at each of these spatial nodes was taken at  $u = 1$  which corresponds to the streaming direction in a 1-D plane geometry problem.

In Fig. 10  $\sigma_T$  was varied from infinity to  $10^{-4}$  /cm thus varying the effect of the odd-parity fluence transformation. For  $\sigma_T = \infty$  an isotropic fluence distribution across the angular domain was generated.

This result was analogous to the first version of the diagnostic problem that generated acceptable results. As illustrated by the other curves in Fig. 10, reducing the value of  $\sigma_T$  increases the weight of the odd-parity fluence transformation in determining the angular distribution of the Boltzmann fluence. The effect of this transformation is most clearly demonstrated by the odd functional nature of the resulting Boltzmann angular fluence distribution for  $\sigma_T = 10^{-4}$  /cm.

For the trial solution presented in Eq. (3.20), the resulting anisotropy is fixed. The collocation method can alter the magnitude of the anisotropy, but can not change its relative angular distribution. Thus the anisotropy demonstrated in Fig. 10 will exist at all spatial locations. This is obviously unsatisfactory since the anisotropy in most transport problems (especially in an air-over-ground problem) varies from one spatial location to another.

In the second interpolation problem a pure spline basis is used as a trial solution for the even-parity fluence. This trial solution can be represented mathematically as

$$\Psi(x, \mu) = \sum_{i=1}^N \sum_{j=1}^M a_{ij} \beta_i(x) \beta_j(\mu) \quad (3.32)$$

where  $\beta_i(x)$  and  $\beta_j(\mu)$  are cubic splines defined respectively over the spatial and angular domain. From this trial solution the Boltzmann fluence is formed for a 1-D plane geometry and appears as

$$\Phi(x, \mu) = \sum_{i=1}^N \sum_{j=1}^M a_{ij} \left( \beta_i(x) \beta_j(\mu) - \frac{\mu}{\sigma_T(x)} \beta_j(\mu) \frac{d\beta_i}{dx} \right) \quad (3.33)$$

Eq. (3.33) was interpolated across a spatial mesh with three nodes located at 1., 10., and 20. cm and an angular mesh with three nodes located at -1, 0, and 1. The spatial and angular nodes also served as collocation

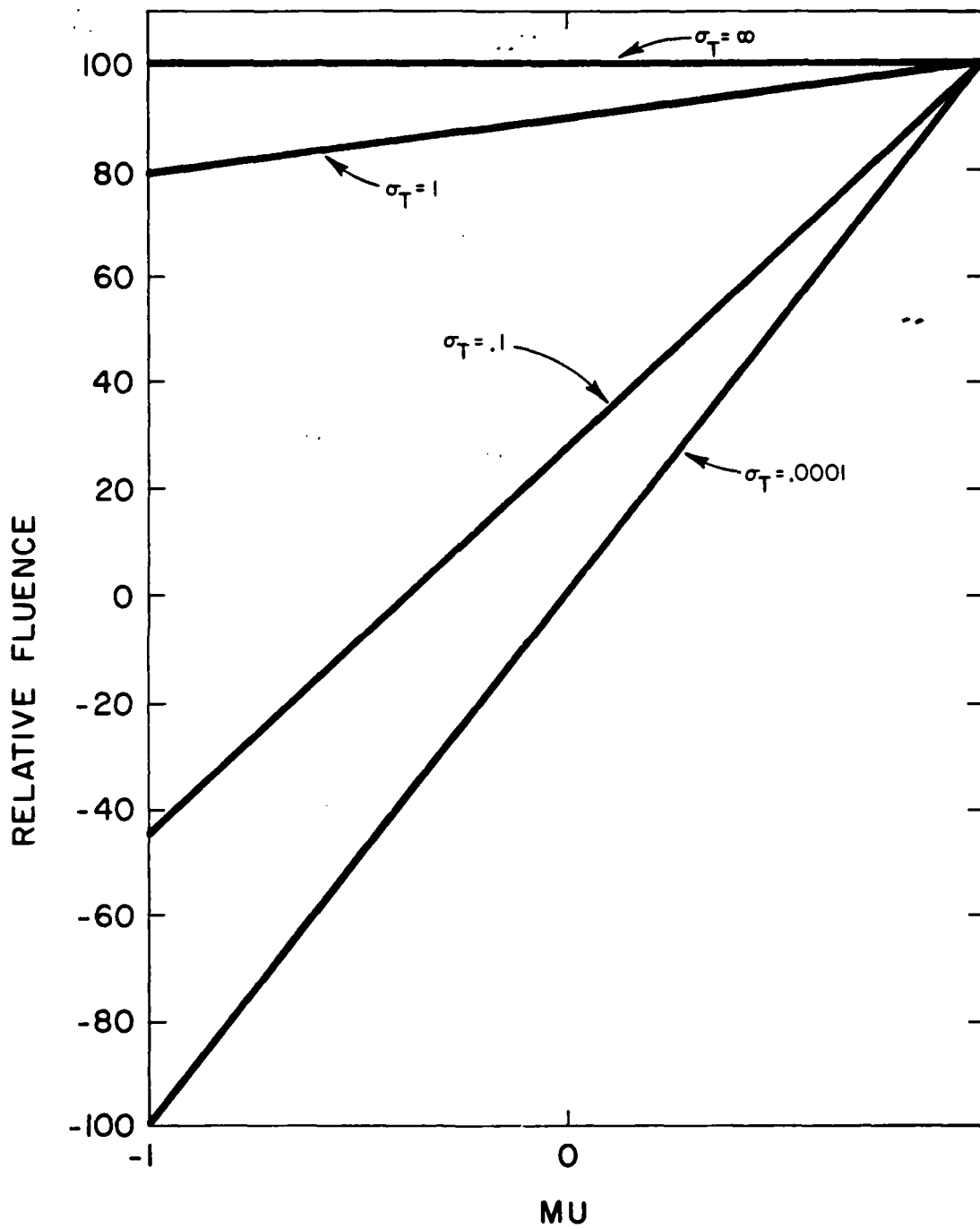


Fig 10. Interpolation Problem 1

coordinates, where the Boltzmann angular fluence (Eq. (3.33)) was forced to equal 100. Again with  $\sigma_T$  set equal to infinity a flat isotropic angular distribution was generated across the spatial domain. In Fig. 11 and Fig. 12 the value of  $\sigma_T$  is continuously decreased. The curves in these figures demonstrate the same trend seen previously with the 1-D synthesis trial solution. As  $\sigma_T$  decreases in value the dominance of the odd-parity fluence transformation increases.

Unlike the synthesis trial solution the pure spline trial solution can alter the anisotropy. This alteration can be achieved by more finely discretizing the angular domain and thus forcing the solution to be constrained at more angular nodes. This approach generates two disadvantages. First, the behavior of the trial solution in Eq. (3.33) would still be dominated by the odd-parity fluence transformation between the nodes for small values of  $\sigma_T$ . This dominance forces an artificial anisotropy between the nodes that in an exact solution would not exist. This artificial anisotropy would affect the evaluation of the boundary condition and first term of the even-parity equation in a manner similar to that observed in the diagnostic problem. The degree to which this effect would alter the final solution is directly related to the number of nodes used in the angular domain. Increasing the number of nodes leads to the second disadvantage. This disadvantage addresses the size of the resulting global matrix that would be generated using a pure spline basis. The total number of coefficients that must be solved for to obtain a solution to the EPFBE is equal to the number of unknown coefficients in the trial solution. The trial solution presented in Eq. (3.33) would result in a global matrix that has a row and column dimension equal to  $NXM$ . Increasing the number of nodes by  $\Delta$  in the angular domain results

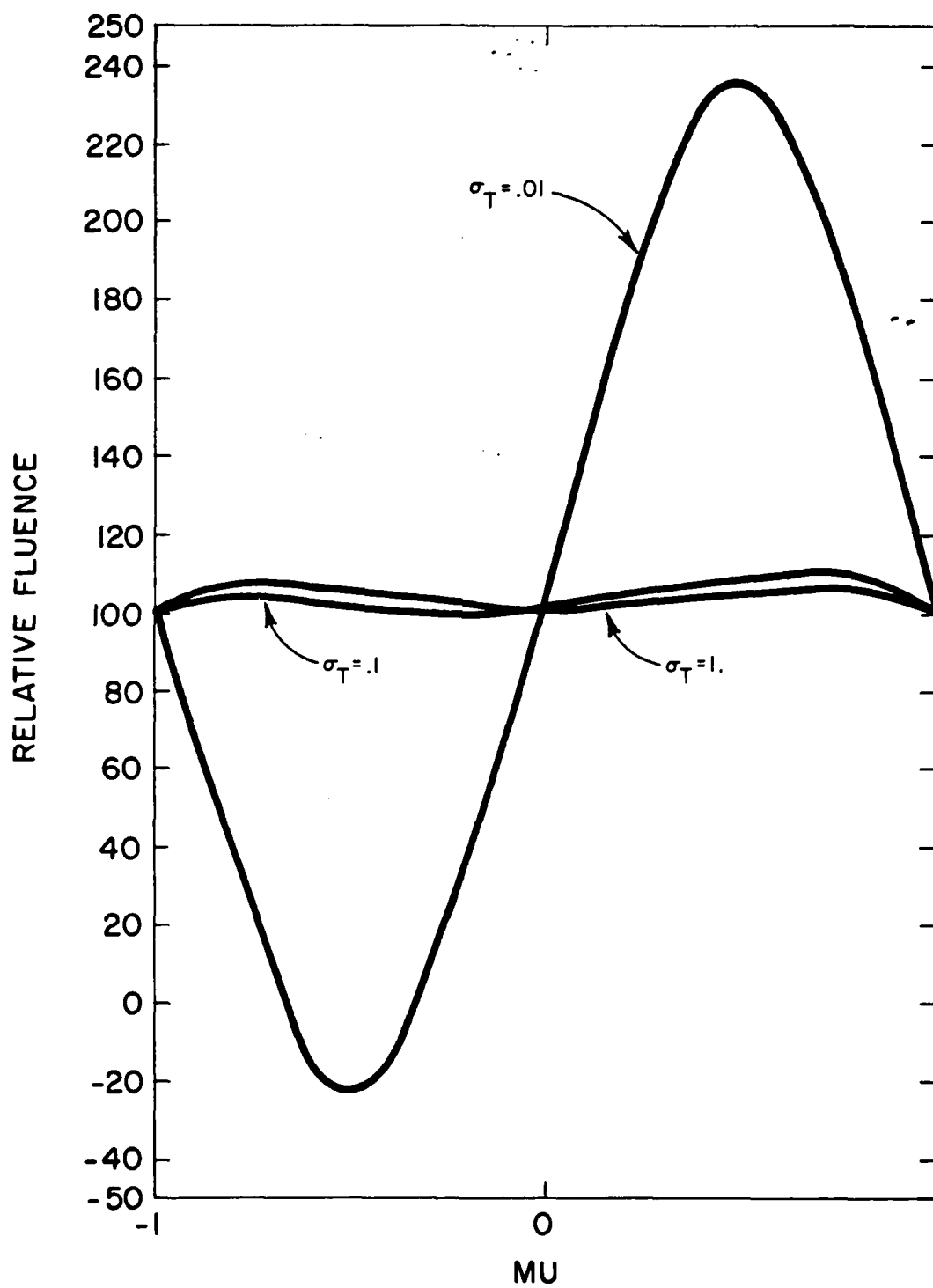


Fig 11. Interpolation Problem 2 (1 of 2)

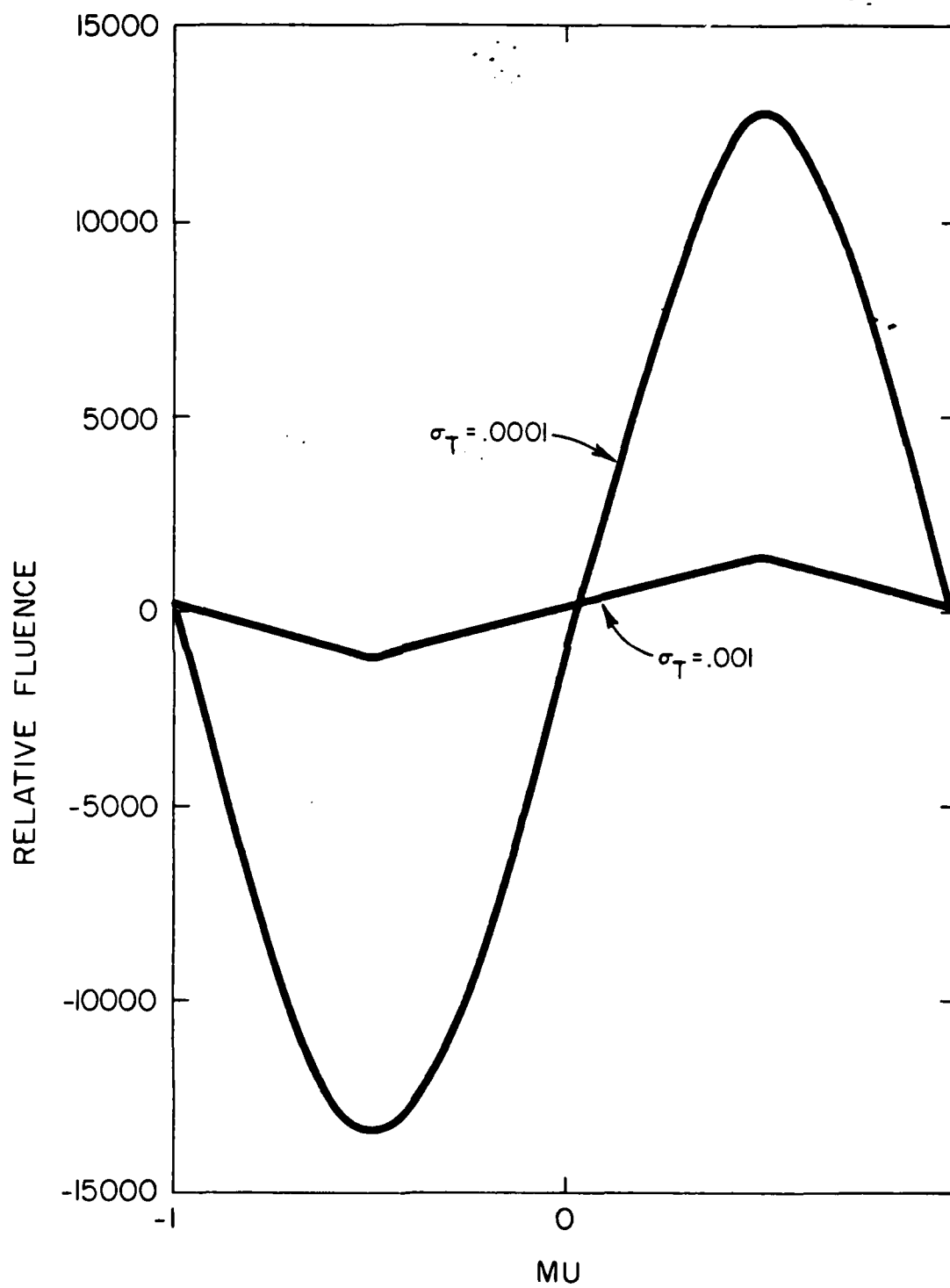


Fig 12. Interpolation Problem 2 (2 of 2)

in an increase in the dimensionality of the global matrix of  $M$ . For an air-over-ground problem a suitable pure spline trial solution for the even-parity fluence is

$$\Psi(\rho, z, \mu, x) = \sum_{i=1}^N \sum_{j=1}^M \sum_{k=1}^Q \sum_{l=1}^P a_{ijkl} \theta_i(\rho) \theta_j(z) \theta_k(\mu) \theta_l(x) \quad (3.34)$$

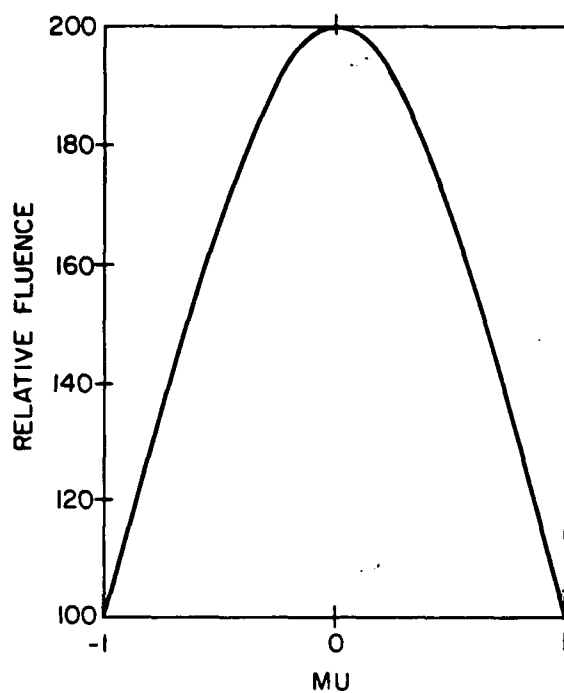
Refining the angular mesh a factor of  $\Delta$  in the  $\mu$  and  $x$  coordinates would result in a  $NM(\Delta(O+P)+\Delta^2)$  increase in the dimensionality of the global matrix. The acceptable value of  $\Delta$  needed to offset the artificial anisotropy effect of the odd-parity fluence transformation is not known, but based on the results of the diagnostic problem and presented figures would appear to be quite large. A large  $\Delta$  would result in a large global matrix. This matrix would be nonsymmetric and costly to compute and solve, thus eliminating the pure spline basis as an efficient means to solve the even-parity equation, especially for an air-over-ground problem.

The third trial solution used to demonstrate the anisotropy effect of the odd-parity fluence transformation was the one presented in Eq. (3.11). For this trial solution an interpolation problem was not formulated. A more simple and direct means of demonstrating the effect of the odd-parity fluence transformation was found. A two-dimensional spatial mesh in the coordinates  $\rho$  and  $z$  was constructed. The nodes in both the  $\rho$  and  $z$  direction were located at 1., 10., and 20. cm. At the coordinate location (10., 10.) the Boltzmann angular fluence distribution was calculated. This calculation was performed by the fluence reconstruction program. Input to this program included the spatial mesh, solution coefficients,  $\sigma_T(\mu)$ , and the location of the point source that determines the pitch of the trial solution at the various spatial locations. All solution

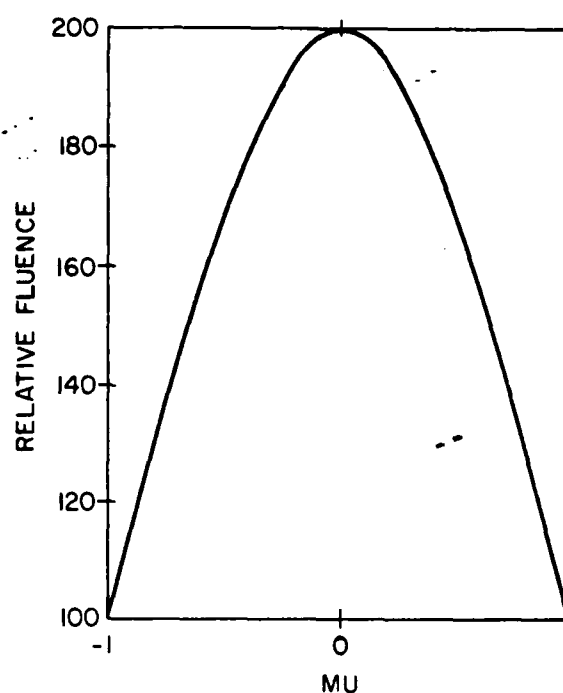
coefficients were set equal to one. The point source was located at the spatial coordinates (0., 10.), thus making the pitch axis of the trial solution parallel with the  $\rho$  axis.

Figs. 13 and 14 illustrate the results of the fluence reconstruction program. Figs. 13a and 13b demonstrate the angular distribution of the even-parity fluence for  $x = 0$  and  $\pi$  respectively. Figs. 13c and 13d show the form of the odd-parity fluence derived from the trial solution of Eq. (3.11) for various  $x$  locations. Figs. 14a thru 14d are plots of the Boltzmann fluence for various  $x$  locations and values of  $\sigma_T$ . The significant thing to note from these plots is the anisotropy that is forced on the Boltzmann fluence by the odd-parity fluence transformation. A polar plot of Figs. 14a and 14b is presented in Fig. 15. This polar plot represents the angular synthesis function for the Boltzmann fluence as derived from the even-parity fluence angular synthesis function and odd-parity fluence transformation. This function is not representative of the angular distribution expected from either the diagnostic problem or an air-over-ground problem. This poor representation is caused by the inadequacy of the selected even-parity angular synthesis function to be transformed into an accurate representation of the anisotropic component of the Boltzmann fluence. As evidenced by Figs. 14c and 14d the derived angular synthesis function becomes worse as the dominance of the odd-parity transformation increases. The negative values seen in Fig. 14c could have contributed to the negative fluence values calculated in the diagnostic and air-over-ground problem.

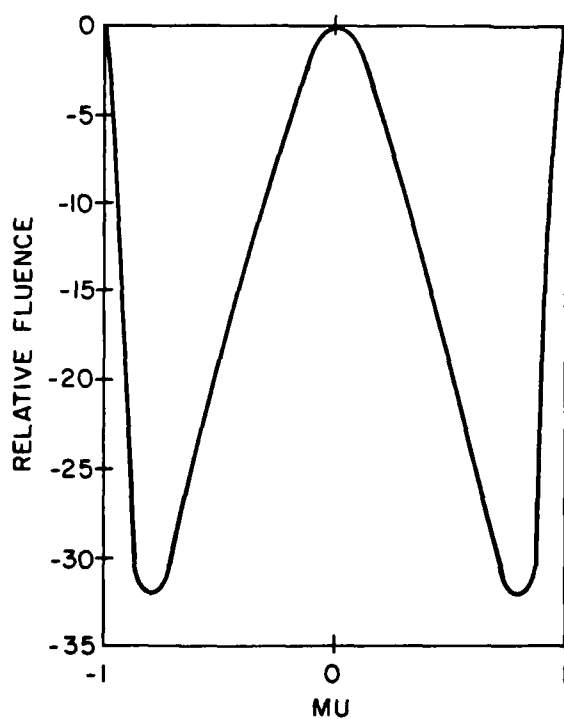
The conclusion of this chapter is that the collocation method is not suitable for solving the EPFBE. The main failure of this technique lies in its point-wise definition. This definition forces the selected



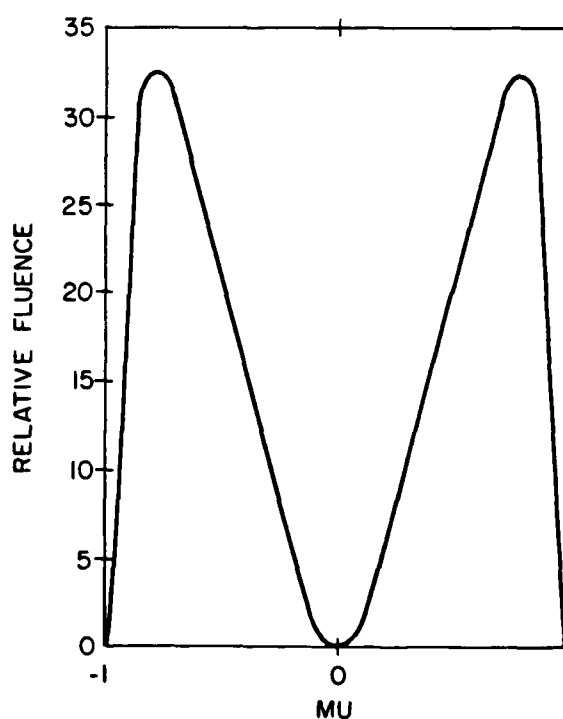
a.  $\sigma_r = 1$   $\chi = 0$



b.  $\sigma_r = 1$   $\chi = \pi$

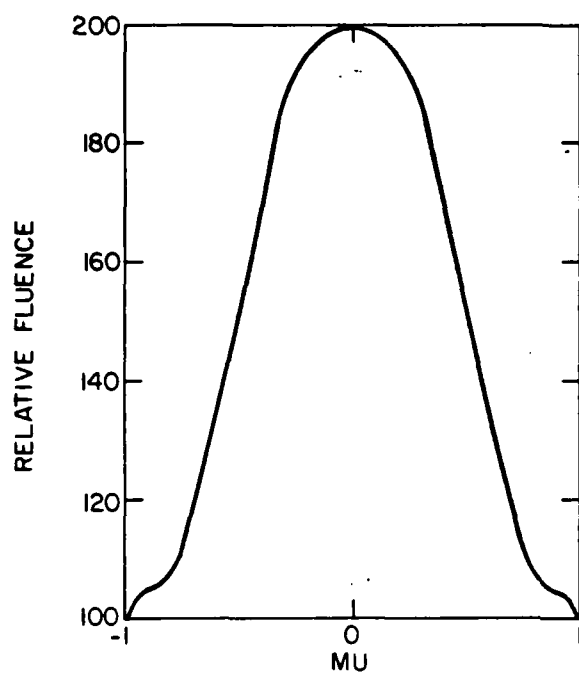


c.  $\sigma_r = 1$   $\chi = 0$

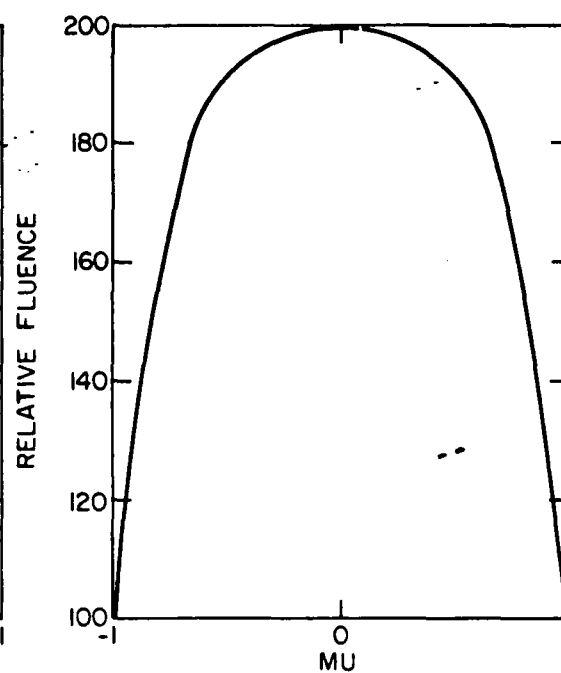


d.  $\sigma_r = 1$   $\chi = \pi$

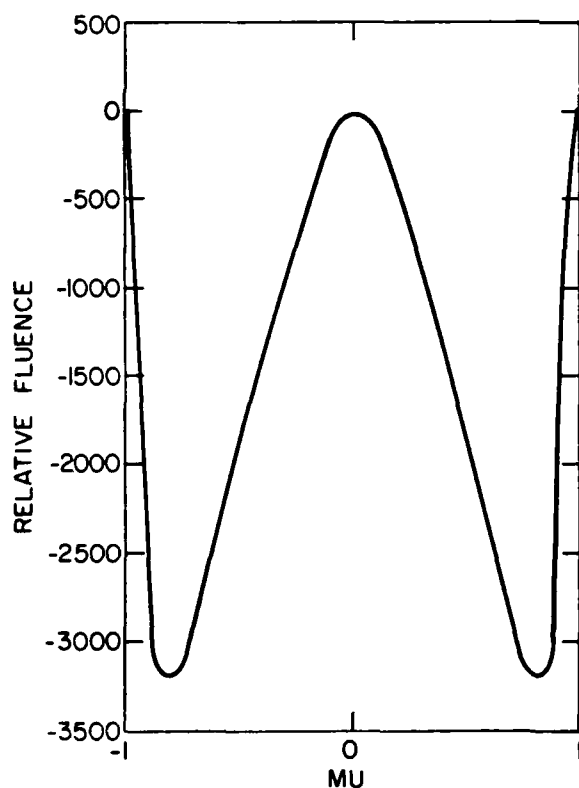
Fig 13. Even and Odd-Parity Fluence



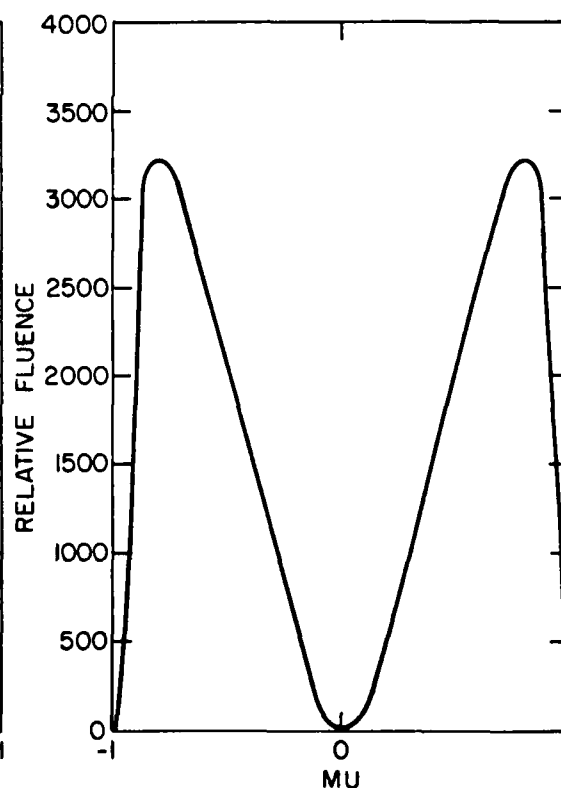
a.  $\sigma_r = 1$   $\chi = 0$



b.  $\sigma_r = 1$   $\chi = \pi$



c.  $\sigma_r = .0001$   $\chi = 0$



d.  $\sigma_r = .0001$   $\chi = \pi$

Fig 14. Boltzmann Fluence

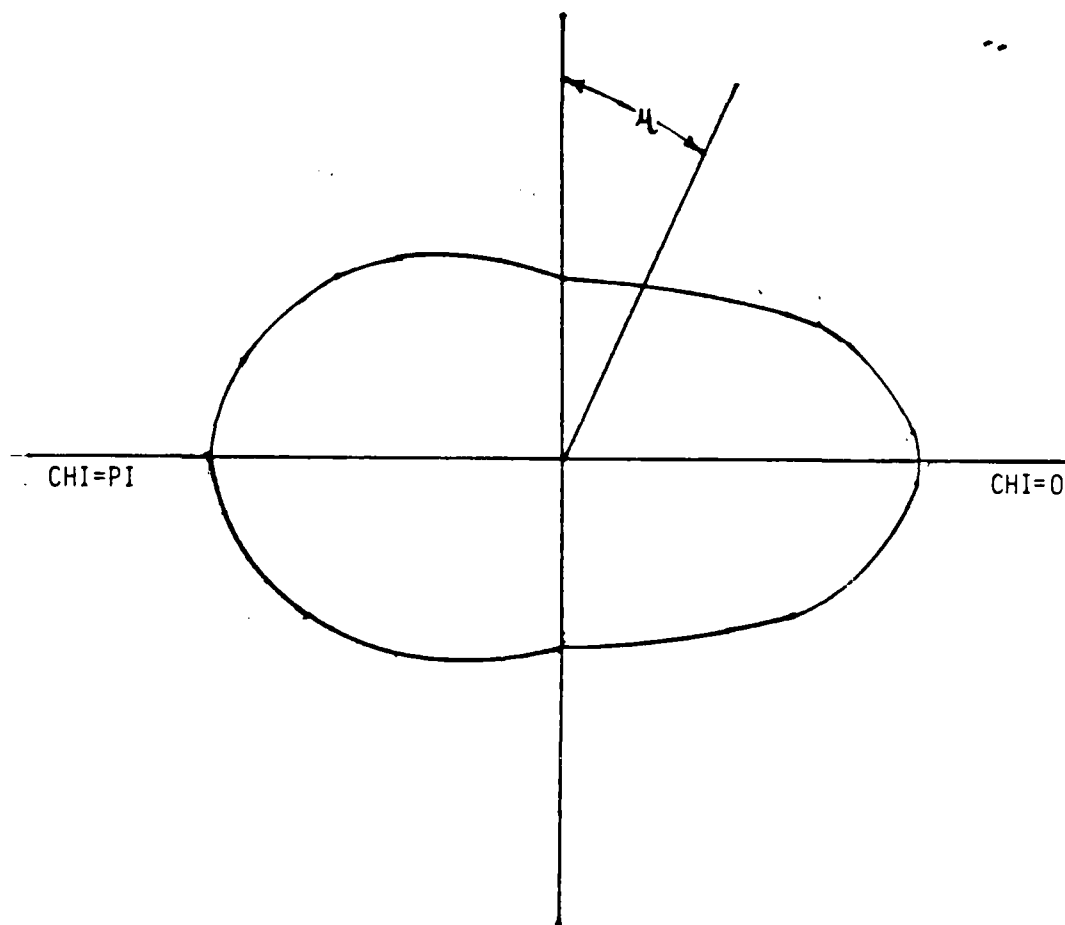


Fig 15. Polar Plot of Boltzmann Fluence

trial solution to accurately represent the even-parity fluence and be transformable into an accurate representation of the odd-parity fluence. As seen in this chapter the standard finite element trial solution (pure spline basis) and combination finite element synthesis function trial solution do not meet this criterion. The Galerkin method reduces these stringent requirements on the trial solution by allowing the even-parity equation to hold in an integral sense rather than a point-wise sense. The integration operations associated with the Galerkin weak form equation act as a smoothing apparatus and shapes the trial solution to meet the phase space volume requirements imposed by the weak form equation. Ironically the very thing that caused the Galerkin method to fail, the nested integrals, is also the reason a finite element method can successfully generate solutions to the EPFBE.

#### IV. Multigroup Considerations

##### Background

The energy dependence of neutral particle fluences must be considered in an air-over-ground problem. The multigroup method (Ref. 1) is used to approximate this dependence. In multigroup theory the definition of various cross sections are modified and new cross sections are defined. Multigroup cross sections have been previously presented in relation to Eq. (1.3) for the regular Boltzmann equation. Similar definitions result from the EPFBE when formulated in a multigroup structure. The EPFBE written for group  $h$  is

$$-\hat{n} \cdot \nabla K_h^{\circ} \hat{n} \cdot \nabla \Psi^h(\hat{r}, \hat{n}) + G_h^{\circ} \Psi^h(\hat{r}, \hat{n}) = S_T^h(\hat{r}, \hat{n}) - \hat{n} \cdot \nabla K_h^{\circ} S_T^h(\hat{r}, \hat{n}) \quad (4.1)$$

where

$\Psi^h(\hat{r}, \hat{n})$  = the even-parity fluence for group  $h$

$K_h$  and  $G_h$  are equivalent to the  $K_u$  and  $G_g$  operators written for group  $h$  and are defined as

$$K_h^{\circ} f^h(\hat{n}) = \frac{1}{\sigma_T^h(\hat{r})} \left( f^h(\hat{n}) + \int_{4\pi} \sigma_{sh}^h(\hat{n}; \hat{n}') f^h(\hat{n}') d\hat{n}' \right) \quad (4.2)$$

$$G_h^{\circ} f^h(\hat{n}) = \sigma_T^h(\hat{r}) f^h(\hat{n}) - \int_{4\pi} \sigma_{sh}^h(\hat{n}; \hat{n}') f^h(\hat{n}') d\hat{n}' \quad (4.3)$$

where

$\sigma_T^h(\hat{r})$  = macroscopic total cross section for group  $h$

$\sigma_{sh}^h(\hat{n}; \hat{n}')$  = in group even-parity differential scattering cross section

$$\sigma_{sh}^h(\hat{n}; \hat{n}') = \sum_{\ell=0,2,4,\dots}^{\infty} \frac{\sigma_{\ell}^h(\hat{r})}{\sigma_T^h(\hat{r}) - \sigma_{\ell}^h(\hat{r})} P_{\ell}(\hat{n} \cdot \hat{n}')$$

( $\sigma_{\ell}^h(\hat{r})$  =  $\ell$ th order Legendre coefficient for group  $h$ )

( $P_{\ell}(\hat{n} \cdot \hat{n}')$  =  $\ell$ th order Legendre polynomial)

${}^eS_T^h(\vec{r}, \lambda)$  and  ${}^oS_T^h(\vec{r}, \lambda)$  are equivalent to the even and odd-parity source terms written for group h. These terms differ from the monoenergetic forms of these source terms in that the down-scatter from higher energy groups must be included as dictated by particle conservation. The even and odd-parity multigroup source terms can be defined respectively as

$${}^eS_T^h(\vec{r}, \lambda) = S_e^h(\vec{r}, \lambda) + \int_{4\pi} \sum_{g=1}^{h-1} \sigma_{sg}^e(\vec{r}, \lambda; \lambda') \Psi^g(\lambda') d\lambda' \quad (4.4)$$

$${}^oS_T^h(\vec{r}, \lambda) = S_o^h(\vec{r}, \lambda) + \int_{4\pi} \sum_{g=1}^{h-1} \sigma_{sg}^o(\vec{r}, \lambda; \lambda') \chi^g(\lambda') d\lambda' \quad (4.5)$$

where

$S_e^h(\vec{r}, \lambda)$  = group h even-parity source term

$S_o^h(\vec{r}, \lambda)$  = group h odd-parity source term

$\sigma_{sg}^e(\vec{r}, \lambda; \lambda')$  = even-parity down scatter cross section from group g to group h

$\sigma_{sg}^o(\vec{r}, \lambda; \lambda')$  = odd-parity down-scatter cross section from group g to group h

$\Psi^g(\vec{r}, \lambda)$  = even-parity fluence in group g

$\chi^g(\vec{r}, \lambda)$  = odd-parity fluence in group g

### Multigroup Analysis

A multigroup solution of Eq. (4.1) was accomplished by Kaper, Leaf, and Lindeman (Ref. 27) using the variational formulation of this equation. These authors assumed that the scattering was isotropic. In an air-over-ground problem this assumption cannot be made, since scattering in air is extremely anisotropic. When the scattering must be modeled as anisotropic, the left hand side of the weak form of the EPFBE becomes extremely complex as evidenced in Chapter II. When the multigroup method is applied

to either the EPFBE or its weak form the source terms increase substantially in complexity. The multigroup method does not significantly affect the left-hand side of either formulation.

To illustrate this increased complexity a comparison is made between using an isotropic and anisotropic scattering representation in the source terms of the multigroup EPFBE. For an isotropic scattering process Eqs. (4.4) and (4.5) can be rewritten as

$$^o S_r^h(\vec{r}, \hat{\lambda}) = S_e^h(\vec{r}, \hat{\lambda}) + \sum_{g=1}^{h-1} \sigma_{sg}^o \int_{4\pi} \Psi^g(\hat{\lambda}') d\hat{\lambda}' \quad (4.6)$$

$$^o S_r^h(\vec{r}, \hat{\lambda}) = S_o^h(\vec{r}, \hat{\lambda}) \quad (4.7)$$

The integral term in Eq. (4.5) is only defined for odd Legendre coefficients and thus for an isotropic scattering process equals zero. Eq. (4.6) is analogous to Eqs. (2.28) and (2.29) in terms of simplicity and once again allows the integral in Eq. (4.6) to be evaluated once to any desired accuracy and stored for future use. The simplifying assumption of isotropic scatter played an essential role in the successful results generated by the previously mentioned authors.

Anisotropic scattering forces the use of the odd-parity fluence term in a multigroup formulation. This term appears in the odd-parity source term as illustrated in Eq. (4.5). Substituting the definition of the odd-parity fluence into Eq. (4.5) yields

$$^o S_r^h(\vec{r}, \hat{\lambda}) = S_o^h(\vec{r}, \hat{\lambda}) + \int_{4\pi} \sum_{g=1}^{h-1} \sigma_{sg}^o(\vec{r}, \hat{\lambda}; \hat{\lambda}') K_h^o(S_r^g(\vec{r}, \hat{\lambda}') \cdot \hat{\lambda}) \Psi^g(\hat{\lambda}') d\hat{\lambda}' \quad (4.8)$$

The complexity of Eq. (4.8) can best be illustrated by assuming a multigroup problem with  $n$  groups. For the first group the odd-parity source term can be written as

$$^{\circ}S'_T(\vec{r}, \hat{\lambda}) = S'_0(\vec{r}, \hat{\lambda}) \quad (4.9)$$

The second group odd-parity source term must include a down-scatter term to account for the neutral particles that scattered from group 1 to group 2.

$$^{\circ}S'_T(\vec{r}, \hat{\lambda}) = S'_0(\vec{r}, \hat{\lambda}) + \int_{4\pi} \sigma_{s_{12}}^{\circ}(\vec{r}, \hat{\lambda}; \hat{\lambda}') \chi'_1(\vec{r}, \hat{\lambda}') d\hat{\lambda}' \quad (4.10)$$

but as previously described

$$\chi'_1(\vec{r}, \hat{\lambda}) = K_1^{\circ} \left( ^{\circ}S'_T(\vec{r}, \hat{\lambda}') - \hat{\lambda}' \cdot \nabla \Psi'_1(\vec{r}, \hat{\lambda}') \right) \quad (4.11)$$

and thus Eq. (4.10) can be written as

$$^{\circ}S'_T(\vec{r}, \hat{\lambda}) = S'_0(\vec{r}, \hat{\lambda}) + \int_{4\pi} \sigma_{s_{12}}^{\circ}(\vec{r}, \hat{\lambda}; \hat{\lambda}') \left\{ K_1^{\circ} \left( S'_0(\vec{r}, \hat{\lambda}') - \hat{\lambda}' \cdot \nabla \Psi'_1(\vec{r}, \hat{\lambda}') \right) \right\} d\hat{\lambda}' \quad (4.12)$$

The complexity of the multigroup method becomes evident in formulating the odd-parity source term for group 3. This source term can be written as

$$^{\circ}S'_T(\vec{r}, \hat{\lambda}) = S'_0(\vec{r}, \hat{\lambda}) + \int_{4\pi} \left\{ \sigma_{s_{13}}^{\circ}(\vec{r}, \hat{\lambda}; \hat{\lambda}') \chi'_1(\vec{r}, \hat{\lambda}') + \sigma_{s_{23}}^{\circ}(\vec{r}, \hat{\lambda}; \hat{\lambda}') \chi'_2(\vec{r}, \hat{\lambda}') \right\} d\hat{\lambda}' \quad (4.13)$$

Expanding the second term in the integral results in

$$\int_{4\pi} \sigma_{s_{23}}^{\circ}(\vec{r}, \hat{\lambda}; \hat{\lambda}') \left\{ K_2^{\circ} \left( ^{\circ}S'_T(\vec{r}, \hat{\lambda}') - \hat{\lambda}' \cdot \nabla \Psi'_2(\vec{r}, \hat{\lambda}') \right) \right\} d\hat{\lambda}' \quad (4.14)$$

Substituting Eq. (4.12) into the first term of Eq. (4.14) generates

$$\int_{4\pi} \sigma_{s_{23}}^{\circ}(\vec{r}, \hat{\lambda}; \hat{\lambda}') K_2^{\circ} \left[ S'_0(\vec{r}, \hat{\lambda}') + \int_{4\pi} \sigma_{s_{12}}^{\circ}(\vec{r}, \hat{\lambda}''; \hat{\lambda}') \left\{ K_1^{\circ} \left( S'_0(\vec{r}, \hat{\lambda}'') - \hat{\lambda}'' \cdot \nabla \Psi'_1(\vec{r}, \hat{\lambda}'') \right) \right\} d\hat{\lambda}'' \right] d\hat{\lambda}' \quad (4.15)$$

If all the terms resulting from the  $K_u$  operator were written out in full form, one term in Eq. (4.15) would appear as

$$\frac{1}{\sigma_T^2(\vec{r})} \frac{1}{\sigma_T^2(\vec{r})} \int_{4\pi} \sigma_{s_{22}}^0(\vec{r}, \hat{\lambda}; \hat{\lambda}) \int_{4\pi} \sigma_{\kappa\mu}^2(\vec{r}, \hat{\lambda}''; \hat{\lambda}') \int_{4\pi} \sigma_{s_{12}}^0(\vec{r}, \hat{\lambda}'''; \hat{\lambda}'') \int_{4\pi} \sigma_{\kappa\mu}^1(\vec{r}, \hat{\lambda}''''; \hat{\lambda}''') S_0^1(\hat{\lambda}''''') d\hat{\lambda}'''' d\hat{\lambda}''' d\hat{\lambda}'' d\hat{\lambda}' \quad (4.16)$$

In a similar manner the term in Eq. (4.15) containing  $\hat{\lambda} \cdot \nabla \Psi(\vec{r}, \hat{\lambda})$  also becomes embedded in a set of nested integrals. When the  $K_h^0$  operator is fully expanded one term of this expansion would appear as

$$\frac{1}{\sigma_T^2(\vec{r})} \frac{1}{\sigma_T^2(\vec{r})} \int_{4\pi} \sigma_{s_{22}}^0(\vec{r}, \hat{\lambda}; \hat{\lambda}) \int_{4\pi} \sigma_{\kappa\mu}^2(\vec{r}, \hat{\lambda}''; \hat{\lambda}') \int_{4\pi} \sigma_{s_{12}}^0(\vec{r}, \hat{\lambda}'''; \hat{\lambda}'') \int_{4\pi} \sigma_{\kappa\mu}^1(\vec{r}, \hat{\lambda}''''; \hat{\lambda}''') \hat{\lambda}'''' \cdot \nabla \Psi(\vec{r}, \hat{\lambda}''''') d\hat{\lambda}'''' d\hat{\lambda}''' d\hat{\lambda}'' d\hat{\lambda}' \quad (4.17)$$

The nesting problem for both Eqs. (4.16) and (4.17) becomes worse when the number of energy groups increases. The problems involved with evaluating the integrals in Eq. (4.17) are similar to those mentioned in Chapter II for both a pure spline and spline synthesis trial solution.

The complexity illustrated in Eqs. (4.16) and (4.17) increases when the odd-parity source is placed in the Galerkin or collocation formulations. For the Galerkin formulation the odd-parity source term appears in the following term

$$\int_{\vec{r}} \int_{4\pi} \langle \hat{\lambda} \cdot \nabla \epsilon(\vec{r}, \hat{\lambda}), K_0^1 \cdot S_T^1(\vec{r}, \hat{\lambda}) \rangle d\hat{\lambda} d\vec{r} \quad (4.18)$$

In the collocation method it appears as

$$\hat{\lambda} \cdot \nabla K_0^1 \cdot S_T^1(\vec{r}, \hat{\lambda}) \quad (4.19)$$

The complexity of doing multigroup calculations using the EPFBE does not exist for the first-order Boltzmann equation. The essential difference is that the first-order Boltzmann fluence is not defined in terms of a source. The odd-parity fluence is dependent on the odd-parity source term due to the requirement of defining this fluence in terms of the even-parity fluence during the derivation of the EPFBE. The complexity introduced by applying the multigroup method to the EPFBE is analogous to the complexity that evolved in the Galerkin method.

This chapter has demonstrated the problems involved with using the EPFBE in a multigroup scheme. These problems must be solved before this equation can be used to generate accurate and cost effective solutions to an air-over-ground problem.

## V. Summary, Conclusions and Recommendations

### Summary and Conclusions

The purpose of this research was to determine the feasibility of using the even-parity equation to calculate the neutral particle fluence distribution for an air-over-ground problem. In pursuing this research several different approaches were attempted. Each of these approaches involved an application of a standard finite element technique to an appropriate form of the EPFBE. The only deviation from this standard approach involved the use of the synthesis method. This deviation can not be considered radical since numerous authors reported its successful use in solving transport problems. The choice of the EPFBE was motivated by its mathematical properties that potentially eliminated ray effects. Combining the finite element and synthesis method to solve the EPFBE appeared to be reasonable.

Two basic problems related to the EPFBE evolved. The first problem involved the complexity that occurred when the weak form of the EPFBE was applied to the air-over-ground problem. The two-dimensional cylindrical geometry required by this problem coupled with the need for a  $P_3$  scattering representation contributed heavily to this complexity. Another contributor was the finite element method. The discretized angular and spatial domain used with this method and the linear Lagrange polynomial trial solution defined over these domains eliminated the use of analytical methods for evaluating the weak form equation integrals. Numerical integration of this trial solution over the same domains was extremely inefficient and would have required a high order quadrature set to generate acceptable results. The cost of numerically evaluating the weak

form integrals to the necessary accuracy proved prohibitive for a full scale air-over-ground problem.

This integral problem originated from the choice of the Galerkin method. Angular integrals were already present in the EPFBE because of the  $K_u$  and  $G_g$  operators. The definition of the Galerkin method added additional angular and spatial integrals that resulted in the nesting of up to six integrals in some terms of the weak form equation. Other finite element methods such as least squares would have generated the same nesting problems and complex integrands as the Galerkin method.

The synthesis method was not successful with the weak form of the EPFBE due to the choice of the function representing the angular distribution. This synthesis function was not analytically integrable and was complex enough to require the use of higher order quadrature sets. Additionally, the form of the function did not allow the pitch parameters of the ellipsoid, which are spatially dependent, to be separated from the angularly dependent variables. This fault eliminated the possibility of separating the angularly and spatially dependent terms in the weak form equation and forced all integral evaluations to be coupled. Such a coupling required all integrals to be reevaluated whenever the spatial mesh was altered.

A conclusion of this research is that the use of a pure linear Lagrange trial solution coupled with any of the integrally defined finite element solution techniques does not provide a viable means for solving the EPFBE formulated for an air-over-ground problem. This conclusion probably applies to any two-dimensional transport problem requiring the use of a  $P_3$  scattering representation.

The second basic problem associated with the EPFBE involves the odd-parity fluence transformation. As demonstrated in Chapter III this transformation forces a certain anisotropy on the solution of a transport problem and adversely affects the collocation evaluation of any term in the EPFBE or boundary condition that contains the odd-parity fluence. The form of this anisotropy is fixed and at best can only be scaled in magnitude by the solution coefficients determined from the collocation method. The only possible situation that would allow an acceptable solution is when the anisotropy generated from the odd-parity fluence transformation matches the anisotropy of the true solution. Such a situation is highly improbable and certainly was not the case for the air-over-ground problem.

Attempting to derive a synthesis trial solution that accurately represented the anisotropy of a particular problem would be extremely difficult. Such a synthesis function would need to satisfy the constraints imposed by the even-parity fluence and be transformable using derivative and integral operations into a function that accurately approximates the odd-parity fluence or anisotropy. The central difficulty of this derivation would be understanding what constitutes a good representation of the anisotropy for a certain problem. Most transport problems are so complex that accurately approximating the anisotropy would be virtually impossible. Additionally, the type of transport problem that the above derivation would be applicable must have a fixed anisotropy across the spatial domain. Few realistic problems meet this constraint.

The forced anisotropy originating from the odd-parity fluence transformation also affects a pure spline trial solution. The effect of

this anisotropy appears between the nodes and modifies the shape of the spline functions in the angular domain. At the nodes the collocation method forces the correct solution. This modification from the original spline shape is the forced anisotropy induced by the odd-parity fluence transformation. The only cure for this problem is to space the nodes closer together in the angular domain. The consequence of this action is to create a global matrix of high order that is costly to compute and inefficient to solve. The optimum spacing of the nodes would have to be determined through experimentation and would vary from one type of transport problem to another.

It is concluded from this research that the collocation method can not be effectively applied to the EPFBE. This statement must be qualified. The synthesis method is totally incompatible with the requirements of forming the odd-parity fluence through the odd-parity fluence transformation and thus an efficient solution method based on synthesis and collocation is not possible. A pure spline trial solution might generate an acceptable transport solution with the collocation method; however, the amount of discretization required in the angular domain to offset the forced anisotropy would prohibit the classification of this approach as efficient.

The multigroup problems described in Chapter IV are common to any solution technique proposed for use with the EPFBE. The structure this method imposes compounds the complexity already inherent in the EPFBE. This complexity increases with the number of energy groups and would restrict the use of the many grouped cross section sets commonly used in an air-over-ground problem. Accurate transport solutions are not possible without using these cross sections. A conclusion of this

research is that the standard multigroup method can not be used with the EPFBE formulated for an air-over-ground problem.

Three significant points concerning the EPFBE have resulted from this research. Miller, Lewis, and Rossow (Refs. 25 and 26) presented a solution technique that successfully eliminated the ray effect. The finite element method applied to the even-parity functional appeared to have potential for other types of transport problems that are affected by this numerical problem. This research has definitively demonstrated that the work of the above authors can not be extended to an air-over-ground problem and is probably limited to the simple geometries and scattering models used in their published work.

This research has also provided the basic criteria for attempting future work with the EPFBE. The solution technique used to solve this equation must be integrally defined and contain the vacuum boundary condition as a natural condition. The trial solution selected for use with the EPFBE must be globally defined, thus eliminating the inefficient numerical integration problems encountered in Chapter II. If the trial solution contains an angular synthesis function it must be simple in form and allow those parameters related to the pitch of the streaming direction to be separated from other angular variables.

The third point addresses the problem of reconstructing the Boltzmann fluence from a numerical solution of the EPFBE. As demonstrated in Chapter III, the odd-parity fluence transformation does not accurately represent the anisotropic portion of the Boltzmann fluence. The central problem with this transformation is its dependence on the spatial and angular derivatives of the selected trial solution. Typical finite element trial

solutions are selected primarily on the requirement of mathematical continuity. Synthesis trial solutions are selected because they accurately approximate some functional variation of interest. For the even-parity equation neither of these types of trial solutions are satisfactory because their angular and spatial derivatives do not accurately approximate the anisotropic portion of the Boltzmann fluence. Additionally, the specification of the EPFBE does nothing to constrain these derivatives for accurately approximating the odd-parity fluence. It is a conclusion of this research that the anisotropic component of the Boltzmann fluence can not be accurately calculated using standard finite element and synthesis techniques. The impact of this conclusion is that the Boltzmann fluence can not be accurately derived from a solution of the EPFBE resulting from the use of these numerical methods. Successful work using this equation was always reported in terms of the scalar fluence. The angular fluence results were never presented.

#### Recommendations

Three facets of future work are proposed for calculating scalar fluences with the monoenergetic form of the EPFBE. First, a parametric study should be performed to determine the effect of reducing the order of the Legendre expansion representing the differential scattering cross section. If a  $P_1$  representation could produce acceptable results, the decrease in complexity would allow the analytical formulation of the weak form of the EPFBE using a pure linear Lagrange trial solution.

Second, the angular synthesis function presented in Chapter III for use with the collocation method should be attempted with the weak form of the EPFBE. The successful analytical formulation of the EPFBE using the collocation method grants much credence to this proposal. Additionally

this angular synthesis function allows the pitch parameter to be separated from the other angular variables. This property would permit a total separation of the spatially and angularly dependent terms and thus the individual integral evaluation of each. Since this angular synthesis function is globally defined all analytical evaluations could be accomplished using definite integrals. These definite integrals would not create the large number of terms in MACSYMA experienced in the indefinite integration process used in Chapter II. This proposal is not without risk. The trigonometric functions in the angular synthesis function must be multiplied by similar functions as specified by the Galerkin method. These products of trigonometric functions are analytically evaluated using reduction formulas that can generate several terms. This increased number of terms coupled with the extra integration over the angular domain required by the Galerkin method could cause problems with MACSYMA's limited memory. If memory problems evolve, a combination of analytical and numerical integration could prove feasible.

The third proposal involves a modified form of the synthesis trial solution presented in Chapter III. This trial solution can be modified for use with the first-order Boltzmann equation. Adding an odd function to this trial solution would result in

$$\Phi(\vec{r}, \hat{n}) = \sum_{i=1}^N \sum_{j=1}^M \theta_i(\rho) \theta_j(z) (a_{1ij} + a_{2ij} \mu_0 + a_{3ij} \mu_0^2) \quad (5.1)$$

$$\mu_0 = \mu \mu_0 + \sqrt{1 - \mu^2} \sqrt{1 - \mu_0^2} \cos(x - x_0) \quad (5.2)$$

and all other terms have been previously defined. This odd term allows the anisotropy of the first-order Boltzmann fluence to be defined and specifically controlled by the  $a_{2i}$  coefficient. This control was not available in the EPFBE.

The trial solution in Eq. (5.1) could be used with several formulations of the first-order Boltzmann equation. The collocation method could be directly applied to this equation, since no odd-parity fluence transformation exists. The one possible drawback to applying this method involves the hyperbolic nature of the first-order Boltzmann equation. Articles do not appear in the literature that successfully demonstrate the application of the collocation method to a hyperbolic equation. The work by Houstis, Lynch, Rice, and Papatheodorou (Ref. 35) considered only elliptic equations. A research project attempting this application should initially study the effects of collocating hyperbolic equations.

Another numerical method that would be compatible with the trial solution in Eq. (5.1) and first-order Boltzmann equation is the weighted residual technique used by Roberds and Bridgman. Their trial solution had the same number of unknowns per spatial point as the one in Eq. (5.1), but only provided a  $P_1$  type of angular approximation. The  $\mu^2$  term in Eq. (5.1) offers a  $P_2$  type of approximation for the same number of unknowns. Roberds and Bridgman used the method of finite differences to evaluate the spatial variation of the fluence. The splines in Eq. (5.1) would serve the same purpose and could be analytically evaluated using MACSYMA.

## BIBLIOGRAPHY

1. Bell, G.I. and Glasstone, S., Nuclear Reactor Theory, New York: Van Nostrand Reinhold Co., 1970.
2. Straker, E.A., The Effect of the Ground on the Steady-State and Time-Dependent Transport of Neutrons and Secondary Gamma Rays in the Atmosphere, Nucl. Sci. Eng., 46:344-355 (1971).
3. Shulstad, R.A., An Evaluation of Mass Integral Scaling as Applied to the Atmospheric Radiation Transport Problem, DS/PH/76-3, Wright-Patterson AFB, OH: AFIT, November 1976.
4. Mynatt, F.R., Muckenthaler, F.J., and Stevens, P.N., "Development of Two-Dimensional Discrete Ordinates Transport Theory for Radiation Shielding," Union Carbide Corporation, Nuclear Division (1969).
5. Carlson, B.G. and Lathrop, K.D., "Transport Theory - The Method of Discrete Ordinates." Computing Methods in Reactor Physics, Chapter III, Greenspan, Kelber, and Okrent, Eds., Gordon and Breach, New York (1968).
6. Lathrop, K.D., "Ray Effects in Discrete Ordinates Equations." Nucl. Sci. Eng., 32:357-369 (1968).
7. Lathrop, K.D., "Remedies for Ray Effects," Nucl. Sci. Eng., 45:255-268 (1971).
8. Jung, Jungchung, "Discrete Ordinate Neutron Transport Equation Equivalent to  $P_L$  Approximation," Nucl. Sci. Eng., 49:1-9 (1972).
9. Reed, W.H., "Spherical Harmonic Solutions of the Neutron Transport Equation from Discrete Ordinate Codes." Nucl. Sci. Eng., 49:10-19 (1972).
10. Jung, Jungchung, "Second Order Discrete Ordinate  $P_L$  Equations in Multi-Dimensional Geometry." Journal of Nuclear Energy, 27:577-590 (1973).
11. Jung, Jungchung, "Solution of Standard Diamond Difference Equations for Discrete-Ordinate Neutron Transport Equations Equivalent to the  $P_L$  Approximation in x-y Geometry." Nucl. Sci. Eng., 53:355-364 (1974).
12. Lathrop, K.D., Private Communication. Energy Division, Los Alamos Scientific Laboratory, January 17, 1978.
13. French, R.L., "A First-Last Collision Model of the Air/Ground Interface Effects on Fast Neutron Distributions," Nucl. Sci. Eng., 19:151-157 (1964).
14. French, R.L., Mooney, L.G., "Last-Collision Model of the Air-Ground Interface Effect on Fast-Neutron Angle Distributions," Nucl. Sci. Eng., 19:151-157 (1964).

15. Guy, R.W., Albert, T.E., and Straker, E.A., "A Comprehensive Model for Initial Weapons Radiation Environments," Tran. Am. Nucl. Soc., 19:452 (1974).
16. Vladimirov, V.S., "Mathematical Problems in the One-Velocity Theory of Particle Transport," Atomic Energy of Canada, Ltd., Ontario (1963), translated from Trans. V.A. Steklov Mathematical Institute, 61 (1961).
17. Kaplan, S. and Davis, J.A., "Canonical and Involuntary Transformation of the Variational Problems of Transport Theory." Nucl. Sci. Eng., 28: 166-176 (1967).
18. Kaplan, S., Davis, J.A., and Natelson, M., "Angle-Space Synthesis--An Approach to Transport Approximations." Nucl. Sci. Eng., 28:364-375 (1967).
19. Natelson, M., "A Strategy for the Application of Space-Angle Synthesis to Practical Problems in Neutron Transport." Nucl. Sci. Eng., 31:325-336 (1968).
20. Kaplan, S., "Synthesis Methods in Reactor Analysis." Advances in Nuclear Science and Technology, 3:233-266 (1966).
21. Stacey, W.M., Jr., "Flux Synthesis Methods in Reactor Physics." Reactor Technology, 15:210-238 (Fall 1972).
22. Kaplan, S., "Some New Methods of Flux Synthesis." Nucl. Sci. Eng., 13:22-31 (1962).
23. Roberds, R. and Bridgman, C., "Application of Space-Angle Synthesis to Two-Dimensional Neutral-Particle Transport Problems of Weapon Physics." Nucl. Sci. Eng., 64:332-343 (1977).
24. Miller, W.F., Lewis, E.E., and Rossow, E.C., "The Application of Phase-Space Finite Elements to the One-Dimensional Neutron Transport Equation." Nucl. Sci. Eng., 51:148-156 (1973).
25. Miller, W.F., Lewis, E.E., and Rossow, E.C., "The Application of Phase-Space Finite Elements to the Two-Dimensional Neutron Transport Equation in x-y Geometry." Nucl. Sci. Eng., 52:12-22 (1973).
26. Reed, W.H., Hill, R.R., Brinkley, F.W., and Lathrop, K.D., "TRIPLET: A Two-Dimensional, Multigroup Triangular Mesh, Planar Geometry, Explicit Transport Code." Los Alamos Scientific Laboratory, LA-5428-MS, October 1973.
27. Kaper, H.G., Leaf, G.K., and Lindeman, A.J., Applications of Finite Element Methods in Reactor Mathematics. Numerical Solution of the Neutron Transport Equation. ANL-8126, Argonne National Laboratory (1974).
28. Briggs, L.L., Miller, W.F., and Lewis, E.E., "Ray-Effect Mitigation in Discrete Ordinate-Like Angular Finite Element Approximations in Neutron Transport," Nucl. Sci. Eng., 57:205-217 (1975).

29. Zachmanoglou, E.C. and Thoe, D.W., Introduction to Partial Differential Equations with Applications, Baltimore: The Williams and Wilkens Company, 1976.
30. Luenberger, D.G., Optimization by Vector Space Methods, John Wiley Co., 1969.
31. Huebner, Kenneth J., The Finite Element for Engineers, John Wiley Co., 1975.
32. Wheaton, Ronald C., AFIT/GNE/PH/78D-15, Wright-Patterson AFB, OH: AFIT, December 1978.
33. Strang, Gilbert, and Fix, George J., An Analysis of the Finite Element Method, Prentice-Hall Inc., 1973.
34. MACSYMA Reference Manual, Massachusetts Institute of Technology, 1977.
35. Houstis, E.N., Lynch, R.E., Rice, J.R., and Papatheodorou, T.S., "Evaluation of Numerical Methods for Elliptic Partial Differential Equations," *Journal of Computational Physics*, 27:323-350 (1978).
36. Davis, Harry F., Introduction to Vector Analysis, Allyn and Bacon, Inc., 1967.

AD-A100 801

AIR FORCE INST OF TECH WRIGHT-PATTERSON AFB OH SCHOO—ETC F/G 12/1  
ANALYTICAL AND NUMERICAL PROBLEMS ASSOCIATED WITH EXTENDING TH—ETC(U)  
JUN 81 J C SOUNDERS

UNCLASSIFIED

AFIT/DS/PH/81-2

NL

2 of 2  
AD-A100 801



END  
DATE  
FILMED  
9-81  
DTIC

# APPENDIX A

## DERIVATION OF EVEN-PARITY FORM OF THE BOLTZMANN NEUTRON TRANSPORT EQUATION

The monoenergetic steady-state Boltzmann neutron transport equation can be written as

$$\hat{\lambda} \cdot \nabla \Phi(\vec{r}, \hat{\lambda}) + \sigma_T(\vec{r}) \Phi(\vec{r}, \hat{\lambda}) - \int_{4\pi} \sigma_s(\vec{r}, \hat{\lambda}' \cdot \hat{\lambda}) \Phi(\vec{r}, \hat{\lambda}') d\hat{\lambda}' - S(\vec{r}, \hat{\lambda}) = 0 \quad (A.1)$$

Since this equation holds for  $\hat{\lambda}$  it must also hold for  $-\hat{\lambda}$

$$-\hat{\lambda} \cdot \nabla \Phi(\vec{r}, -\hat{\lambda}) + \sigma_T(\vec{r}) \Phi(\vec{r}, -\hat{\lambda}) - \int_{4\pi} \sigma_s(\vec{r}, \hat{\lambda}' \cdot -\hat{\lambda}) \Phi(\vec{r}, \hat{\lambda}') d\hat{\lambda}' - S(\vec{r}, -\hat{\lambda}) = 0 \quad (A.2)$$

If Eqs. (A.1) and (A.2) are added together the following results:

$$\begin{aligned} & \hat{\lambda} \cdot \nabla (\Phi(\vec{r}, \hat{\lambda}) - \Phi(\vec{r}, -\hat{\lambda})) + \sigma_T(\vec{r}) (\Phi(\vec{r}, \hat{\lambda}) + \Phi(\vec{r}, -\hat{\lambda})) - \\ & \int_{4\pi} (\sigma_s(\vec{r}, \hat{\lambda}' \cdot \hat{\lambda}) + \sigma_s(\vec{r}, \hat{\lambda}' \cdot -\hat{\lambda})) \Phi(\vec{r}, \hat{\lambda}') d\hat{\lambda}' - (S(\vec{r}, \hat{\lambda}) + S(\vec{r}, -\hat{\lambda})) = 0 \end{aligned} \quad (A.3)$$

Subtracting Eq. (A.2) from Eq. (A.1) results in

$$\begin{aligned} & \hat{\lambda} \cdot \nabla (\Phi(\vec{r}, \hat{\lambda}) + \Phi(\vec{r}, -\hat{\lambda})) + \sigma_T(\vec{r}) (\Phi(\vec{r}, \hat{\lambda}) - \Phi(\vec{r}, -\hat{\lambda})) - \\ & \int_{4\pi} (\sigma_s(\vec{r}, \hat{\lambda}' \cdot \hat{\lambda}) - \sigma_s(\vec{r}, \hat{\lambda}' \cdot -\hat{\lambda})) \Phi(\vec{r}, \hat{\lambda}') d\hat{\lambda}' - (S(\vec{r}, \hat{\lambda}) - S(\vec{r}, -\hat{\lambda})) = 0 \end{aligned} \quad (A.4)$$

Now define the following quantities:

$$\Psi(\vec{r}, \hat{\lambda}) = \frac{1}{2} [\Phi(\vec{r}, \hat{\lambda}) + \Phi(\vec{r}, -\hat{\lambda})] \quad (1.10)$$

$$\chi(\vec{r}, \hat{\lambda}) = \frac{1}{2} [\Phi(\vec{r}, \hat{\lambda}) - \Phi(\vec{r}, -\hat{\lambda})] \quad (A.5)$$

$$\sigma_{sg}(\vec{r}, \hat{\lambda}' \cdot \hat{\lambda}) = \frac{1}{2} [\sigma_s(\vec{r}, \hat{\lambda}' \cdot \hat{\lambda}) + \sigma_s(\vec{r}, \hat{\lambda}' \cdot -\hat{\lambda})] \quad (1.16)$$

$$\sigma_{5\mu}(\vec{r}, \hat{n}; \hat{n}) = \frac{1}{2} [\sigma_5(\vec{r}, \hat{n}; \hat{n}) - \sigma_5(\vec{r}, \hat{n}; -\hat{n})] \quad (\text{A.6})$$

$$S_{\mu}(\vec{r}, \hat{n}) = \frac{1}{2} [S(\vec{r}, \hat{n}) - S(\vec{r}, -\hat{n})] \quad (\text{1.11})$$

$$S_g(\vec{r}, \hat{n}) = \frac{1}{2} [S(\vec{r}, \hat{n}) + S(\vec{r}, -\hat{n})] \quad (\text{1.12})$$

Substituting these definitions into Eqs. (A.3) and (A.4) respectively results in

$$\begin{aligned} \hat{n} \cdot \nabla X(\vec{r}, \hat{n}) + \sigma_T(\vec{r}) \Psi(\vec{r}, \hat{n}) - \int_{4\pi} \sigma_{5g}(\vec{r}, \hat{n}; \hat{n}') \Phi(\vec{r}, \hat{n}') d\hat{n}' \\ - S_g(\vec{r}, \hat{n}) = 0 \end{aligned} \quad (\text{A.7})$$

$$\begin{aligned} \hat{n} \cdot \nabla \Psi(\vec{r}, \hat{n}) + \sigma_T(\vec{r}) X(\vec{r}, \hat{n}) - \int_{4\pi} \sigma_{5\mu}(\vec{r}, \hat{n}; \hat{n}') \Phi(\vec{r}, \hat{n}') d\hat{n}' \\ - S_{\mu}(\vec{r}, \hat{n}) = 0 \end{aligned} \quad (\text{A.8})$$

Now define the following operators

$$G_g f(\vec{r}, \hat{n}) = \sigma_T(\vec{r}) f(\vec{r}, \hat{n}) - \int_{4\pi} \sigma_{5g}(\vec{r}, \hat{n}; \hat{n}') f(\vec{r}, \hat{n}') d\hat{n}' \quad (\text{1.14})$$

$$G_{\mu} f(\vec{r}, \hat{n}) = \sigma_T(\vec{r}) f(\vec{r}, \hat{n}) - \int_{4\pi} \sigma_{5\mu}(\vec{r}, \hat{n}; \hat{n}') f(\vec{r}, \hat{n}') d\hat{n}' \quad (\text{A.9})$$

To use the above two equations the following must be proved

$$\int_{4\pi} \sigma_{5g}(\vec{r}, \hat{n}; \hat{n}') \Phi(\vec{r}, \hat{n}') d\hat{n}' = \int_{4\pi} \sigma_{5g}(\vec{r}, \hat{n}; \hat{n}') \Psi(\vec{r}, \hat{n}') d\hat{n}' \quad (\text{A.10})$$

This can be done by using the previously presented definitions

$$\int_{4\pi} \sigma_{5g}(\vec{r}, \hat{n}; \hat{n}') \Psi(\vec{r}, \hat{n}') d\hat{n}' = \frac{1}{4} \int_{4\pi} (\sigma_5(\vec{r}, \hat{n}; \hat{n}') + \sigma_5(\vec{r}, \hat{n}; -\hat{n}')) (\Phi(\vec{r}, \hat{n}') + \Phi(\vec{r}, -\hat{n}')) d\hat{n}' \quad (\text{A.11})$$

The term on the right hand side of Eq. (A.11) can be expanded to give

$$\frac{1}{4} \int_{4\pi} (\sigma_3(\mathbf{r}, \hat{\mathbf{r}}; \hat{\mathbf{r}}) \Phi(\mathbf{r}, \hat{\mathbf{r}}) + \sigma_3(\mathbf{r}, \hat{\mathbf{r}}; -\hat{\mathbf{r}}) \Phi(\mathbf{r}, \hat{\mathbf{r}}) + \sigma_3(\mathbf{r}, \hat{\mathbf{r}}; \hat{\mathbf{r}}) \Phi(\mathbf{r}, -\hat{\mathbf{r}}) + \sigma_3(\mathbf{r}, \hat{\mathbf{r}}; -\hat{\mathbf{r}}) \Phi(\mathbf{r}, -\hat{\mathbf{r}})) d\hat{\mathbf{r}} \quad (\text{A.12})$$

however, the following relationships are true

$$\frac{1}{4} \int_{4\pi} \sigma_3(\mathbf{r}, \hat{\mathbf{r}}; \hat{\mathbf{r}}) \Phi(\mathbf{r}, \hat{\mathbf{r}}) d\hat{\mathbf{r}} = \frac{1}{4} \int_{4\pi} \sigma_3(\mathbf{r}, \hat{\mathbf{r}}; -\hat{\mathbf{r}}) \Phi(\mathbf{r}, \hat{\mathbf{r}}) d\hat{\mathbf{r}} \quad (\text{A.13})$$

$$\frac{1}{4} \int_{4\pi} \sigma_3(\mathbf{r}, -\hat{\mathbf{r}}; \hat{\mathbf{r}}) \Phi(\mathbf{r}, \hat{\mathbf{r}}) d\hat{\mathbf{r}} = \frac{1}{4} \int_{4\pi} \sigma_3(\mathbf{r}, \hat{\mathbf{r}}; \hat{\mathbf{r}}) \Phi(\mathbf{r}, -\hat{\mathbf{r}}) d\hat{\mathbf{r}} \quad (\text{A.14})$$

Substituting the results of Eqs. (A.13) and (A.14) into Eq. (A.12) gives

$$\frac{1}{2} \int_{4\pi} (\sigma_3(\mathbf{r}, \hat{\mathbf{r}}; \hat{\mathbf{r}}) + \sigma_3(\mathbf{r}, \hat{\mathbf{r}}; -\hat{\mathbf{r}})) \Phi(\mathbf{r}, \hat{\mathbf{r}}) d\hat{\mathbf{r}} \quad (\text{A.15})$$

Using Eqs. (1.16) and (A.15) gives

$$\int_{4\pi} \sigma_{3g}(\mathbf{r}, \hat{\mathbf{r}}; \hat{\mathbf{r}}) \Phi(\mathbf{r}, \hat{\mathbf{r}}) d\hat{\mathbf{r}}$$

thus proving the equality in Eq. (A.10). A similar proof can be constructed to show

$$\int_{4\pi} \sigma_{3\mu}(\mathbf{r}, \hat{\mathbf{r}}; \hat{\mathbf{r}}) \Phi(\mathbf{r}, \hat{\mathbf{r}}) d\hat{\mathbf{r}} = \int_{4\pi} \sigma_{3\mu}(\mathbf{r}, \hat{\mathbf{r}}; \hat{\mathbf{r}}) \chi(\mathbf{r}, \hat{\mathbf{r}}) d\hat{\mathbf{r}} \quad (\text{A.16})$$

Using the results of Eqs. (A.10) and (A.16) with the definitions of

Eqs. (1.14) and (A.9) in Eqs. (A.7) and (A.8) gives

$$G_y \Psi(\mathbf{r}, \hat{\mathbf{r}}) = S_g(\mathbf{r}, \hat{\mathbf{r}}) - \hat{\mathbf{r}} \cdot \nabla \chi(\mathbf{r}, \hat{\mathbf{r}}) \quad (\text{A.17})$$

$$G_\mu \chi(\mathbf{r}, \hat{\mathbf{r}}) = S_\mu(\mathbf{r}, \hat{\mathbf{r}}) - \hat{\mathbf{r}} \cdot \nabla \Psi(\mathbf{r}, \hat{\mathbf{r}}) \quad (\text{A.18})$$

Eqs. (A.17) and (A.18) represent a first order set of coupled integro-differential equations. Now define two new operators such that

$$K_g G_g f(\vec{r}, \hat{\Omega}) = f(\vec{r}, \hat{\Omega}) \quad (\text{A.19})$$

$$K_\mu G_\mu f(\vec{r}, \hat{\Omega}) = f(\vec{r}, \hat{\Omega}) \quad (\text{A.20})$$

$K_g$  and  $K_\mu$  are the inverse operators of  $G_g$  and  $G_\mu$  respectively. The derivation of these two operators is presented in Appendix B. Applying these inverse operators to Eqs. (A.17) and (A.18) results in

$$\Psi(\vec{r}, \hat{\Omega}) = K_g (S_g(\vec{r}, \hat{\Omega}) - \hat{\Omega} \cdot \nabla \chi(\vec{r}, \hat{\Omega})) \quad (\text{A.21})$$

$$\chi(\vec{r}, \hat{\Omega}) = K_\mu (S_\mu(\vec{r}, \hat{\Omega}) - \hat{\Omega} \cdot \nabla \Psi(\vec{r}, \hat{\Omega})) \quad (\text{A.22})$$

Substituting Eqs. (A.21) and (A.22) into Eqs. (A.17) and (A.18) gives

$$\hat{\Omega} \cdot \nabla K_\mu S_\mu(\vec{r}, \hat{\Omega}) - \hat{\Omega} \cdot \nabla K_\mu (\hat{\Omega} \cdot \nabla \Psi(\vec{r}, \hat{\Omega})) + G_g \Psi(\vec{r}, \hat{\Omega}) - S_g(\vec{r}, \hat{\Omega}) = 0 \quad (\text{A.23})$$

$$\hat{\Omega} \cdot \nabla K_g S_g(\vec{r}, \hat{\Omega}) - \hat{\Omega} \cdot \nabla K_g (\hat{\Omega} \cdot \nabla \chi(\vec{r}, \hat{\Omega})) + G_\mu \chi(\vec{r}, \hat{\Omega}) - S_\mu(\vec{r}, \hat{\Omega}) = 0 \quad (\text{A.24})$$

Eq. (A.23) is called the second order even-parity form of the Boltzmann neutron transport equation. Eq. (A.24) is the odd-parity form of this same equation. Rearranging Eq. (A.23) gives

$$-\hat{\Omega} \cdot \nabla K_\mu (\hat{\Omega} \cdot \nabla \Psi(\vec{r}, \hat{\Omega})) + G_g \Psi(\vec{r}, \hat{\Omega}) = S_g(\vec{r}, \hat{\Omega}) - \hat{\Omega} \cdot \nabla K_\mu S_\mu(\vec{r}, \hat{\Omega}) \quad (1.9)$$

## APPENDIX B

### DERIVATION OF THE $K_U$ OPERATOR

The  $K_U$  operator as seen from Appendix A takes the inverse of the  $G_U$  operator. The  $G_U$  operator is defined as

$$G_U f(\hat{r}) = \sigma_T f(\hat{r}) - \int_{4\pi} \sigma_{SU}(\hat{r}; \hat{r}') f(\hat{r}') d\hat{r}' \quad (B.1)$$

(The  $\vec{r}$  variable has been omitted, since it does not effect this derivation.) Let  $\sigma_{SU}(\hat{r}; \hat{r}')$  be defined in terms of a Legendre polynomial expansion

$$\sigma_{SU}(\hat{r}; \hat{r}') = \sum_{\ell=0}^{\infty} \sigma_{\ell}^u \left( \frac{2\ell+1}{4\pi} \right) P_{\ell}(\hat{r}; \hat{r}') \quad (B.2)$$

From the addition theorem of Legendre polynomials the following can be stated

$$P_{\ell}(\hat{r}; \hat{r}') = \frac{4\pi}{2\ell+1} \sum_{m=-\ell}^{\ell} Y_{\ell,m}(\hat{r}) Y_{\ell,m}^*(\hat{r}') \quad (B.3)$$

where  $Y_{\ell,m}(\hat{r})$  is a normalized spherical harmonic and  $Y_{\ell,m}^*(\hat{r}')$  is the complex conjugate of  $Y_{\ell,m}(\hat{r}')$ . Substituting Eq. (B.3) into Eq. (B.2) yields

$$\sigma_{SU}(\hat{r}; \hat{r}') = \sum_{\ell=0}^{\infty} \sum_{m=-\ell}^{\ell} \sigma_{\ell}^u Y_{\ell,m}(\hat{r}) Y_{\ell,m}^*(\hat{r}') \quad (B.4)$$

Now assume that  $f(\hat{r})$  can be represented in a spherical harmonic expansion

$$f(\hat{r}) = \sum_{\ell=0}^{\infty} \sum_{m=-\ell}^{\ell} f_{\ell} Y_{\ell,m}(\hat{r}) \quad (B.5)$$

Placing Eqs. (B.4) and (B.5) in Eq. (B.1) gives

$$G_U f(\hat{r}) = \sigma_T \sum_{\ell=0}^{\infty} \sum_{m=-\ell}^{\ell} f_{\ell} Y_{\ell,m}(\hat{r}) - \int_{4\pi} \sum_{\ell=0}^{\infty} \sum_{m=-\ell}^{\ell} \sigma_{\ell}^u Y_{\ell,m}(\hat{r}) Y_{\ell,m}^*(\hat{r}') \sum_{j=0}^{\infty} \sum_{k=-j}^j f_j Y_{j,k}(\hat{r}') d\hat{r}' \quad (B.6)$$

Rearranging Eq. (B.6) leads to

$$G_{\mu} f(\hat{r}) = \sigma_r \sum_{\ell=0}^{\infty} \sum_{m=-\ell}^{\ell} f_{\ell} Y_{\ell,m}(\hat{r}) - \sum_{\ell=0}^{\infty} \sum_{m=-\ell}^{\ell} \sigma_{\ell}^{\mu} Y_{\ell,m}(\hat{r}) \int \sum_{j=0}^{\infty} \sum_{k=-j}^j f_j Y_{j,k}(\hat{r}') Y_{\ell,m}^*(\hat{r}') d\hat{r}' \quad (B.7)$$

The orthogonality property of spherical harmonics states

$$\int_{4\pi} Y_{\ell,m}(\hat{r}) Y_{j,k}(\hat{r}) d\hat{r} = \delta_{\ell,j} \delta_{m,k} \quad (B.8)$$

where

$$\delta_{\ell,j} \begin{cases} = 1 & \text{if } \ell=j \\ = 0 & \text{if } \ell \neq j \end{cases}$$

Using the orthogonality property in Eq. (B.7) results in

$$G_{\mu} f(\hat{r}) = \sigma_r \sum_{\ell=0}^{\infty} \sum_{m=-\ell}^{\ell} f_{\ell} Y_{\ell,m}(\hat{r}) - \sum_{\ell=0}^{\infty} \sum_{m=-\ell}^{\ell} \sigma_{\ell}^{\mu} f_{\ell} Y_{\ell,m}(\hat{r}) \quad (B.9)$$

Combining terms in Eq. (B.9) gives

$$G_{\mu} f(\hat{r}) = \sum_{\ell=0}^{\infty} \sum_{m=-\ell}^{\ell} (\sigma_r - \sigma_{\ell}^{\mu}) f_{\ell} Y_{\ell,m}(\hat{r}) \quad (B.10)$$

Eq. (B.10) illustrates that the  $G_{\mu}$  operator alters the spherical harmonic coefficient  $f_{\ell}$  by a factor of  $(\sigma_r - \sigma_{\ell}^{\mu})$ . By definition an inverse operator to  $G_{\mu}$  must do the following

$$K_{\mu} G_{\mu} f(\hat{r}) = f(\hat{r}) \quad (B.11)$$

Therefore if  $K_{\mu}$  is defined as

$$K_{\mu} f(\hat{r}) = \sum_{\ell=0}^{\infty} \sum_{m=-\ell}^{\ell} \left( \frac{1}{\sigma_r - \sigma_{\ell}^{\mu}} \right) f_{\ell} Y_{\ell,m}(\hat{r}) \quad (B.12)$$

then

$$K_{\mu} G_{\mu} f(\hat{r}) = \sum_{\ell=0}^{\infty} \sum_{m=-\ell}^{\ell} \left( \frac{1}{\sigma_r - \sigma_{\ell}^{\mu}} \right) (\sigma_r - \sigma_{\ell}^{\mu}) f_{\ell} Y_{\ell,m}(\hat{r}) = f(\hat{r}) \quad (B.13)$$

thus satisfying Eq. (B.11)

Eq. (B.12) can be rearranged into the following form:

$$K_{\mu} f(\hat{r}) = \sum_{\ell=0}^{\infty} \sum_{m=-\ell}^{\ell} \left( \frac{1}{\sigma_r} + \frac{1}{\sigma_r} \left( \frac{\sigma_{\ell}^{\mu}}{\sigma_r - \sigma_{\ell}^{\mu}} \right) f_{\ell} Y_{\ell m}(\hat{r}) \right) \quad (B.14)$$

Rearranging Eq. (B.14) and again using the orthogonality property of spherical harmonics, the following results:

$$K_{\mu} f(\hat{r}) = \frac{1}{\sigma_r} \left( \sum_{\ell=0}^{\infty} \sum_{m=-\ell}^{\ell} f_{\ell} Y_{\ell m}(\hat{r}) \right) + \int_{4\pi} \sum_{\ell=0}^{\infty} \sum_{m=-\ell}^{\ell} \frac{\sigma_{\ell}^{\mu}}{\sigma_r - \sigma_{\ell}^{\mu}} Y_{\ell m}(\hat{r}) Y_{\ell m}^*(\hat{r}') \sum_{j=0}^{\infty} \sum_{k=-j}^j f_j Y_{j k}(\hat{r}') d\hat{r}' \quad (B.15)$$

Now make the following definition

$$\sigma_{\mu}(\hat{r}, \hat{r}') = \sum_{\ell=0}^{\infty} \sum_{m=-\ell}^{\ell} \frac{\sigma_{\ell}^{\mu}}{\sigma_r - \sigma_{\ell}^{\mu}} Y_{\ell m}(\hat{r}) Y_{\ell m}^*(\hat{r}') \quad (B.16)$$

Using the addition theorem on Eq. (B.16) gives

$$\sigma_{\mu}(\hat{r}, \hat{r}') = \sum_{\ell=0}^{\infty} \frac{\sigma_{\ell}^{\mu}}{\sigma_r - \sigma_{\ell}^{\mu}} \left( \frac{2\ell+1}{4\pi} \right) P_{\ell}(\hat{r} \cdot \hat{r}') \quad (B.17)$$

Using the results of Eq. (B.16) and previous definitions the following can be stated:

$$K_{\mu} f(\hat{r}) = \frac{1}{\sigma_r} \left( f(\hat{r}) + \int_{4\pi} \sigma_{\mu}(\hat{r}, \hat{r}') f(\hat{r}') d\hat{r}' \right) \quad (1.13)$$

Using a similar derivation the following form of  $K_g$  can be determined:

$$K_g f(\hat{r}) = \frac{1}{\sigma_r} \left( f(\hat{r}) + \int_{4\pi} \sigma_{\mu g}(\hat{r}, \hat{r}') f(\hat{r}') d\hat{r}' \right) \quad (B.18)$$

## APPENDIX C

### DERIVATION OF THE WEAK FORM OF SECOND ORDER EVEN-PARITY FLUENCE EQUATION

The classical technique for deriving the weak form of an equation can be illustrated in the following general example. Let the equation be represented by

$$L \Psi(\vec{x}) = f(\vec{x}) \quad (C.1)$$

where  $L$  is an operator,  $\Psi(\vec{x})$  is the dependent variable,  $f(\vec{x})$  is the source term, and  $\vec{x}$  is a vector representing the independent variables. If Eq. (C.1) is rearranged and multiplied through by a weight function,  $\varepsilon(\vec{x})$ , the following results:

$$(L \Psi(\vec{x}) - f(\vec{x})) \varepsilon(\vec{x}) = 0 \quad (C.2)$$

Integrating Eq. (C.2) over its domain of definition gives

$$\int_{\vec{x}} (L \Psi(\vec{x}) - f(\vec{x})) \varepsilon(\vec{x}) d\vec{x} = 0 \quad (C.3)$$

Eq. (C.3) is the weak form of Eq. (C.1). This equation is "weak" in that it holds in an integral sense rather than a point-wise sense as in Eq. (C.1).

The derivation of the weak form of the even-parity equation follows the above illustration. The even-parity equation is given by

$$-\hat{n} \cdot \nabla K_{\mu} \hat{n} \cdot \nabla \Psi(\vec{r}, \hat{n}) + G_g \Psi(\vec{r}, \hat{n}) = S_g(\vec{r}, \hat{n}) - \hat{n} \cdot \nabla K_{\mu} S_{\mu}(\vec{r}, \hat{n}) \quad (C.4)$$

where the operator for this equation is

$$L = -\hat{n} \cdot \nabla K_{\mu} \hat{n} \cdot \nabla + G_g \quad (C.5)$$

and the source term is

$$f(\vec{r}, \hat{n}) = S_g(\vec{r}, \hat{n}) - \hat{n} \cdot \nabla K_\mu S_\mu(\vec{r}, \hat{n}) \quad (C.6)$$

Rearranging Eq. (C.4) and multiplying through by the weight function results in

$$(-\hat{n} \cdot \nabla K_\mu \hat{n} \cdot \nabla \Psi(\vec{r}, \hat{n}) + G_g \Psi(\vec{r}, \hat{n}) - S_g(\vec{r}, \hat{n}) + \hat{n} \cdot \nabla K_\mu S_\mu(\vec{r}, \hat{n})) E(\vec{r}, \hat{n}) = 0 \quad (C.7)$$

Now integrate over the phase space defined by  $\vec{r}$  and  $\hat{n}$

$$\int_{\vec{r}} \int_{\hat{n}} [(-\hat{n} \cdot \nabla K_\mu \hat{n} \cdot \nabla \Psi(\vec{r}, \hat{n})) E(\vec{r}, \hat{n}) + (G_g \Psi(\vec{r}, \hat{n})) E(\vec{r}, \hat{n}) - S_g(\vec{r}, \hat{n}) E(\vec{r}, \hat{n}) + (\hat{n} \cdot \nabla K_\mu S_\mu(\vec{r}, \hat{n})) E(\vec{r}, \hat{n})] d\hat{n} d\vec{r} = 0 \quad (C.8)$$

For simplification the following definition is presented

$$\langle h(\vec{r}, \hat{n}), g(\vec{r}, \hat{n}) \rangle = \int_{\hat{n}} h(\vec{r}, \hat{n}) g(\vec{r}, \hat{n}) d\hat{n} \quad (C.9)$$

Substituting Eq. (C.9) into Eq. (C.8) results in

$$\int_{\vec{r}} [ \langle -\hat{n} \cdot \nabla K_\mu \hat{n} \cdot \nabla \Psi(\vec{r}, \hat{n}), E(\vec{r}, \hat{n}) \rangle + \langle G_g \Psi(\vec{r}, \hat{n}), E(\vec{r}, \hat{n}) \rangle - \langle S_g(\vec{r}, \hat{n}), E(\vec{r}, \hat{n}) \rangle + \langle \hat{n} \cdot \nabla K_\mu S_\mu(\vec{r}, \hat{n}), E(\vec{r}, \hat{n}) \rangle ] d\vec{r} = 0 \quad (C.10)$$

Again for simplification let

$$q(\vec{r}, \hat{n}) = K_\mu \hat{n} \cdot \nabla \Psi(\vec{r}, \hat{n}) \quad (C.11)$$

and operate on each term in Eq. (C.10) individually. Using Eq. (C.11)

in the first term of Eq. (C.10) results in

$$- \int_{\vec{r}} \langle \hat{n} \cdot \nabla q(\vec{r}, \hat{n}), E(\vec{r}, \hat{n}) \rangle d\vec{r} \quad (C.12)$$

Since  $\hat{n}$  and  $\nabla$  have independent coordinate systems, Eq. (C.12) can be

modified to

$$-\int_{\vec{r}} \langle \nabla \cdot \hat{n} q(\vec{r}, \hat{n}), \epsilon(\vec{r}, \hat{n}) \rangle d\vec{r} \quad (C.13)$$

Using the following vector identity (Ref. 36)

$$\nabla \cdot \epsilon(\vec{r}, \hat{n}) (\hat{n} q(\vec{r}, \hat{n})) = \epsilon(\vec{r}, \hat{n}) \nabla \cdot (\hat{n} q(\vec{r}, \hat{n})) - (\hat{n} q(\vec{r}, \hat{n})) \cdot \nabla \epsilon(\vec{r}, \hat{n}) \quad (C.14)$$

$$\epsilon(\vec{r}, \hat{n}) \nabla \cdot (\hat{n} q(\vec{r}, \hat{n})) = \nabla \cdot \epsilon(\vec{r}, \hat{n}) (\hat{n} q(\vec{r}, \hat{n})) - (\hat{n} q(\vec{r}, \hat{n})) \cdot \nabla \epsilon(\vec{r}, \hat{n}) \quad (C.15)$$

in Eq. (C.13) results in

$$-\int_{\hat{n}} \int_{\vec{r}} (\nabla \cdot \hat{n} q(\vec{r}, \hat{n})) \epsilon(\vec{r}, \hat{n}) d\vec{r} d\hat{n} = \int_{\hat{n}} \int_{\vec{r}} (\nabla \cdot \epsilon(\vec{r}, \hat{n})) \hat{n} q(\vec{r}, \hat{n}) d\vec{r} d\hat{n} + \int_{\hat{n}} \int_{\vec{r}} (\hat{n} q(\vec{r}, \hat{n}) \cdot \nabla \epsilon(\vec{r}, \hat{n})) d\vec{r} d\hat{n} \quad (C.16)$$

Applying the divergence theorem to the first term on the right hand side of Eq. (C.16)

$$-\int_{\vec{r}} \int_{S_v} \epsilon(\vec{r}, \hat{n}) q(\vec{r}, \hat{n}) (\hat{n} \cdot \hat{n}) d\vec{s} d\hat{n} \quad (C.17)$$

Where  $S$  represents the boundary of the spatial domain. Substituting the definition of  $q(\vec{r}, \hat{n})$  into Eq. (C.16) and using the results of the divergence theorem modifies the first term of Eq. (C.10) to

$$\int_{\vec{r}} \langle K_{\mu} \hat{n} \cdot \nabla \Psi(\vec{r}, \hat{n}), \hat{n} \cdot \nabla \epsilon(\vec{r}, \hat{n}) \rangle d\vec{r} - \int_{S_v} \langle \epsilon(\vec{r}, \hat{n}) (\hat{n} \cdot \hat{n}), K_{\mu} \hat{n} \cdot \nabla \Psi(\vec{r}, \hat{n}) \rangle d\vec{s} \quad (C.18)$$

Operating on the fourth term in Eq. (C.10) with both the vector identity in Eq. (C.15) and the divergence theorem results in the following new form

$$-\int_{\vec{r}} \langle K_{\mu} S_{\mu}(\vec{r}, \hat{n}), \hat{n} \cdot \nabla \epsilon(\vec{r}, \hat{n}) \rangle d\vec{r} + \int_{S_v} \langle \epsilon(\vec{r}, \hat{n}) (\hat{n} \cdot \hat{n}), K_{\mu} S_{\mu}(\vec{r}, \hat{n}) \rangle d\vec{s} \quad (C.19)$$

The weak form of Eq. (C.4) is now given by

$$\int_{\vec{r}} \left[ \langle K_{\mu} \hat{n} \cdot \nabla \Psi(\vec{r}, \hat{n}), \hat{n} \cdot \nabla E(\vec{r}, \hat{n}) \rangle + G_g \Psi(\vec{r}, \hat{n}), E(\vec{r}, \hat{n}) \rangle - \langle E(\vec{r}, \hat{n}), S_g(\vec{r}, \hat{n}) \rangle - \right. \\ \left. \langle K_{\mu} S_{\mu}(\vec{r}, \hat{n}), \hat{n} \cdot \nabla E(\vec{r}, \hat{n}) \rangle \right] d\vec{r} + \int_{S_v} \langle E(\vec{r}, \hat{n}) (\hat{n} \cdot \hat{n}), K_{\mu} (S_{\mu}(\vec{r}, \hat{n}) - \hat{n} \cdot \nabla \Psi(\vec{r}, \hat{n})) \rangle d\vec{s} = 0 \quad (C.20)$$

By the definition of the odd-parity fluence presented in Eq. (A.22), the term in Eq. (C.20) representing and integration around the spatial domain can be modified to

$$\int_{S_v} \langle E(\vec{r}, \hat{n}) (\hat{n} \cdot \hat{n}), \chi(\vec{r}, \hat{n}) \rangle d\vec{s} \quad (C.21)$$

Assuming a vacuum boundary condition the following is true

$$\Psi(\vec{r}, \hat{n}) + \chi(\vec{r}, \hat{n}) = 0, \quad \vec{r} \in S_v, \quad \hat{n} \cdot \hat{n} < 0 \quad (C.22)$$

$$\Psi(\vec{r}, \hat{n}) - \chi(\vec{r}, \hat{n}) = 0, \quad \vec{r} \in S_v, \quad \hat{n} \cdot \hat{n} > 0 \quad (C.23)$$

Eqs. (C.22) and (C.23) can be rewritten as

$$\Psi(\vec{r}, \hat{n}) = -\chi(\vec{r}, \hat{n}), \quad \vec{r} \in S_v, \quad \hat{n} \cdot \hat{n} < 0 \quad (C.24)$$

$$\Psi(\vec{r}, \hat{n}) = \chi(\vec{r}, \hat{n}), \quad \vec{r} \in S_v, \quad \hat{n} \cdot \hat{n} > 0 \quad (C.25)$$

Using the results of Eqs. (C.24) and (C.25) the following modification to Eq. (C.21) can be made:

$$\int_{S_v} \langle E(\vec{r}, \hat{n}) (\hat{n} \cdot \hat{n}), \chi(\vec{r}, \hat{n}) \rangle d\vec{s} = \int_{S_v} \int_{\hat{n} \cdot \hat{n} < 0} -E(\vec{r}, \hat{n}) \Psi(\vec{r}, \hat{n}) (\hat{n} \cdot \hat{n}) d\hat{n} d\vec{s} + \\ \int_{S_v} \int_{\hat{n} \cdot \hat{n} > 0} E(\vec{r}, \hat{n}) \Psi(\vec{r}, \hat{n}) (\hat{n} \cdot \hat{n}) d\hat{n} d\vec{s} \quad (C.26)$$

Eq. (C.26) is equivalent to the following:

$$\int_{S_v} \langle E(\vec{r}, \hat{n}) |\hat{n} \cdot \hat{n}|, \Psi(\vec{r}, \hat{n}) \rangle d\vec{s} \quad (C.27)$$

Thus the weak form of the even-parity equation that naturally satisfies the vacuum boundary condition is

$$\begin{aligned} \int_F [ < K_\mu \hat{n} \cdot \nabla \Psi(\vec{r}, \hat{n}), \hat{n} \cdot \nabla E(\vec{r}, \hat{n}) > + < G_g \Psi(\vec{r}, \hat{n}), E(\vec{r}, \hat{n}) > - \\ < S_g(\vec{r}, \hat{n}), E(\vec{r}, \hat{n}) > - < K_\mu S_\mu(\vec{r}, \hat{n}), \hat{n} \cdot \nabla E(\vec{r}, \hat{n}) > d\vec{r} + \end{aligned} \quad (2.1)$$

$$\int_{S_v} < E(\vec{r}, \hat{n}) | \hat{n} \cdot \hat{n} |, \Psi(\vec{r}, \hat{n}) > d\vec{s} = 0$$

## APPENDIX D

### BILINEAR LAGRANGE POLYNOMIALS

A bilinear Lagrange polynomial can be represented as

$$L(x,y) = a_1 xy + a_2 x + a_3 y + a_4 \quad (D.1)$$

If a rectangular element is defined as shown in Fig. 16, Eq. (D.1) can be properly constrained to give the tent function used as a trial solution in Chapter II. Let  $L_1, L_2, L_3, L_4$  be the value of Eq. (D.1) at the nodes defined in Fig. . Then the following system of equation can be written

$$L_1(x_1, y_1) = a_1 x_1 y_1 + a_2 x_1 + a_3 y_1 + a_4 \quad (D.2)$$

$$L_2(x_2, y_2) = a_1 x_2 y_2 + a_2 x_2 + a_3 y_2 + a_4$$

$$L_3(x_3, y_3) = a_1 x_3 y_3 + a_2 x_3 + a_3 y_3 + a_4$$

$$L_4(x_4, y_4) = a_1 x_4 y_4 + a_2 x_4 + a_3 y_4 + a_4$$

Now define the matrix H such the

$$[H] = \begin{vmatrix} x_1 y_1 & x_1 & y_1 & 1 \\ x_2 y_2 & x_2 & y_2 & 1 \\ x_3 y_3 & x_3 & y_3 & 1 \\ x_4 y_4 & x_4 & y_4 & 1 \end{vmatrix}$$

and the vector  $\vec{A}$  and  $\vec{L}$  where

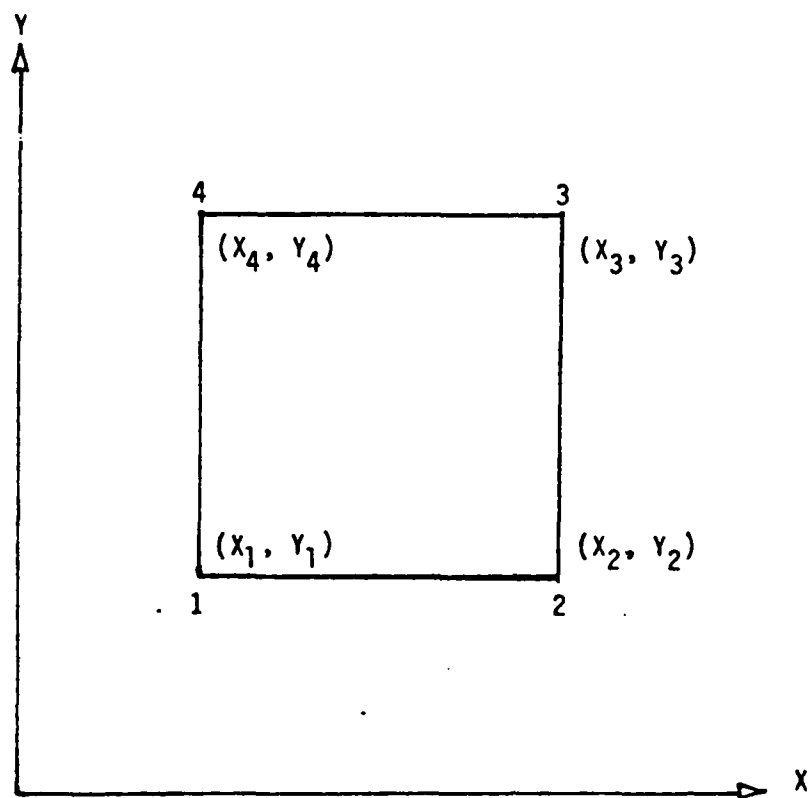


Fig 16. Rectangular Element

$$\vec{A}^T = [a_1, a_2, a_3, a_4] \quad (D.4)$$

$$\vec{L}^T = [L_1, L_2, L_3, L_4]$$

The system of equations represented in Eq. (D.1) can now be represented as

$$[H]\vec{A} = \vec{L} \quad (D.5)$$

Multiplying the inverse of the H matrix on both sides of Eq. (D.5) yields

$$\vec{A} = [H]^{-1}\vec{L} \quad (D.6)$$

Eq. (D.1) can be expressed as a product of a row vector P and the column vector a, if

$$\vec{P}^T = [x_y, x, y, 1] \quad (D.7)$$

then

$$L_{(x,y)} = \vec{P}^T \vec{A} \quad (D.8)$$

Substituting the values of  $\vec{A}$  from Eq. (D.6) into Eq. (D.8) gives

$$L_{(x,y)} = \vec{P}^T [H]^{-1} \vec{L} \quad (D.9)$$

By letting the  $\vec{L}$  assume the following values the tent function of nodes 1, 2, 3, 4 can be found respectively:

$$(1, 0, 0, 0)$$

$$(0, 1, 0, 0)$$

$$(0, 0, 1, 0)$$

$$(0, 0, 0, 1)$$

## APPENDIX E

### CANONICAL TECHNIQUES

#### CANONICAL ELEMENTS/INTEGRATION

The concept of a canonical element is used in the finite element method to simplify the integral evaluations associated with the chosen numerical technique. In Fig. 17 a standard rectangular element with sides parallel to the coordinate axis (x,y) is presented.

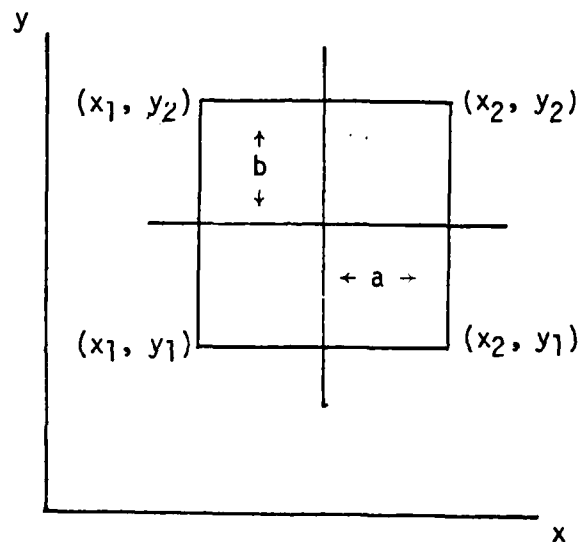


Fig. 17. Standard Rectangular Element

Inscribed in this element is a natural coordinate system defined by (n, ). The relationship between the natural coordinates and axis coordinates is given by

$$\xi = \frac{x - x_c}{a} \quad (E.1)$$

$$\eta = \frac{y - y_c}{b} \quad (E.2)$$

This coordinate transformation defines a canonical element that represents the rectangular element in Fig. 18.

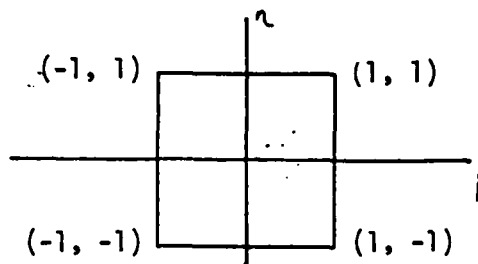


Fig. 18. Canonical Element

From Eqs. (E.1) and (E.2) the following can be generated

$$\frac{d\xi}{dx} = \frac{1}{a} \Rightarrow dx = a d\xi \quad (E.3)$$

$$\frac{d\eta}{dy} = \frac{1}{b} \Rightarrow dy = b d\eta \quad (E.4)$$

Let  $f(x,y)$  be a function that is identically defined over all finite elements in the  $(x,y)$  coordinate system shown in Fig. 17. Using the coordinate transformation equations this function can be redefined in the natural coordinate system as  $f(\xi, \eta)$ . Since this function is identically defined in all elements the transformation equations will generate exactly the same functional representation in the canonical element for all the elements in the  $(x,y)$  coordinate system. The only difference is the scaling factors  $a$  and  $b$  that are related to the dimension of the element. Thus the following equality holds

$$\int_{x_1}^{x_2} \int_{y_1}^{y_2} f(x,y) dx dy = ab \int_{-1}^1 \int_{-1}^1 f(\xi, \eta) d\xi d\eta \quad (E.5)$$

This relationship allows the integral evaluation of  $f(x,y)$  over a finite element to be done once over the canonical element. If a finer discretization is necessary the canonical evaluation need be changed only by the new dimension parameters  $a, b$  caused by this mesh refinement.

### GALERKIN WEAK FORM EQUATION/ISOTROPIC SCATTER

The global integrals in the Galerkin weak form equation resulting from the  $G_g$  operator and using isotropic scatter is

$$\sigma_{s\phi}(\bar{r}) \int_{4\pi} \Psi(\bar{r}, \hat{n}) d\hat{n} \quad (E.6)$$

If  $\Psi(\bar{r}, \hat{n})$  is represented by the trial solution of Eq. (2.20), Eq. (E.6) gives

$$\sigma_{s\phi}(\bar{r}) L_i(\bar{r}) \int_{\mu} \int_x L_j(\mu, x) dx d\mu \quad (E.7)$$

The bilinear Lagrange polynomials meet the requirement of being identically defined over all elements, thus the integral in Eq. (E.7) can be evaluated over a canonical element as

$$ab \int_{-1}^1 \int_{-1}^1 L_j(t, n) dt dn \quad (E.8)$$

The evaluation of Eq. (E.8) can be done once and the result used for all other angular elements.

### GALERKIN WEAK FORM EQUATION/ANISOTROPIC SCATTERING

The global integral resulting from the  $K_u$  operator using a  $P_1$  anisotropic scattering representation is

$$\frac{\sigma_{s1}(\bar{r})}{\sigma_T(\bar{r})} \int_{4\pi} (\mu\mu' + \sqrt{1-\mu^2}\sqrt{1-\mu'^2}\cos(x-x')) \hat{n} \cdot \nabla \Psi(\bar{r}, \hat{n}) d\hat{n} \quad (E.9)$$

If the even-parity fluence is again represented as a tensor product of bilinear Lagrange polynomials, then the derivatives that result from the gradient operator are identical over each angular element. The integrand of Eq. (E.9) contains other functions besides these derivatives. These functions vary differently over each angular element, thus eliminating a single canonical evaluation that would represent all these

elements. Eq. (E.9) can be evaluated over the canonical element; however, it must be separately evaluated for each element defined in the angular domain since the location of the element now affects the value of this term.

## APPENDIX F

### TOTAL TERMS IN $\hat{\mathbf{r}} \cdot \nabla E(\mathbf{r}, \hat{\mathbf{r}}) K_{\mu} \hat{\mathbf{r}} \cdot \nabla \Psi(\mathbf{r}, \hat{\mathbf{r}})$

The MACSYMA program did not have enough available core to expand the first term in the Galerkin weak form equation into all its distinct terms. The reason this core limit was reached can be seen from the following evaluation. The first term of the Galerkin weak form equation can be expressed as

$$\int_{\mathbf{r}} \int_{4\pi} \hat{\mathbf{r}} \cdot \nabla E(\mathbf{r}, \hat{\mathbf{r}}) K_{\mu} \hat{\mathbf{r}} \cdot \nabla \Psi(\mathbf{r}, \hat{\mathbf{r}}) d\hat{\mathbf{r}} d\mathbf{r} \quad (\text{F.1})$$

Using the definition of the  $K_{\mu}$  operator expands the integrand in Eq. (F.1) to give

$$\hat{\mathbf{r}} \cdot \nabla E(\mathbf{r}, \hat{\mathbf{r}}) \left[ \frac{1}{\sigma_T(\mathbf{r})} (\hat{\mathbf{r}} \cdot \nabla \Psi(\mathbf{r}, \hat{\mathbf{r}}) + \int_{4\pi} \sigma_{KM}(\hat{\mathbf{r}} \cdot \hat{\mathbf{r}}') \hat{\mathbf{r}} \cdot \nabla \Psi(\mathbf{r}, \hat{\mathbf{r}}') d\hat{\mathbf{r}}') \right] \quad (\text{F.2})$$

For this evaluation only the following is used

$$\hat{\mathbf{r}} \cdot \nabla E(\mathbf{r}, \hat{\mathbf{r}}) \int_{4\pi} \sigma_{KM}(\hat{\mathbf{r}} \cdot \hat{\mathbf{r}}') \hat{\mathbf{r}} \cdot \nabla \Psi(\mathbf{r}, \hat{\mathbf{r}}') d\hat{\mathbf{r}}' \quad (\text{F.3})$$

Applying the definition of the  $\hat{\mathbf{r}} \cdot \nabla$  operator in cylindrical geometry expands the integrand to

$$\hat{\mathbf{r}} \cdot \nabla E(\mathbf{r}, \hat{\mathbf{r}}) \int_{4\pi} \sigma_{KM}(\hat{\mathbf{r}} \cdot \hat{\mathbf{r}}') \left( \frac{\sqrt{1-\mu^2} \cos(\chi)}{\rho} \frac{\partial(\rho \Psi(\mathbf{r}, \hat{\mathbf{r}}'))}{\partial \rho} - \frac{1}{\rho} \frac{\partial(\sqrt{1-\mu^2} \Psi(\mathbf{r}, \hat{\mathbf{r}}') \sin(\chi))}{\partial \chi} + \mu \frac{\partial \Psi(\mathbf{r}, \hat{\mathbf{r}}')}{\partial z} \right) d\hat{\mathbf{r}}' \quad (\text{F.4})$$

If  $\Psi(\mathbf{r}, \hat{\mathbf{r}})$  is represented by linear Lagrange interpolating functions in a four-dimensional phase space  $(\rho, z, \mu, \chi)$  the following general expression can be written

$$\Psi(\mathbf{r}, \hat{\mathbf{r}}) = (a + b\rho)(c + dz)(e + f\mu)(g + h\chi) \quad (\text{F.5})$$

Substituting Eq. (E.5) into the first term in brackets in Eq. (E.4) gives

$$\frac{\sqrt{1-\mu'^2} \cos(x')}{\rho} (c+dz) (e+f\mu) (g+hx) (u+2b\rho) \quad (F.6)$$

Eq. (F.6) contains sixteen distinct terms. Proceeding in the same manner with the other two terms in the brackets results in

$$\frac{\sqrt{1-\mu'^2}}{\rho} (a+b\rho) (c+dz) (e+f\mu) (g \cos(x) + h \sin(x) + hx \sin(x)) \quad (F.7)$$

$$\mu (a+b\rho) (e+f\mu) (g+hx) d \quad (F.8)$$

Eq. (F.7) contains twenty-four distinct terms and Eq. (F.8) contains eight. The total number of distinct terms resulting from the bracketed terms in the integrand of Eq. (F.4) is forty-eight.

The odd-parity differential scattering cross section can be represented for a  $P_3$  legendre expansion as

$$\sigma_{KM}(\mu_0) = \sigma_{K1} \mu_0 + \sigma_{K3} \mu_0^3 \quad (F.9)$$

where

$$\mu_0 = \mu \mu' + \sqrt{1-\mu'^2} \sqrt{1-\mu^2} \cos(x) \cos(x') + \sqrt{1-\mu'^2} \sqrt{1-\mu^2} \sin(x) \sin(x') \quad (F.10)$$

Eq. (F.10) represents three distinct terms and cubing this equation results in ten for a total of thirteen distinct terms. Therefore, the integrand in Eq. (F.4) contains 624 distinct terms.

For now ignore the integration over  $\lambda'$  and define the weight function as

$$E(\vec{r}, \lambda) = (aa + bb\rho) (cc + ddz) (ee + ff\mu) (gg + hhx) \quad (F.11)$$

The coefficients are different than those in Eq. (F.5), because in the Galerkin method different combinations of Lagrange polynomials all defined over the same finite element are multiplied together (see Eq. (2.18)). The  $\hat{A} \cdot \nabla \varepsilon(\rho, \lambda)$  has forty-eight distinct terms just as  $\hat{A} \cdot \nabla \psi(\rho, \lambda)$ . Multiplying the forty-eight distinct terms of Eq. (F.11) by the 624 terms resulting from the previous work generates a total of 29,952 distinct terms. This number is an absolute minimum since the integration operation was not included. The integral evaluation over a rectangular element of arbitrary dimension would generate at least four more terms for each term evaluated. If the integral was complex, then more than four terms could result.

Obviously many of the terms are similar and could be combined to reduce the total. MACSYMA can only begin this simplification after all the distinct terms are generated. Several approaches were attempted to alleviate this shortcoming in MACSYMA, but all proved unsuccessful. The main problem was the limited core capacity of the DEC 10 on which this program resided.

## APPENDIX G

### DERIVATION OF ANGULAR SYNTHESIS FUNCTION

In Chapter III an angular synthesis function was derived for use with the collocation method. The selection of this function was guided by two basic criteria. The first criterion dictated that the form of an angular synthesis function must be simple to avoid the problems encountered in Chapter II. The second criterion is the basic tenet of using a synthesis function that accurately approximates the angular variation of the neutron fluence. As mentioned in Chapter II, the choice of an appropriate synthesis function is made from experience, previous calculations, or intuition.

The collocation angular synthesis function was selected from the definition of the even-parity fluence. This fluence can be represented as

$$\psi(\vec{r}, \lambda) = \frac{1}{2} [\Phi(\vec{r}, \lambda) + \Phi(\vec{r}, -\lambda)] \quad (G.1)$$

The work accomplished by Roberds and Bridgman (Ref. 23) demonstrated that a spheroid can be used as an angular synthesis function for the regular Boltzmann fluence. Fig. 19a illustrates a spheroid that could be used to represent  $\Phi(\vec{r}, \lambda)$  for some anisotropic angular distribution.

Fig. 19b is a polar plot of  $\Phi(\vec{r}, \lambda)$  using the same spheroid synthesis function. If the two spheroids in Figs. 19a and 19b are added together the result is the even-parity fluence and the polar plot of this addition is presented in Fig. 19c.

The selected synthesis function must have the general form represented by Fig. 19c. In Chapter II a centered ellipsoid was proposed as an angular synthesis function. Though this function would adequately

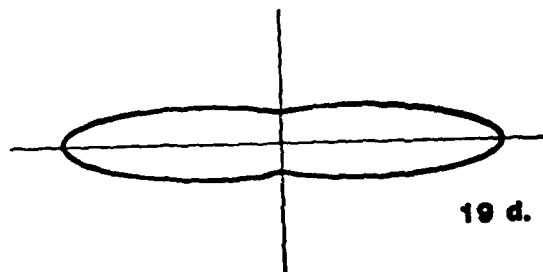
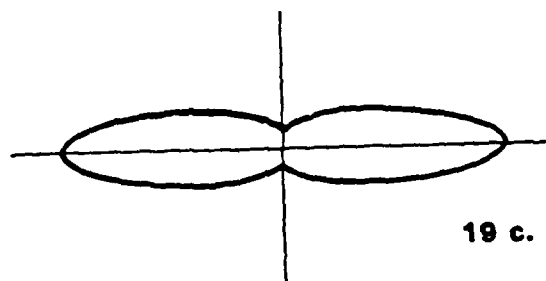
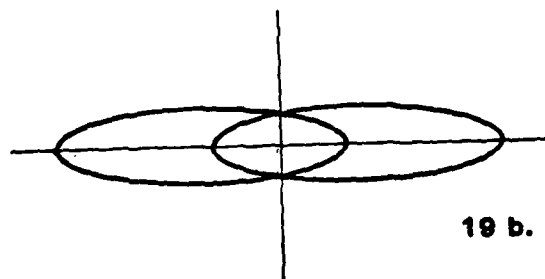
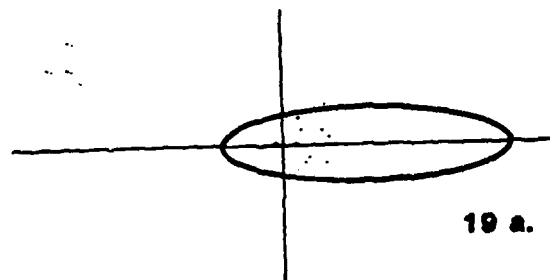


Fig. 19. Derivation of Collocation Angular Synthesis Function

approximate the angular distribution of Fig. 19c, it does not meet the first criterion as already demonstrated. A function that would accurately approximate Fig. 19c is

$$A(\mu_0) = 1 + \mu_0^2 \quad (G.2)$$

A polar plot of this function appears in Fig. 19d. A comparison of Fig. 19c and Fig. 19d demonstrates the adequacy of Eq. (G.2) to approximate the angular distribution of the even-parity fluence in an air-over-ground problem.

The largest component of the Boltzmann fluence in an air-over-ground problem is aligned parallel with a ray drawn from the spatial location of the point source to the spatial location of interest. The angular coordinates of this streaming direction in the local coordinate system changes from one spatial location to another. Let the streaming direction for a spatial location be represented by  $\mu_0$  and  $\chi_0$  in the local coordinate system. If the  $\mu_0$  variable in Eq. (G.2) is defined in terms of the law of cosines, the following results

$$A(\mu, \chi) = 1 + (\mu_0 \mu + \sqrt{1-\mu_0^2} \sqrt{1-\mu^2} \cos(\chi - \chi_0))^2 \quad (G.3)$$

Eq. (G.3) represents the angular shape presented in Fig. 19d and has the capability of being aligned in the streaming direction at any spatial location. Fig. 20 is a polar plot of Eq. (G.3).

The synthesis function represented in Eq. (G.3) satisfied the two criteria previously presented. In the collocation method Eq. (G.3) is used in the following form

$$\Psi(r, \mu, \chi) = \sum_{i=1}^M \sum_{j=1}^N \theta_i(\rho) \theta_j(z) (a_{ij} + a_{2ij} (\mu_0 \mu + \sqrt{1-\mu_0^2} \sqrt{1-\mu^2} \cos(\chi - \chi_0))^2) \quad (G.4)$$

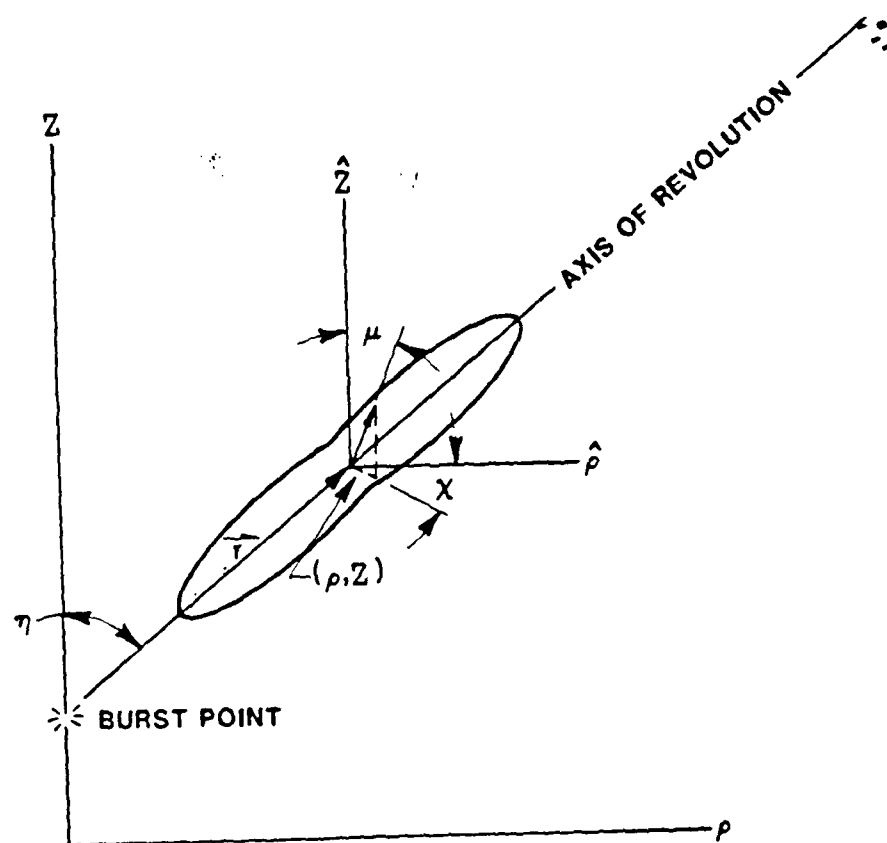


Fig. 20. Definition of Collocation Angular Synthesis Function

The coefficients  $\alpha_{ij}$  and  $\alpha_{ij}$  are determined from solving the global matrix formed from applying the collocation method to the EPFBE. These two coefficients can be adjusted to represent even-parity angular fluence shapes varying from highly anisotropic to isotropic. The form of Eq. (G.4) is simple and was analytically integrable when placed in the EPFBE used in the collocation method.

## APPENDIX H

### FLOW CHARTS

This appendix contains the flow diagrams for both the Galerkin and collocation program presented in Chapters II and III respectively for generating a matrix representation of the EPFBE. An explanation of the numbers in the diagrams is presented below.

#### Galerkin Program (Fig. 21)

1. The following parameters are inputed.
  - a. Maximum number of mesh lines in  $\rho, z, \mu, \chi$  directions.
  - b. Number of spatial and angular test functions per finite element.
  - c. Global spatial node and angular node matrix that relates nodes to elements.
  - d. Mesh node values for  $\rho, z, \mu$ , and  $\chi$  coordinates.
  - e. Order of differential scattering cross section.
  - f. Cross sections.
2. Quadrature sets for use with spatial and angular numerical integration are selected and inputed.
3. Print out all input data as a check.
4. Zero all elements in the global matrix and load vector.
5. Determine coordinates for defining all angular finite elements.  
--- Start loop over spatial finite elements.
6. Select a spatial finite element and define its location in the spatial mesh.  
--- Start loop over angular finite elements.
7. Select an angular finite element and from step 5 identify its location in the angular mesh.

8. From the coordinates of these selected elements calculate the parameters needed to transform each into a canonical element representation.
9. Select a quadrature point for the  $\rho$ ,  $z$ ,  $\mu$ , and  $\chi$  variables and an accompanying weight function.
10. Select a combination of bilinear Lagrange polynomials representing the spatial and angular test functions.
11. The numerical evaluation of the integrals involved with the source term of the Galerkin weak form equation is performed. The integrands of these integrals are expressed in terms of the test function and their derivatives selected in step 10 and are evaluated at the quadrature points defined in step 9. These evaluated terms are multiplied by the corresponding weight function associated with these quadrature points and the product is stored in an element of the load vector. The location of this element in the load vector is determined by the test function combination. This element represents the evaluated integrals in the source term when all quadrature points and weights have been used and their resultant products summed. The value of the test functions and their derivatives that appear in the source term integrands are determined by a series of function routines and subroutine programs. These subprograms define the test functions in a canonical element, evaluate these functions for the selected quadrature points, and assemble these evaluated functions into a representation of the source term integrands.
12. Select a combination of bilinear Lagrange polynomials representing the spatial and angular trial functions.
13. The numerical evaluation of the local integrals containing the even-parity fluence in the Galerkin weak form equation is performed. The integrands of these integrals are expressed in terms of the trial

functions and test functions selected in steps 12 and 10 respectively. These integrands are evaluated at the quadrature points defined in step 9 and the result of this evaluation is multiplied by the weight functions associated with the quadrature points. This product which represents a partial evaluation of the weak form integrals is stored in one element of the global stiffness matrix. The position of this element is determined by the test and trial function combinations. This element represents the full evaluation of the Galerkin weak form local integrals for the selected test and trial function combination after the contribution of all quadrature point evaluations have been summed. As mentioned in step 11 several subprograms contribute to this evaluation.

14. Has a different spatial trial function been selected in step 12 since the last iteration?
15. Select an angular finite element for global evaluation of the global integrals in Galerkin weak form equation.
16. Calculate the parameters needed to transform the angular element selected in step 15 into a canonical element representation.
17. Select quadrature points for the  $u'$  and  $x'$  variables and the accompanying weight functions.
18. Select a bilinear Lagrange polynomial trial function defined in the angular element selected in step 15. The test functions and spatial trial functions are the same as previously chosen.
19. The numerical evaluation of the global integrals (integrals defined over the entire angular domain) resulting from the  $K_u$  and  $G_g$  operators is performed. The integrands of these integrals are expressed in terms of the test function selected in step 10, spatial trial function selected in step 12, and angular trial function in step 18. The result of this

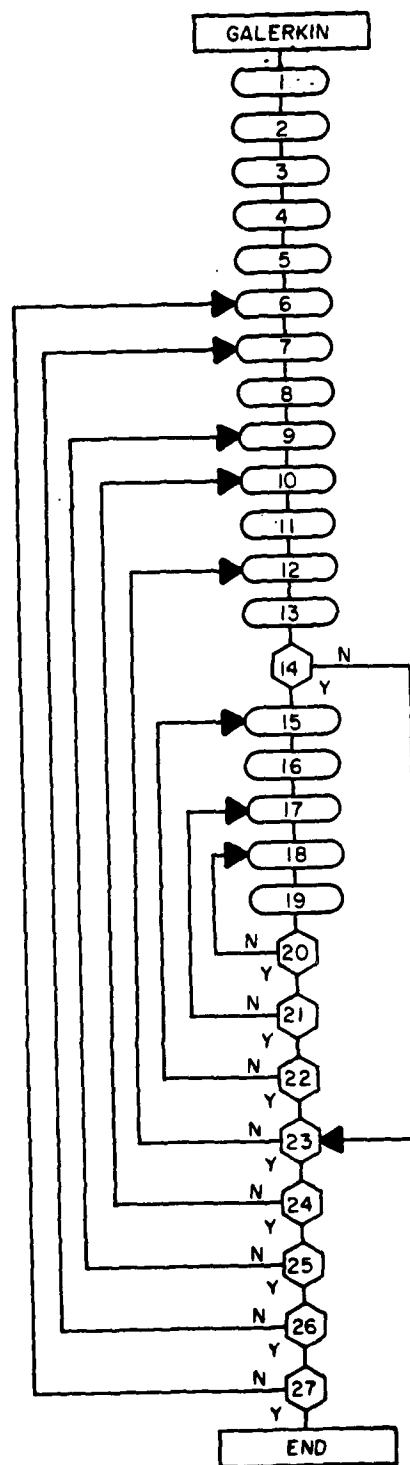


Fig. 21. Galerkin Program Flow Chart

- evaluation is stored or added to existing values in the global stiffness matrix in a position determined by the test and trial function combination. The subprograms mentioned in step 11 and 13 perform the evaluations.
20. Have all angular trial functions for the global integral evaluation been used?
  21. Have all quadrature points for the  $u'$  and  $x'$  variables been used to evaluate the global integrals?
  22. Have all angular elements been used for the global integral evaluations?
  23. Have all spatial and angular trial function combinations in step 12 been used?
  24. Have all spatial and angular test functions combinations in step 10 been used?
  25. Have all quadrature points for the  $\rho$ ,  $z$ ,  $\mu$ , and  $x$  variables been used?
  26. Have all angular elements from step 7 been used?
  27. Have all spatial elements from step 6 been used?

Collocation Program (Fig. 22)

1. The following parameters are inputted.
  - a. Number of collocation points in  $\rho$  direction.
  - b. Number of collocation points in  $z$  direction.
  - c. Number of mesh points in  $\rho$  direction.
  - d. Number of mesh points in  $z$  direction.
  - e.  $r$  coordinate collocation points.
  - f.  $z$  coordinate collocation points.
  - g. Mesh coordinates in  $\rho$  direction.
  - h. Mesh coordinates in  $z$  direction.

- i. Total macroscopic cross section and  $P_3$  cross sections.
- j. Height of burst.
2. All global matrix elements zeroed.
3. Start of  $\rho$  coordinate collocation loop. A  $\rho$  coordinate collocation point is selected and used for evaluation.
4. Splines in  $\rho$  coordinate that have a value at selected  $\rho$  coordinate mesh point are identified.
5. Start of  $Z$  coordinate collocation loop. A  $Z$  coordinate collocation point is selected and used for evaluation.
6. The streaming direction and 90 degrees off the streaming direction in the  $x=0$  plane at the selected spatial collocation points are determined.
7. Ellipsoidal synthesis function pitch is set based on the streaming direction. Spatial derivatives of the pitch function ( $\cos\eta$  or  $\sin\eta$ ) are determined for the selected spatial collocation points.
8. Splines in  $Z$  coordinate that have a value at selected  $Z$  coordinate are identified.
9. Start loop over all splines in  $\rho$  coordinate that were previously identified in 4.
10. Start loop over all splines in  $Z$  coordinate that were previously defined in 8.
11. Evaluate all terms in EPFBE that have spatial dependence. This encompasses an evaluation of the  $\theta_i(\rho)$ ,  $\theta_j(z)$  terms in Eq. (3.11) and their derivatives.
12. Decision block to determine if all splines in  $Z$  coordinate identified in 8 have been evaluated (Y=Yes, N=No).

13. Decision block to determine if all splines in  $p$  coordinate identified in 4 have been evaluated.
  14. Evaluate all terms in EPFBE that have angular dependence. This encompasses an evaluation of the  $a_{ij} + a_{z,j} (\mu\mu_0 + \sqrt{1-\mu^2}\sqrt{1-\mu_0^2} \cos(x-x_0))^2$  term in Eq. (3.11) and its derivative with respect to the  $u$  and  $x$  variables. (Primed and unprimed.)
  15. The spatial and angular contributions of the EPFBE found from 11 and 14 respectively are combined to calculate the value of all terms in the EPFBE.
  16. Value of EPFBE calculated in 15 is stored in appropriate global matrix element. The value of the source terms is stored in the load vector. The position of these elements in the global matrix and load vector is determined by the spatial spline combination and angular collocation points.
  17. Decision block to determine if both angular collocation points have been evaluated.
  18. Decision block to determine if all  $z$  coordinate collocation points have been evaluated.
  19. Decision block to determine if all  $p$  coordinate collocation points have been evaluated.
- Global matrix formed.

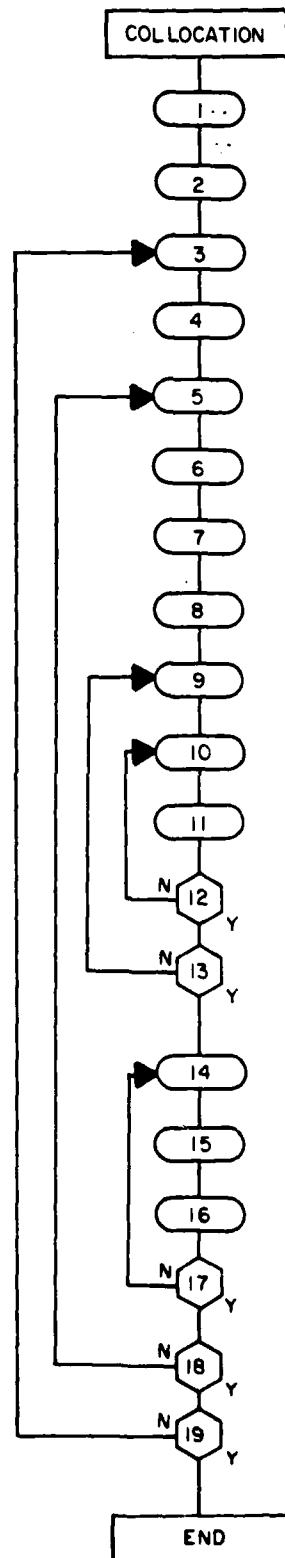


Fig. 22. Collocation Program Flow Diagram

## APPENDIX I

### DERIVATION OF NORMALIZED B-SPLINES OF ORDER 4

In Chapter III the spatial variation of neutral particle fluence was approximate by cubic spline functions defined in the  $x$  and  $z$  variables. The value of these functions for various spatial locations was calculated in the collocation program by a subroutine called BS. The following derivation generates the equations used in this routine for defining and evaluating these splines.

Assume the node sequence  $t_1, t_2, t_3, t_4, t_5$  illustrated in Fig. 23.

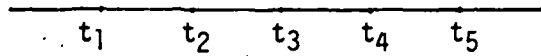


Fig. 23. B Spline Node Sequence

Define the expression  $(s-t)_+^{k-1}$  such that

$k$  = order of the spline

$k-1$  = degree of the spline

$$(s-t)_+^{k-1} = \begin{cases} (s-t)^{k-1} & \text{if } s \geq t \\ 0 & \text{if } s < t \end{cases}$$

Using the above definitions define a new variable  $N_{i,k}(t)$  as

$$N_{i,k}(t) = (t_{i+k} - t_i) [t_i, \dots, t_{i+k}]_s (s-t)_+^{k-1} \quad (I.1)$$

where

$i$  = number of the first node

$[t_i, \dots, t_{i+k}]$  = divided difference operator operating on the  $s$  variable and defined in the following manner.

$$\begin{aligned} [x,]_s f(s) &= f(x) \\ [x_1, x_2]_s f(s) &= \frac{f(x_2) - f(x_1)}{x_2 - x_1} \\ [x_0, \dots, x_n]_s f(s) &= ([x_1, \dots, x_n] f(s) - [x_0, \dots, x_{n-1}] f(s)) / (x_n - x_0) \end{aligned}$$

Using Eq. (I.1) and setting  $K=4$  the following representation of the B splines can be written for the node sequence in Fig. 23

$$N_{i,4}(t) = (t_5 - t_1) [t_1, t_2, t_3, t_4, t_5]_s (s - t)_+^3 \quad (I.2)$$

Now apply the definition of the divided difference operator

$$[t_1, t_2, t_3, t_4, t_5]_s (s - t)_+^3 = \frac{[t_2, t_3, t_4, t_5]_s (s - t)_+^3 - [t_1, t_2, t_3, t_4]_s (s - t)_+^3}{t_5 - t_1} \quad (I.3)$$

The following series of equations represent a repeated application of the divided difference operator to the two terms on the right hand side of equation I.3

$$A = [t_3, t_4, t_5]_s (s - t)_+^3 = \frac{[t_3, t_4, t_5]_s (s - t)_+^3 - [t_2, t_3, t_4]_s (s - t)_+^3}{t_5 - t_2} \quad (I.4)$$

$$B = [t_1, t_2, t_3, t_4]_s (s - t)_+^3 = \frac{[t_2, t_3, t_4]_s (s - t)_+^3 - [t_1, t_2, t_3]_s (s - t)_+^3}{t_4 - t_1} \quad (I.5)$$

To A and B the following reductions can be made

$$C = [t_3, t_4, t_5]_s (s - t)_+^3 = \frac{[t_4, t_5]_s (s - t)_+^3 + [t_4, t_3]_s (s - t)_+^3}{t_5 - t_3} \quad (I.6)$$

$$D = E = [t_1, t_2, t_3, t_4]_s (s - t)_+^3 = \frac{[t_3, t_4]_s (s - t)_+^3 - [t_2, t_3]_s (s - t)_+^3}{t_4 - t_2} \quad (I.7)$$

$$F = [t_1, t_2, t_3]_s (s - t)_+^3 = \frac{[t_2, t_3]_s (s - t)_+^3 - [t_1, t_2]_s (s - t)_+^3}{t_3 - t_1} \quad (I.8)$$

Applying the definition of the divided difference operator to C, D, E, and F results in

$$G = [t_4, t_5]_s (s - t)_+^3 = \frac{(t_5 - t)_+^3 - (t_4 - t)_+^3}{t_5 - t_4} \quad (I.9)$$

$$H = [t_4, t_3]_s (s - t)_+^3 = \frac{(t_3 - t)_+^3 - (t_4 - t)_+^3}{t_3 - t_4} \quad (I.10)$$

$$I = [t_2, t_3]_s (s-t)_+^2 = \frac{(t_3-t)_+^3 - (t_2-t)_+^3}{t_3 - t_2} \quad (I.11)$$

$$J = [t_1, t_2]_s (s-t)_+^2 = \frac{(t_2-t)_+^3 - (t_1-t)_+^3}{t_2 - t_1} \quad (I.12)$$

By back substituting the following relationships are formed.

$$C = \frac{G-H}{t_5-t_3} \quad (I.13)$$

$$D=E = \frac{H-I}{t_4-t_2} \quad (I.14)$$

$$F = \frac{I-J}{t_3-t_1} \quad (I.15)$$

Further back substituting results in

$$A = \frac{C-E}{t_5-t_2} \quad (I.16)$$

$$B = \frac{D-F}{t_4-t_1} \quad (I.17)$$

Finally the form of the B spline used in the collocation program is defined as

$$Q(t) = (t_5-t_1) \frac{A-B}{(t_5-t_1)} = A-B \quad (I.18)$$

The spline in Eq. (I.18) is normalized such that

$$\int_{t_1}^{t_5} N_{1,4}(t) dt = 1 \quad (I.19)$$

### Vita

Captain John C. Souders graduated with distinction from Texas A&M University in May 1971. He received his Master of Engineering degree at this same institution in October 1972 studying under an Atomic Energy Commission Traineeship.

Captain Souders' first active duty assignment was in the Foreign Technology Division located at Wright-Patterson AFB, Ohio. In this assignment he monitored Soviet developments related to surface-to-air missiles. In April 1973 he was selected as aide-de-camp to the base commander of Wright-Patterson AFB. Captain Souders served in this job until August 1974 when he was reassigned to the Air Force Weapons Laboratory at Kirtland AFB, New Mexico. For the next two years he served as a nuclear research officer working in the area of nuclear safety. For his work during this period he was awarded the Air Force Association's Citation of Honor. Captain Souders entered the Doctoral Program at the Air Force Institute of Technology in August 1976. He is currently assigned at Field Command Defense Nuclear Agency working as a Technical Director in the Underground Nuclear Test Program.

John Souders was born in Lancaster, Pennsylvania, in March 1949, and is the son of John C. Souders and Janet E. Souders. He was married in 1968 to the former Marilyn McKinney of Carrollton, Texas. He and Marilyn have three children: John, age 10, Amy, age 9, and Wade, age 5.

Permanent Address: 14743 Tanglewood Dr., Dallas, Texas 75234.

UNCLASSIFIED

SECURITY CLASSIFICATION OF THIS PAGE (When Data Entered)

REPORT DOCUMENTATION PAGE		READ INSTRUCTIONS BEFORE COMPLETING FORM
1. REPORT NUMBER AFIT/DS/PH/81-2	2. GOVT ACCESSION NO. AD-100801	3. RECIPIENT'S CATALOG NUMBER
4. TITLE (and Subtitle) Analytical and Numerical Problems Associated with Extending the Use of the Second Order Even-Parity Transport Equation		5. TYPE OF REPORT & PERIOD COVERED Ph.D. Dissertation
7. AUTHOR(s) John C. Souders, Jr.		6. PERFORMING ORG. REPORT NUMBER
9. PERFORMING ORGANIZATION NAME AND ADDRESS Air Force Institute of Technology (AFIT-EN) Wright-Patterson AFB, Ohio 45433		8. CONTRACT OR GRANT NUMBER(s)
11. CONTROLLING OFFICE NAME AND ADDRESS Air Force Weapons Laboratory NTYV Kirtland AFB, New Mexico 87117		10. PROGRAM ELEMENT, PROJECT, TASK AREA & WORK UNIT NUMBERS PE 62601F JON 88090132 DC W10
14. MONITORING AGENCY NAME & ADDRESS (if different from Controlling Office)		12. REPORT DATE June 1981
		13. NUMBER OF PAGES
		15. SECURITY CLASS. (of this report) UNCLASSIFIED
		15a. DECLASSIFICATION DOWNGRADING SCHEDULE
16. DISTRIBUTION STATEMENT (of this Report)  Approved for public release; distribution unlimited		
17. DISTRIBUTION STATEMENT (of the abstract entered in Block 20, if different from Report)  Approved for public release; distribution unlimited		
18. SUPPLEMENTARY NOTES  Approved for public release; IAW AFR 190-17  16 JUN 1981  Frederick C. Lynch, Major, USAF Director of Public Affairs Air Force Institute of Technology (AFIT-EN) Wright-Patterson AFB, OH 45433		
19. KEY WORDS (Continue on reverse side if necessary and identify by block number) Transport Theory      Finite Element Method Numerical Methods      Weapon Physic Problem Galerkin Method      Even-Parity Form of Boltzmann Equation Collocation Method      Air-Over-Ground Problem Ray Effect		
20. ABSTRACT (Continue on reverse side if necessary and identify by block number) The purpose of this research was to determine the feasibility of extending the use of the even-parity form of the Boltzmann Equation (EPFBE) to complex linear transport problems. Previous applications had been limited to problems involving simple geometry and low order scatter approximations. The air-over-ground problem was selected for this more complex extension since it required two-dimensional cylindrical geometry, anisotropic scatter, and a multigroup solution. To eliminate the ray effect in this problem, both the		

DD FORM 1 JAN 73 1473

EDITION OF 1 NOV 65 IS OBSOLETE

UNCLASSIFIED

SECURITY CLASSIFICATION OF THIS PAGE (When Data Entered)

UNCLASSIFIED

SECURITY CLASSIFICATION OF THIS PAGE(When Data Entered)

finite element and synthesis method were used. With these methods the Galerkin and collocation numerical techniques were applied. The Galerkin method proved infeasible because the integrals that resulted could not be efficiently evaluated either numerically or analytically. The collocation method allowed the analytic evaluation of all derivative and integral operations, but forced a fixed anisotropy on the solution. The multigroup method applied to the EPFBE produced a nested integral problem that increased proportionately with the number of energy groups. This research demonstrated that the finite element method can not be cost effectively used in solving the EPFBE for transport problems requiring complex geometries, anisotropic scatter, and a multigroup method. Criteria developed during this research for pursuing future work with the EPFBE is presented.

UNCLASSIFIED

SECURITY CLASSIFICATION OF THIS PAGE(When Data Entered)

